UiT The Arctic University of Norway

Faculty of Health Sciences
Department of Medical Biology

Myocardial metabolic, structural and functional remodelling following nutritional and hormonal stress

Synne Simonsen Hansen

A dissertation for the degree of Philosophiae Doctor (PhD) - 2022

Table of content:

Summary of thesis

The overall aim of this thesis was to increase our knowledge related to the underlying mechanisms of diabetes-induced cardiomyopathy. The primary objective of the first two papers was to elucidate the role of the reactive oxygen species (ROS) producing enzyme, NADPH oxidase 2 (NOX2), in the development of cardiac dysfunction in obesity/diabetes. We also wanted to examine the potential link between activators of NOX2, such as Angiotensin II (AngII) and fatty acids, in mediating cellular stress, myocardial oxygen wasting and impaired energetics in the heart. In paper I, we investigated whether NOX2 activity would influence cardiac function, energetics and substrate utilization following obesity by using ablation or pharmacological inhibition of NOX2. In paper II, we examined the direct effects of AngII on cardiac function, efficiency, substrate utilization, and mitochondrial respiration using a cardiac specific NOX2 overexpressing mouse model. Lastly, in paper III, we investigated whether hydrolysed wax ester (WE_H) from the marine supplementation Calanus oil could promote protective effects during palmitate-induced nutritional stress in cardiomyoblasts.

Our main findings were that inhibition of NOX2 attenuated obesity-induced left ventricular remodelling and dysfunction. NOX2 inhibition also improved myocardial energetics due to decreased myocardial oxygen demand for non-mechanical work. In addition, obesity-induced mitochondrial ROS production was abrogated. Cardiac-specific overexpression of NOX2 resulted in an aggravation of AngII-induced metabolic, structural, and functional remodelling in the heart. WE_H from Calanus oil prevented palmitate-induced cell death in cardiomyoblasts. The protective effects of WE_H were not mediated through reduced oxidative stress, but it ameliorated the palmitate-induced endoplasmic reticulum stress and impairment of autophagic flux.

Acknowledgment

This work was financed by The University of Tromsø – The Arctic University of Norway. Experiments were carried out in the Cardiovascular Research Group, at the Institute of Medical Biology, Faculty of Health Science.

I want to thank my main supervisor, Anne Dragøy Hafstad. Working with you has taught me so much about science, about struggling, trying harder when I fail, to not give up and lastly to always question my results. Thank you for believing in me, for pushing me forward and for making this PhD possible.

To Ellen Aasum, my second supervisor, thank you for all your help on this PhD journey and for being a supportive confident. Your door is always open which I really appreciate that. I want to thank you for helping me to realize my love for teaching, for giving me so many teaching opportunities and for always trusting in my abilities.

To Neoma, I want to thank you for supporting me, for sharing your experience, knowledge and helping me with both articles and the thesis. Your understanding and kindness have seen me through both ups and downs. I also want to thank everyone at the Cardiovascular Research Group for all the feedback, help and acceptance. A special thanks to Trine for being so patient, for contributing to my papers, for the hours of small talk, and for being a good friend.

To Trine K, Åsa, Hege, Victoria, and Jenny, thank you for countless lunches, cakes, coffees, talks and laughs. To Leif, Lars, and Kirsten, without you I would have quit this PhD so many times. Thank you for all the fun times, for funny texts, dinners, and beers. You guys have taught me so much about life, work, politics, and friendship. I can't even imagine what this PhD-journey would have been like without you.

To my parents Kirsten and Øystein and my brother Oscar, thank you for your unconditional love, for listening, giving me advice and for supporting me.

Last, but most importantly, to my family. To my daughters Adele and Mathilde, you are everything to me and I'm so proud of you. Before anything ells, I am your mom and without the two of you I'm nothing. To Andreas for being my husband, my best friend and the one I want by my side in everything I do. Thank you for believing in me, for rooting for me always, and for being my person. I love the three of you to the moon and back, the most important thing is that we have each other!
Synne Simonsen Hansen, March 2022

Papers included in this thesis

Paper I

Anne D. Hafstad, Synne S. Hansen, Jim Lund, Celio X. C. Santos, Neoma T. Boardman, Ajay M. Shah and Ellen Aasum. NADPH Oxidase 2 Mediates Myocardial Oxygen Wasting in Obesity. *Antioxidant* 2020; 9, 171; doi.org/10.3390/antiox9020171 ePub: 2020 February 19.

Paper II

Synne S. Hansen* and Tina M. Pedersen*, Julie Marin, Neoma T. Boardman, Ajay M. Shah, Ellen Aasum and Anne D. Hafstad. Overexpression of NOX2 Exacerbates AngII-Mediated Cardiac Dysfunction and Metabolic Remodelling. *Antioxidant* 2022; 11, 143; doi.org/10.3390/antiox11010143 ePub: 2022 January 10.

Paper III

Synne S. Hansen* and Kirsten M. Jansen*, Kenneth B. Larsen, Anne D. Hafstad, Ragnar L. Olsen, Terje S. Larsen and Ellen Aasum. Hydrolysed Wax Ester from Calanus Oil Protects H9c2 Cardiomyoblasts from Palmitate-Induced Lipotoxicity. (Manuscript).

* Both authors contribute equally and shared first authorship

Related publications

Synne S. Hansen, Ellen Aasum and Anne D. Hafstad. The Role of NADPH Oxidases in Diabetic Cardiomyopathy. *BBA – Molecular Basis of Disease* 2018; 1864 (5), 1908-1913, doi.org/10.1016/j.bbadis.2017.07.025. ePub; 2017 July 25. PMID: 28754449

Abbreviations

AngII	Angiotensin II
BM	Basal metabolism
BMI	Body mass index
DAG	Diacylglycerol
DIO	Diet-induced obesity
EC	Excitation-contraction
ECC	Excitation-contraction coupling
ER	Endoplasmic reticulum
ETC	Electron transport chain
FA	Fatty acid
FAO	Fatty acid oxidation
HFD	High fat diet
HF	Heart failure
KO	Knock-out
LD	Lipid droplets
LV	Left ventricle
MVO_2	Myocardial oxygen consumption
NADPH	Nicotinamide adenine dinucleotide phosphate
NOX	NADPH oxidase
OCR	Oxygen consumption rate
PKC	Protein kinase C
PUFA	Poly-unsaturated fatty acid
PVA	Pressure-volume area
RAAS	Renin-angiotensin-aldosteron system
ROS	Reactive oxygen species
ROX	Residual oxygen consumption
TG	Transgenic
WD	Western diet
WE	Wax ester
WE_H	Wax ester hydrolysate
WT	Wild type

Introduction

Clinical perspective

Despite modern treatment options, heart failure (HF) is a major public health issue with both social and economic consequences [1-3]. The cardiac pathophysiology in HF is complex and includes processes such as myocardial metabolic remodelling, hypertrophy, ventricular dilation, increased wall stress as well as cardiomyocyte apoptosis [4,5]. Systolic HF is characterized by reduced left ventricle (LV) ejection fraction, while diastolic HF is associated with impaired relaxation and a stiffening of the ventricles which results in impaired filling. A reduced ejection fraction may cause low renal perfusion, which activates the renin-angiotensin-aldosterone system (RAAS) as a compensatory mechanism of the perceived hypotension. RAAS-activation results in salt and water retention, increasing the load on the heart which may further exacerbate the progression of HF [6,7]. Consequently, uncompensated HF may lead to physical symptoms like congestion, shortness of breath, exercise intolerance and oedema [4-6].

Obesity-induced heart failure

There are several risk factors associated with the development of HF. The Framingham study, a community-based long-term cohort study started in 1948, has provided solid epidemiological and pathophysiological data on the development of HF [2]. Several risk factors for HF has been identified, these include hypertension, smoking, ischemic heart disease, as well as diabetes and obesity [1]. The association between obesity and HF is demonstrated by the fact that a Body Mass Index (BMI) within the obesity range (female 30-38 kg/m^2, male 30-35 kg/m^2), doubles the risk of developing HF when compared to subjects with BMI within the normal range (female 20.5-24 kg/m^2, male 21.5-24 kg/m^2) [8]. Obesity and type II diabetes have been referred to as twin epidemics as several epidemiological studies reveal parallel

escalation of both conditions [9]. Accordingly, in approximately 90% of patients with type II diabetes, the disease is attributable to obesity [10]. Although the cause of this obesity pandemic is multifactorial, decreased physical activity in combination with highly processed food is at the core [11].

Even in absence of coronary artery disease and hypertension [12], obese and diabetic individuals have increased risk of HF, a condition referred to as diabetic cardiomyopathy [12,13]. Then pathophysiology in cardiomyopathy is multifactorial and complex (Figure 1), and several systemic changes such as hyperglycaemia, dyslipidaemia, hyperinsulinemia as well as activation of RAAS and low-grade inflammation can induce these pathophysiologic changes within the cardiomyocyte. Common hallmarks of diabetic cardiomyopathy include altered substrate utilization [14-16], altered calcium handling [17], increased endoplasmic reticulum (ER) stress [18], impaired autophagy [19], mitochondrial dysfunction [14,20] and oxidative stress [14,20,21].

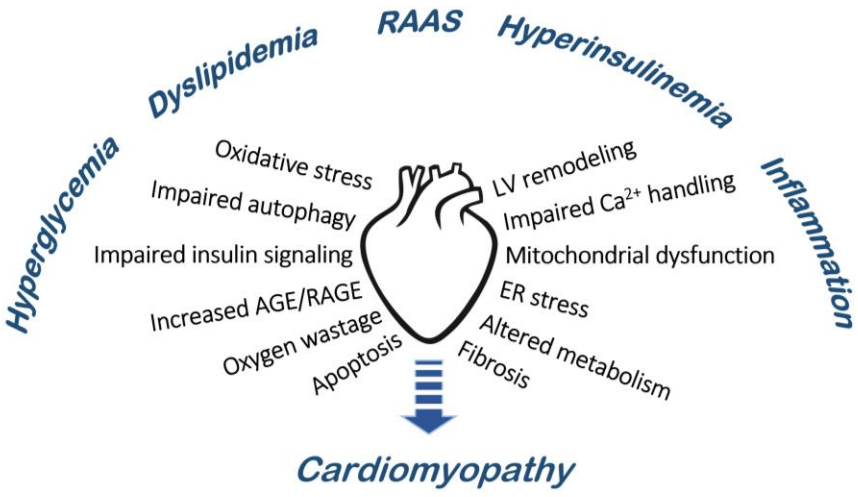

Figure 1: Overview of systemic changes in obesity and diabetes that drive cellular changes and consequently leads to the development of cardiomyopathy. Renin-angiotensin-aldosteron-system (RAAS), endoplasmic reticulum (ER), left ventricular (LV), advanced glycation end-product (AGE)/receptor for AGE (RAGE). Modified from Hansen *et al*. 2018 [22].

Myocardial metabolism and energetics

The heart consumes large amounts of energy in the form of ATP that is continuously replenished by oxidative phosphorylation in mitochondria and to a lesser extent, by glycolysis. To adapt the ATP supply efficiently to the constantly varying demand of cardiomyocytes, a complex network of enzymatic and signalling pathways controls the metabolic flux of substrates towards their oxidation in mitochondria [23]. The heart is an omnivore which can utilize a wide range of substrates supplied by the coronary circulation, and it can rapidly change substrates for its ATP production, depending on the supply, neurohormonal condition and oxygen supply. Under aerobic conditions, there is a regulatory interaction between metabolism of fat and glucose in the cardiomyocyte, where the increased oxidation of one substrate will result in decrease oxidation of the other, and vice versa, described as the Randle cycle [24]. Under normal resting conditions, the heart derives about 75% of its energy from fatty acids (FA) [25-27] and the remaining 25% is mainly oxidation of glucose in addition to lactate, ketones and amino acids [26]. However, under conditions of elevated circulating FAs, the heart can increase its reliance on fat [27]. In a healthy individual, the plasma concentration of FA can vary up to fourfold a day, depending on dietary choices, time between meals and exercise or stress [28]. Importantly, metabolic stress factors such as fasting, diabetes or ischemia have also been shown to increase the concentration of FA in the plasma [16].

In HF patients reduced energetics measured as lowered myocardial phosphocreatine-to-ATP ratio, is a predictor of cardiovascular mortality [29]. Metabolic remodelling as well as decreased cardiac efficiency has also been suggested to be a central component leading to HF [30,31]. In accordance with this, altered metabolism and inefficiency are early findings in both clinical and experimental models of HF [14,15,32]. The mechanisms leading to impaired cardiac energetics and efficiency are not fully elucidated, however, increased reliance on FA

oxidation (FAO), altered calcium handling, mitochondrial uncoupling, as well as structural changes, such as fibrosis and hypertrophy, are suggested to play important roles. Experimental studies have shown impaired mechanoenergetic properties, leading to mechanical inefficiency in obese/diabetic hearts [14,15], and also that this reduction in efficiency is mainly caused by increased myocardial oxygen demand for non-contractile work, such as basal metabolism (BM) and processes associated with excitation-contraction (EC) coupling [14,15,33-35].

Although altered substrate metabolism is also a hallmark in many types of HF [16], the observed metabolic phenotype will vary [26]. In obesity/diabetes-mediated cardiomyopathy, experimental studies consistently describe a myocardial switch towards increased FAO and accompanied decreased glucose oxidation [15,30,31]. This was also confirmed clinically in obese females by Peterson *et al* [32]. The high reliance on FAO is mediated by an increased expression of proteins and enzymes that are involved in FAO, induced by the transcription factor peroxisome proliferator-activated receptor α [36]. The metabolic shift has been shown to precede development of cardiac dysfunction [14,32], and is therefore suggested to be involved in the development of cardiac dysfunction [37].

Although FA are the primary energy substrate for the heart, exposure to high FA levels may activate harmful processes in the cardiomyocyte. In *ex vivo* analysis of hearts from healthy mice, an acute FA load has been found to increase myocardial oxygen consumption (MVO_2), decrease cardiac efficiency [38], and increase ischemic susceptibility [39,40]. In diabetes, long-term exposure to high circulating levels of FA is likely to play a role in the development of cardiomyopathy and although the underlying mechanisms are far from elucidated, they are generally referred to as lipotoxicity [41,42]. These adverse effects of high lipid load are specifically related to saturated FA acids such as palmitate. If FA availability vastly exceeds what the cardiomyocyte is capable of oxidizing, it results in an accumulation of acyl-CoAs as

well as other FA intermediates such as diacylglycerol (DAG) and ceramides. In cardiomyocytes, acute exposure to palmitate was found to impair the FAO rate [27] and cause intracellular accumulation of DAG and ceramides, disturbing normal cellular signaling [43]. The pathology of lipotoxicity are generally linked to increased oxidative stress, but may also involve impaired autophagy [19,44,45], which is closely linked to increased ER stress [45]. Accordingly, palmitate has been shown to cause prolonged ER stress and activation of specific ER stress-induced apoptotic signaling pathways [41].

Both diabetes and obesity are associated with activation of RAAS , however, the effects of this on cardiac metabolism are complex and not fully elucidated [46]. Experimental studies have previously demonstrated a cardiac metabolic shift in the heart with decreased FAO and subsequent increased glucose oxidation induced by increased plasma levels of angiotensin II (AngII) [47-49]. This was thought to be mediated by a downregulation of key regulatory transcription factors of FAO [47]. A similar switch towards glucose reliance has been described in ischemic HF, as well as models of overt hypertension induced by aortic banding [26]. On the other hand, Mori and colleagues have demonstrated impaired glucose oxidation, in addition to insulin resistance following AngII-treatment [50,51]. The AngII-induced shifts in metabolism seem to be dependent on AngII-treatment regimens and the progression and severity of HF [46].

Oxidative stress and NADPH oxidases

Increased oxidative stress is shown to contribute to the pathophysiology in many forms of HF, including ischemic HF, obesity or diabetes-induced cardiomyopathy as well as HF caused by hypertension [52]. Reactive oxygen species (ROS) are oxygen-based chemicals that include both free radicals, such as superoxide's ($O_2^{\cdot-}$), hydroxyl radical ($^{\cdot}OH$) and nonradicals that generate free radicals, such as hydrogen peroxide

(H_2O_2). Although the main production of ROS is linked to the electron transport system in mitochondria, there are also many other sources of ROS within the cardiomyocyte. These includes xanthine oxidase, nitric oxide synthases, and nicotinamide adenine dinucleotide phosphate (NADPH) oxidases (NOX) (Figure 2). In low concentration, ROS have important roles in cell signalling and are closely linked to the redox state of the cardiomyocyte. However, excessive ROS can cause oxidative damage and even cell death. To counteract ROS production during transient changes in cardiac workload, energy demand, and substrate supply, there are a number of coordinated and complex systems in place including ROS scavenging enzymes such as superoxide dismutase, glutathione peroxidase, catalase, in addition to the nonenzymatic antioxidants systems. These systems are important to prevent intracellular ROS accumulation and consequently oxidative stress.

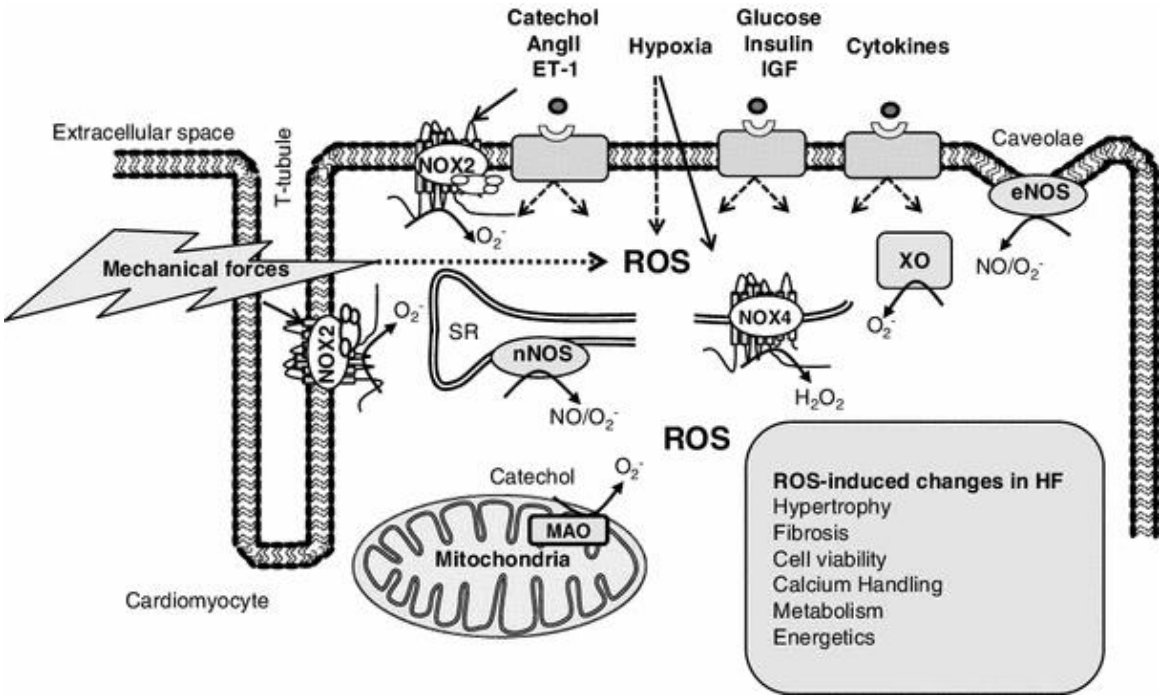

Figure 2. Sources and stimuli leading to reactive oxygen species (ROS) production in the cardiomyocyte, as well as different ROS-mediated effects in the failing heart. Uncoupled nitric oxide synthases (eNOS, nNOS), endothelin-1 (ET-1), insulin-like growth factor (IGF), monoamine oxidase (MAO), xanthine oxidase (XO). This figure is modified from Hafstad *et al*. 2013 [53].

Several isoforms of NOXs have been discovered, NOX2 and NOX4 being the two isoforms predominantly expressed in the cardiomyocyte. While NOX2 is a transmembrane enzyme that functions through recruiting multiple cytosolic subunits, NOX4 is found intracellularly, however the exact location is still controversial [54]. NOX2 is a heterogenic flavocytochrome with a $p22^{phox}$ subunit, where cytosolic subunits needed to activate NOX2 includes $p47^{phox}$, $p67^{phox}$, $p40^{phox}$ and Rac1. Once activated, it uses the NADPH substrate to reduce molecular oxygen to superoxide [55]. NOX2 activation and subsequent ROS production triggers the opening of mitochondrial membrane channel, which releases bursts of ROS into the cytosol. This has a consolidating effect because the increased ROS activates membrane channels on neighbouring mitochondria resulting in additional endogenous ROS release, referred to as ROS-induced ROS release [56]. NOX4 is a flavocytochrome with a $p22^{phox}$ subunit, it is transcriptionally regulated and produce mainly H_2O_2.

When ROS production exceeds the endogenous antioxidant capacity of the cardiomyocyte it results in oxidative stress which can damage proteins, lipids and DNA [7]. The pathological changes in the cardiomyocyte following oxidative stress induce a whole range of processes in the heart, such as fibrosis, impaired calcium handling, mitochondrial dysfunction, and impaired energetics [52,54].

Interestingly, many of the systemic changes associated with obesity and diabetes are also potent activators of NOXs (Figure 2). It is well documented that hyperglycaemia leads to activation of NOX2 [57-61], and NOX2-produced ROS have been shown to play an important role in glucotoxicity, resulting in increased cell death [57]. Under these conditions recruitment of necessary subunits occurs through different intracellular pathways, among these being activation of protein kinase C (PKC) [19,62,63]. Both chronic [62,64,65] and acute [19,63,66] high lipid load have also been shown to cause activation of NOX2 in the cardiomyocyte. In addition, AngII

increases ROS production [7,67,68] by binding to the angiotensin receptor 1 located in the cell membrane, causing a rapid ROS production through PKC-activation of NOX2 [69].

An important finding is that NOX activation seems to be a double edge sword, being both protective and damaging. While NOX2 activation serves an important role in several signalling pathways in the cardiomyocyte such as stretch-induced calcium release and the EC-coupling [68,70], NOX2 activation can also promote detrimental processes in sustained cardiac stress, leading to hypertrophy, contractile dysfunction, myocardial stiffening and myocardial cell death [54]. Similarly, NOX4 has been demonstrated to mediate protective effects against hemodynamic stress [71] and to play an important role in many intracellular processes, including regulation of ER stress response [72], reprograming of substrate utilization [73], and activation of autophagy [74], even though NOX4 is also a known contributor to oxidative stress in HF [75]. Taken together, these inconsistent findings regarding NOXs might be explained by differences in animal models, HF severity, and variance in experimental methods, and also demonstrate that there is need for more understanding of the individual roles of NOX homologues.

Knowledge gaps in obesity-induced development of cardiomyopathy

The mechanisms behind obesity-induced cardiomyopathy are not fully elucidated, but metabolic alternations including impaired energetics, and increased oxygen consumption seems to precede development of cardiac dysfunction [14,32]. Although the increased reliance on FA utilization and oxidation is considered to be a major contributor to obesity-induced oxygen wasting, myocardial oxygen wasting may also be reduced without major effects on substrate utilization [14]. Moreover, an acute lipid load was only shown to induce myocardial oxygen wasting effects in hearts from lean, but not obese mice despite an increase in FAO in both hearts [35].

Interestingly, myocardial oxygen wasting has been shown to be associated with increased levels of cardiac ROS in obese models [14,21]. Although the significance of NOX2 in the development of diabetic cardiomyopathy is still largely unknown, the cardiac expression of NOX2 is increased in experimental models of obesity and diabetes [64,76,77] and several of the systemic changes occurring in obesity and diabetes are potent activators of NOX2. We therefore hypothesized that increased NOX2 activity plays an important role in the pathogenesis of diabetes-induced cardiomyopathy. Whether myocardial NOX2 activation will influence cardiac energetics or the progression of cardiac dysfunction following obesity has been the subject of this thesis. Given the ability of NOX enzymes to influence calcium handling [62,68,70] and mitochondrial ROS release [78,79] there is reason to believe that NOX2 activation may also play an important role in the obesity/diabetes related impairment of cardiac energetics due to impaired calcium homeostasis and mitochondrial function. Finally, as obesity is associated with increased RAAS, and AngII is a potent activator of NOX2, AngII-signaling may also be a candidate for oxygen wasting effects in the myocardium.

Omega 3-poly-unsatturated FAs (PUFAs) have been suggested as a potential strategy to combat lipotoxicity, as they have been shown to both reduce ROS production in vascular cells [80] as well as attenuate ER stress in hepatocytes [81]. In recent studies from our group, we have investigated the effect of a marine oil derived from marine crustacean *Calanus finmarchicus*. This is a commercially available dietary supplement which has recently been rebranded "Zooca". Despite this, it will be referred to as Calanus in this thesis. The major component (approximately 80%) of calanus oil is wax esters (WE) [82], which consist of FA (including omega 3-PUFAs) esterified to a fatty alcohol. Studies from our own group have shown that supplementation of calanus oil and/or the WE from this oil reduced obesity-induced inflammation [83] and improved recovery of heart function following ischemia and reperfusion in a

mouse model of diet-induced obesity (DIO) [84]. To what extent this oil or its WE can have a more direct effect on cardiomyocyte during lipotoxic-stress is yet to be explored.

Aim of the thesis

The overall goal for this thesis was to elucidate underlying mechanism of diabetes-induced cardiomyopathy.

Paper I

The aim of this paper was to investigate the effects of NOX2 activity on ventricular function, cardiac energetics and metabolism following obesity by using both ablation and pharmacological inhibition of NOX2 in mouse models of obesity.

Paper II

The aim of paper II was to examine the direct effects of AngII on cardiac function, substrate utilization, efficiency, and mitochondrial respiration. We also investigate whether overexpression of NOX2 exacerbates the effect of AngII-treatment.

Paper III

The aim of paper III was to investigate whether hydrolysed wax ester from the marine supplementation Calanus oil could promote protective effects during palmitate-induced nutritional stress in cardiomyoblasts.

Methodological considerations

Animal models of obesity-induced heart failure

Obesogenic diets are extensively used in experimental studies of obesity-induced HF [85-88]. As compared to the congenital leptin deficient mice models (*db*/*db* and *ob*/*ob*), diet-induced obesity produces a less severe model of insulin resistance without overt type II diabetes [89,90]. The mouse strain most often used in these models are the C57Bl/6J strain, as it is particularly susceptible to diet-induced obesity. They express a mutation in the Nicotinamide nucleotide transhydrogenase gene resulting in low pancreatic insulin secretion and consequently reduced glucose clearance [87]. In addition, they exhibit reduced response to both leptin and β-adrenergic signalling which hampers lipolysis [86,91]. The progression of obesity is comparable to the human development of the same conditions [86,92]. In the current thesis, we induced obesity using two different diet regimes in C57Bl/6J male mice 1) high fat diet (HFD) with 60% of the calories derived from fat (TestDiet, London, UK), and 2) a western palatable diet (WD), with 35% kcal derived from fat (TestDiet, London, UK). The feeding period was 18 and 28 weeks starting when the mice were 5-6 weeks of age. Both HFD and WD have previously produced obesity with insulin resistant phenotypes in our lab [14,21]. In addition, these models have consistently displayed a cardiometabolic phenotype with increased reliance on FAO, myocardial oxygen wasting and development of ventricular diastolic dysfunction [14,21]. The assessment of the diabetic phenotype included body weight and analysis of blood glucose, plasma free FA as well as plasma insulin levels. Insulin resistance was assessed with a glucose tolerance test, as well as a homeostatic model assessment (HOMA) calculated from the product of fasted blood glucose and insulin (μU/ml) and then divided by 22.5 [93].

In this thesis, male NOX2 knock-out (KO) mice, obtained from a colony established at King's College, London, UK, were used to investigate the role of NOX2 in DIO.

These NOX2 KO mice are based on the C57Bl/6J strain but they lack the gp91^{phox} /Cybb gene (B6.129S-*Cybb^{tm1Din}*/J) [94]. Importantly, the basal cardiac phenotype is unaltered in this model. In addition, pharmacological inhibition of NOX2 activity in the DIO mice was obtained by adding 4-hydroxy-3-methoxy-acetophenone, acetovanillone (apocynin, Sigma-Aldrich CO, Munich, Germany) to the drinking water (2.4g/L) throughout week 11 until week 21 of feeding period with WD. This dose has previously been shown to improve glucose tolerance and reduce inflammatory markers in long-term DIO C57Bl/6J mice [95]. Although apocynin is a commonly used NOX2 inhibitor, the mechanism by which it works is not fully elucidated. One of the common theories is that it prevents the translocation of cytoplastic sub-units p47^{phox} and p67^{phox} to the NOX2 complex [96,97]. However, one study on vascular cells has suggested that apocynin might not be a NADPH inhibitor but rather works as an antioxidant [98]. Apocynin, at very high concentrations has also been shown to inhibit NOX4 activity, even though it is not subunit dependent [99].

Animal model of AngII-induced heart failure

In experimental animals, AngII-treatment is known to induce hypertension and to be a potent activator of NOX2 [7]. In experimental studies, AngII-treatment with high doses >1000ng/kg/min caused overt hypertension as well as cardiac hypertrophy, creating a severe model of HF with cachexic properties [100-102]. At such high doses it is hard to distinguish the initial effects of AngII from other stressors on the heart. In order to investigate the direct effects of AngII without inflicting overt hypertension, we treated the mice for two weeks with a non-pressor (50 ng/kg/min) [103] or a slow pressor dose (400ng/kg/min) [104] of AngII. The treatment was administered through a subcutaneous, micro-osmotic pump (Model 1002, Alzet, California, USA) inserted in the midscapular region. The pumps contained either a solution of AngII in saline, or saline exclusively (sham). Chronic infusion of slow pressor dose of AngII has

previously been shown to initiate a pre-hypertensive period, characterized by trophic stimulation of vasculature, muscle as well as potentiation of pressor and vasoconstrictor responses to AngII itself [105].

To elucidate the role of NOX2 activation in AngII-induced HF we also included cardiomyocyte specific NOX2 overexpressing (csNOX2) transgenic (TG) male mice, obtained from a colony established at King's College, London, UK. The csNOX2 TG were created on a C57Bl/6J strain by cloning a 1.8 kb human NOX2 cDNA downstream of the myosin light chain-2 promoter. They show a cardiac expression of the NOX2 protein that is approximately five times higher than their wild type (WT) litter mates and the basal cardiac phenotype and the activity of NOX2 is not different from their WT littermates. However, when subjected to stress, for instance AngII-treatment, the NOX2 activity increases with 50% in the TG compared to WT [68].

Assessment of blood pressure

To evaluate the hypertensive effect of AngII, we measured blood pressure using tail-cuff plethysmography (Coda, Kent Scientific, Connecticut USA). In comparison to telemetry with a transmitter-catheter systems, tail-cuff measuring is less invasive and may therefore inflict less stress on the animal. Studies comparing the two methods have shown a strong correlation between measured blood pressure, although tail cuff seems to be less sensitive in terms of determining minor changes in blood pressure [106]. To limit the effect of stress during the recordings, we familiarised the mice to the procedure, by exposing them to the process on three consecutive days prior to the experiment. Baseline blood pressure was obtained prior to AngII-treatment.

Assessment of ventricular function

Cardiac function was assessed both *in vivo* using echocardiography, as well as *ex vivo* using an isolated heart perfusion system. Paper II includes conventional

echocardiographic examinations in 2D B-/M-mode and pulsed wave Doppler, using the VisualSonics 2100 (Vevo Imaging System, Toronto, Canada) with a 40 MHz probe. The animals were anaesthetized with isoflurane (1.5-2%), examined in a supine position on a heated platform and body temperature was maintained at 37°C. Images of parasternal short-axis M-mode and apical four-chamber doppler images were obtained and analysed by a blinded operator. Results include assessments of global LV function, including wall thickness, volume, and systolic and diastolic function in M-mode. Additionally, the diastolic function was further evaluated with a pulsed-wave and tissue doppler. Echocardiography was performed the day before initializing AngII-treatment as well as on day 14 of treatment, allowing monitoring of changes in ventricular function in each animal.

Cardiac function was also evaluated in isolated perfused hearts. The isolated heart model was first described by Langendorff in 1895, where the heart is perfused in a retrograde mode. This technique was further evolved to a "working heart model", described by Neely and Morgen in 1967 [107]. In the working mode, the heart is perfused antegradely and therefore it more closely resembles normal cardiac physiology [107]. The advantages of heart perfusion, regardless of the mode, is the control of external factors such as loading conditions, heart rate, substrate supply and if necessary, drug administration. The control of these factors gives a high level of comparability within measured data [90,108,109]. In the present thesis, all hearts were perfused with a modified Krebs-Henseleit buffer containing 5 mM glucose as well as 0.4-0.5mM palmitate bound to 3% bovine serum albumin in a recirculating mode. In paper I and II, both coronary flow (CF) and aortic flow was measured, and cardiac output (CO) was calculated as the sum of these.
In paper I, intraventricular pressure and volume (PV) in the LV was measured using a conductance catheter. Systolic functional parameters included LV developed pressure and the maximum positive derivative of the pressure development

(dP/dt_{max}), while parameters of diastolic function included LV end-diastolic pressure and volume and the maximum negative derivative of the pressure development (dP/dt_{min}), as well as the relaxation constant (Tau). In addition, a preload occlusion allowed assessment of load-independent parameters such as the preload recruitable stroke work index and end-diastolic pressure volume relationship, parameters of systolic and diastolic function, respectively.

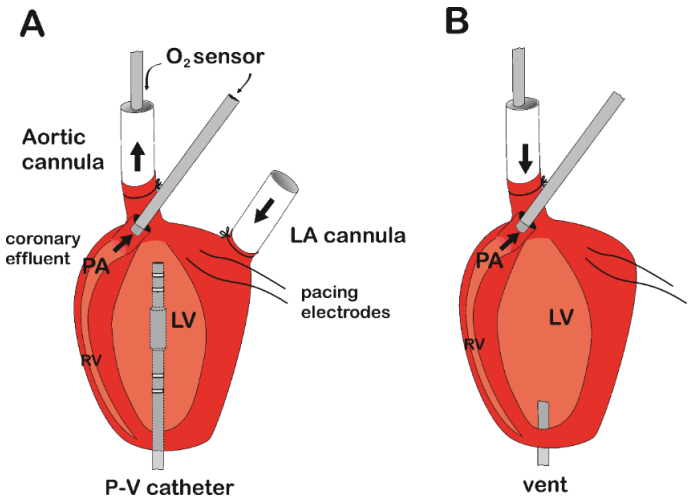

Figure 3. Illustrations of the different modes of isolated perfused hearts. **A** working heart mode with pressure-volume catheter inserted in the left ventricle, O_2 sensors and pacing electrodes. **B** Unloaded Langendorff mode with vent and pacing electrodes. Left atrial (LA), left ventricle (LV), right ventricle (RV), pressure-volume (P-V), pulmonary artery (PA).

MVO_2 was obtained by using two fibre optic sensors to measure the difference in PO_2 in the perfusion buffer entering and leaving the heart (Figure 3). MVO_2 was then calculated as [PO_2 (oxygenated perfusate) – PO_2 (coronary effluent)] * Benson solubility coefficient of O_2 * CF [15].

Cardiac mechanical efficiency was assessed as the ratio between LV stroke work (SW) and MVO_2 under a steady state condition. In paper I, SW obtained using the PV catheter (SW = LV developed pressure * stroke volume). In paper II, the pressure

catheter was placed in the aortic line and the SW was calculated as stroke volume (CO/heart rate) * estimated LV develop pressure (peak systolic pressure$_{\text{aortic line}}$ - LV filling pressure).

In studies from our research group a regression analysis of the relationship between the MVO_2 and the cardiac work (pressure-volume area, PVA), has been used to determine the work-dependent and non-work-dependent oxygen consumption [110] (Figure 4).

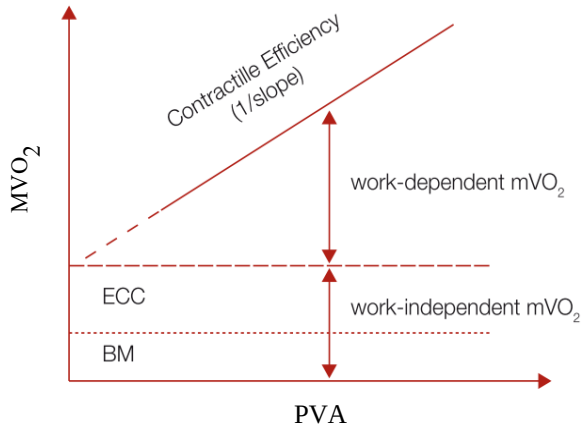

Figure 4. The linear relationship between myocardial oxygen consumption (MVO_2) and pressure-volume area (PVA). The y-intercept defines work-independent MVO_2, and the slope of the relationship represent the contractile efficiency. Excitation-contraction coupling (ECC) and basal metabolism (BM) together represent the work-independent oxygen expenditure. Figure borrowed with permission from Aasum 2011 [23].

In this thesis an alternative method was used [34], where the non-work-dependent oxygen consumption was directly measured by altering the perfusion mode to a Langendorff mode and further "unloading" the heart by inserting a vent into the LV to remove any excess fluid in the ventricle (Figure 3B). This measurement is referred to as the unloaded MVO_2 ($MVO_{2\text{unloaded}}$) and includes processes associated with BM (MVO_{2BM}) and EC-coupling (MVO_{2ECC}). By adding potassium chloride to the

circulating buffer, cardioplegic arrest is induced to obtain MVO_{2BM}, which allows calculation of MVO_{2ECC} ($MVO_{2\ unloaded}$ - MVO_{2BM}).

Assessments of myocardial substrate utilization

Altered substrate metabolism and loss of metabolic flexibility is a hallmark of HF [15,16,38,111]. We therefore measured both glucose and FAO rates as previously described by our group [111]. Radio-labelled isotopes ([U-^{14}C]-glucose) and ([9,10-^{3}H]-palmitate) were added in trace amounts to the recirculating perfusion buffer. At regular time intervals, samples of the perfusion buffer were collected, and glucose and FAO rates could later be calculated as the accumulated $^{14}CO_2$ and $^{3}H_2O$. $^{14}CO_2$ was measured by injecting a sample of the perfusion buffer to a sealed test tube containing sulphuric acid, where the subsequent released $^{14}CO_2$ was trapped on filter paper with hyamine hydroxide. $^{3}H_2O$ was separated from the buffer sample using vacuum sublimation, where the water in the frozen buffers sample will sublimate at room temp under vacuum. The total $^{14}CO_2$ and $^{3}H_2O$ were determined using a liquid scintillation counter, where the slope of increased isotope concentration represents the rate of substrate oxidation.

Assessment of mitochondrial respiration

Mitochondrial respiration in LV tissue was assessed using the Oroboros oxygraph (Oroboros Instruments, Innsbruck; Austria), which is a high-resolution respirometer that measures the changes in oxygen concentration over time (O_2 flux). The oxygraph can be used to analyse respiration in tissue, isolated mitochondria or intact/permeabilized cells [112]. In paper I, mitochondria were isolated using a slightly modified method, based on Palmer *et al*. [113]. The oxygen consumption in the presence of substrates alone without the presence of ADP is known as LEAK respiration. We used either malate (2.5mM), glutamate (5mM) and pyruvate (10mM) (carbohydrate oxidation) or malate (2.5mM) and palmitoyl-carnitine (10mM) (FAO)

as substrates. A saturated amount of ADP was then added to determine the maximal OXPHOS-capacity ($OXPHOS_{max}$). Lastly, Cytochrome C (10μM) was used to evaluate the integrity of the mitochondria.

In paper II, we followed the protocol described by Acin-Perez *et al*., where mitochondrial respiration was measured in previously frozen tissue [114,115]. When isolating mitochondria from frozen tissue there seems to be a predominant loss of diseased mitochondria, potentially masking mitochondrial pathology, however, tissue homogenate has 90-95% preservation of the maximal respiratory capacity compared to fresh tissue [114]. Thus, we chose to analyse homogenate of LV tissue, that had been frozen at -70°C. As the freezing/thawing process breaks down the inner and outer mitochondrial membrane, thereby disrupting the enzymatic processes involved in the citric acid cycle (CAC), it is not possible to add substrates which produce nicotinamide adenine dinucleotide (NADH) via the CAC. Hence, we added NADH (1mM) as a complex I substrate and in addition cytochrome C (10μM) was added to compensate for the loss during the freeze -thaw process. Succinate feeds directly to complex II via FADH in the electron transport chain (ETC), therefor, after first inhibiting complex I respiration with rotenone (0.5μM), succinate (10mM) was added as a substrate to evaluate complex II respiration. Finally, malonic acid (5mM) and antimycin A (2.5mM) were added sequentially to inhibit complex II and complex III respectively to assess the non-mitochondrial residual oxygen consumption rate (ROX). It should be noted that using this strategy, we do not measure coupled respiration; OXPHOS, but rather quantify the maximal respiratory capacity of the ETC during non-coupled respiration.

Cell model of lipotoxicity

To create a cell model of nutritional stress, H9c2 cells were treated with toxic levels of palmitate. Isolated adult cardiomyocytes have low proliferative capacity which

makes them difficult to culture and sustain over time. We therefore used the H9c2 cardiomyoblast cell line (Sigma-Aldrich, Darmstadt, Germany). This cell line was originally derived from embryonic rat ventricle heart tissue in 1976 [116]. One major drawback with the H9c2 cells is their glycolytic nature, whereas adult cardiomyocytes primarily have an oxidative metabolism [117]. This might be explained by the foetal origin of H9c2s , where their environment is more hypoxic with higher levels of lactate and lower levels of FA compared to the adult heart [117]. H9c2 cells were incubated in 5% CO_2 at 37°C, in a high glucose Dulbecco's modified eagle's medium (Sigma-Aldrich, St. Louis MO, USA), including 10% foetal bovine serum (FBS, Sigma-Aldrich) and 1% streptomycin (p0781, Sigma-Aldrich). Incubation with 100μM palmitate resulted in cell death over time. Cell line ageing can be a source of variable results with toxicity testing [118], therefore we only included cells from passages between 10-15.

Preparation of hydrolysed wax ester from Calanus

The major component (approximately 80%) of calanus is WE, [82], which consist of FA esterified to a fatty alcohol. By hydrolysing the WE, the bond between the FA and the fatty alcohol is broken. The biological availability of FA is correlated with FA-binding to carrier proteins, specifically albumin. The ratio between albumin-bound and free FA will be an indicator of the biological availability [119]. We chose to dissolve the WE_H in ethanol which enables maximal biological availability.

Assessment of lipotoxicity and cell survival

Live cell imaging was used to visualisation of cell proliferation as well as time of death. Manual, blinded counting of live and dead cells were performed in three randomly chosen areas, from three different wells per treatment, at different timepoints (0, 10 and 20 hours). In addition, the xCELLigence real-time cell analysis (xCELLigence® Biosensor Technology RTCA, ACEA, Etterbeek, Belgium) was used

to confirm our findings from the live cell imaging. The instrument measures the electrical conduction through gold microelectrodes that are fused to the bottom surface of a microtiter plate well. As the number of cells increase, they inhibit electron flow through the plate, thereby reducing the current. The adherence of cells is reported as Cell Index (CI = (impedance at time point – impedance in the absence of cells)/nominal impedance value).

Assessment of ROS production

This thesis includes three different methods to assess the ROS production. In paper I, ROS production in the myocardium was measured with dihydroethidium (DHE) - high pressure liquid chromatography (DHE-HPLC) where fluorescence from hydroxyethidium (EOH) and ethidium (E) was measured. The DHE-derived products were expressed as ratio of either EOH or E per DHE consumed, or per gram of wet tissue. This method assesses overall superoxide production, while at the same time specifying the measurement by separating fluorescence derived from EOH, a superoxide specific product, versus E, which relates to H_2O_2 [120]. ROS production was also measured in isolated mitochondria simultaneously with mitochondrial respiration using a fluorescent Amplex UltraRed dye (10 μM Thermo Fischer Massachusetts, USA) that reacts with H_2O_2, a reaction that is catalysed by adding horseradish peroxidase (10uU) to produce a red fluorescent compound. This fluorescence is recorded by the Fluo LED2-Module in the oxygraph. In paper II, we evaluated mitochondrial ROS production from previously frozen LV homogenates, but we found very little response in ROS production to both inhibitors as well as different substrates. Finally, in paper III, ROS production was measured utilizing flow cytometry and a redox sensitive probe 2′,7′dichlorofluorescin diacetate. A drawback with this method is that this probe irreversible binds to all endogenous ROS, which unlike the DHE-HPLC method, does not provide information on the individual sources of ROS.

Assessment of gene expression

Real time PCR was performed to evaluate gene expression, specifically the metabolic mediator genes, hypertrophy markers, inflammatory markers in adipose tissue, as well as to verify the TG and KO mice. In addition, in paper III, the gene expression of transcriptional factor C/EBP homologous protein (CHOP) was analysed to evaluate the ER stress in H9c2 cells. RNA was isolated from perirenal fat stored in Allprotect Tissue Reagent (Qiagen, Hilden, Germany) with RNeasy Lipid Tissue Mini Kit protocol (Qiagen, Hilden, Germany). mRNA from H9c2 cells were isolated using the RNeasy plus mini kit protocol (Qiagen, Hilden, Germany). Liver samples were stored in RNA later (Qiagen, Hilden, Germany) at -20°C and then RNA was isolated using the RNeasy Fibrous Mini Kit. The RNA concentration and purity were determined using spectrophotometer, NanoDrop 2000 (Thermo Fisher, Waltham, Massachusetts, USA). RNA was reverse transcribed into cDNA using High-Capacity cDNA Reverse Transcription Kit (Thermo Fisher, Waltham, Massachusetts, USA) and real-time PCR was performed in a LightCycler®96 System (Roche, Basel, Switzerland) with the cDNA and FastStart Essential DNA Green Master (Roche, Basel, Switzerland). Target gene expression levels were normalized to a stable expressed housekeeping gene. The stability of the housekeeping gene was determined by geNorm. Quantification cycle value was defined as the cycle number at which the fluorescent signal was recorded above background level, defined by the LightCycle software [121].

Immunofluorescence and fluorescence microscopy

Paper III includes immunofluorescence and fluorescence microscopy performed in collaboration with the Advanced Microscopy Core Facility at this university. This was used to visualise and analyse ER stress marker (CHOP), as well as accumulation of autophagy markers (p62 and LC3B) in H9c2 cell treated with palmitate or palmitate in combination with WE_H. Cells were incubated with primary antibodies

against CHOP (Cell Signalling, Danvers, Massachusetts, USA), LC3B (Sigma-Aldrich, Saint-Louis, Missouri, USA), and p62/SQSTM1 (Progen, Heidelberg, Germany), followed by an AlexaFluor-conjugated secondary antibodies. Cells were imaged using a confocal microscope (LSM880 or CD7 – both Carl Zeiss Microscopy, Oberkochen, Germany), using a 40x NA1.2 W C-Apochromat objective for the confocal microscopy, or a 50x NA1.2 W Plan-Apochromat objective for the widefield microscopy. Optimal emission and excitation setting for each fluorophore were determined using ZEN software and all fluorescence channels were recorded at non-saturating levels. Acquisition settings were constant between samples used for comparisons or quantifications and random areas were selected for image analysis, performed using a customized protocol in Velocity ver. 6.3 (PerkinElmer, Waltham, Massachusetts, USA). Antibodies can vary in their degree of specificity, from high to low based on its unspecific binding, representing a major challenge in immunoblotting. The primary antibodies used in this thesis (CHOP, p62 and LC3B) are regarded as highly specific and are extensively used within this field.

Statistics

The results in articles included in this thesis are presented as mean ± standard error of the mean (SEM) in tables and graphs, with individual data points also presented in some of the graphs. The overall significance level was set to $p < 0.05$. All experiments included in this thesis have a relatively small sample size, ranging from 6-10, which increases the risk of type II errors, also known as false negatives. We estimated the required sample size based on variance in standard deviation of earlier experiments together with an appropriate power 0.8, which reduces the likelihood of type II errors. In paper I, the difference between groups were analysed using one-way ANOVA. A post-hoc test, Holm-Sidak was used due to multiple comparisons between groups when using different genotypes and comparison against control when using the same genotype. In paper II the difference between individual and

groups were analysed using paired and unpaired Student's t-test, respectively. Lastly, in paper III cells derived from one passage were regarded as n=1. The difference between treatment groups were analysed with paired one-way ANOVA together with Tukey's post hoc test, which is used to compare mean to mean between groups. Post hoc tests are used to explore difference when there are multiple groups in one experiment and reduces the likelihood of making at least one type I error, also called false positive.

Ethical considerations

The experiments were designed according to the guidelines from the Federation of European Laboratory Animal Science Associations (FELASA), EU animal research directive (86/609/EEC), Council of Europe (ETS 123), and the EU directive (2010/63/EU). The local authority of the National Animal Research Authority in Norway approved the ethical protocols (FOTS id: 4772, 7435 and 3946). The 3R's (Replacement, Reduction, and Refinement) have specifically been addressed when designing the study. All mice received chow ad libitum, free access to drinking water, and were housed at 23° C. All experiments took place in our laboratory at the UiT, The Arctic University of Norway. When working with animals we always aimed to minimize harm and stress. In addition, in paper III we replaced animals with a cell line. Unfortunately, there are still many aspects of heart physiology that cannot be elucidated in a cell model and in therapeutic development [122]. Because the scope of this thesis is largely revolved around the development of obesity- or AngII-induced cardiomyopathy, both *in vivo* and *ex vivo* measurements were performed, and we could not replace the use of animals. Acknowledging this, ethically sound experiments were conducted, and the number of animals used was reduced to an absolute minimum, by performing statistical power analysis before starting. We aimed to optimize the conditions for the mice throughout the experiment starting with the choice of animal model and assuring proper handling

and familiarisation to experimental environments and procedures. The DIO mice model is far less severe compared to other models of obesity such as the *db*/*db* or *ob*/*ob*, where the mice exhibit both a very rapid onset of obesity and diabetes in addition to increased risk of systemic complications such as subcutaneous inflammation, altered kidney and liver morphology, neuropathy, and lymphoma. Moreover, in paper II, we used low doses of AngII and avoided both overt hypertension and cachexia, which has been reported with higher doses [101,102]. We also included proper score sheets to assess post-operative care, pain identification and clearly defined humane endpoints as described by Baertschi and Gyger 2011 [122]. No animals were removed from the studies due to stress and harm, or due to other unforeseen events.

Summary of results

Paper I. NADPH Oxidase 2 Mediates Myocardial Oxygen Wasting in Obesity

Anne D. Hafstad, Synne S. Hansen, Jim Lund, Celio X. C. Santos, Neoma T. Boardman, Ajay M. Shah and Ellen Aasum. *Antioxidant* 2020; 9, 171; doi.org/10.3390/antiox9020171 ePub: 2020 February 19.

To investigate whether ablation and pharmacological inhibition of NOX2 would affect the development of HF following DIO, we studied the cardiac consequence of a NOX2 ablation using a global NOX2 knock-out (DIO_{KO}) as well as NOX2 inhibition using apocynin-treatment (DIO_{APO}).

Main findings

- Ablation or inhibition of NOX2 had only subtle systemic effects in DIO mice, with a slight improvement of pro-inflammatory markers in adipose- and liver tissue, as well as minor improvement of glucose tolerance seen with apocynin-treatment.
- Obesity-induced increase in 2-hydroxyethidium (a specific superoxide product) in cardiac tissue was significantly reduced in DIO_{KO} and DIO_{APO} mice.
- Obesity-induced increase in cardiac mitochondrial ROS which was attenuated in DIO_{APO} mice.
- Obesity-induced LV dysfunction, most prominent as diastolic dysfunction was normalized in both DIO_{KO} and DIO_{APO} mice.
- Obesity-induced reduction in mechanical efficiency was significantly improved in both DIO_{KO} and DIO_{APO} mice.
- Obesity-induced myocardial oxygen wasting in unloaded hearts ($MVO_{2unloaded}$) was improved in both DIO_{KO} and DIO_{APO} mice. In DIO_{KO} mice, this reduction was associated with reduced oxygen expenditure for ECC (MVO_{2ECC}).
- Inhibiting NOX2 did not influence myocardial substrate oxidation rates.

- Obesity had only modest effects on cardiac mitochondrial function. Nevertheless, the respiratory coupling ratio was significantly higher in DIO_{APO} as compared to DIO when using palmitoyl-carnitine as a substrate.

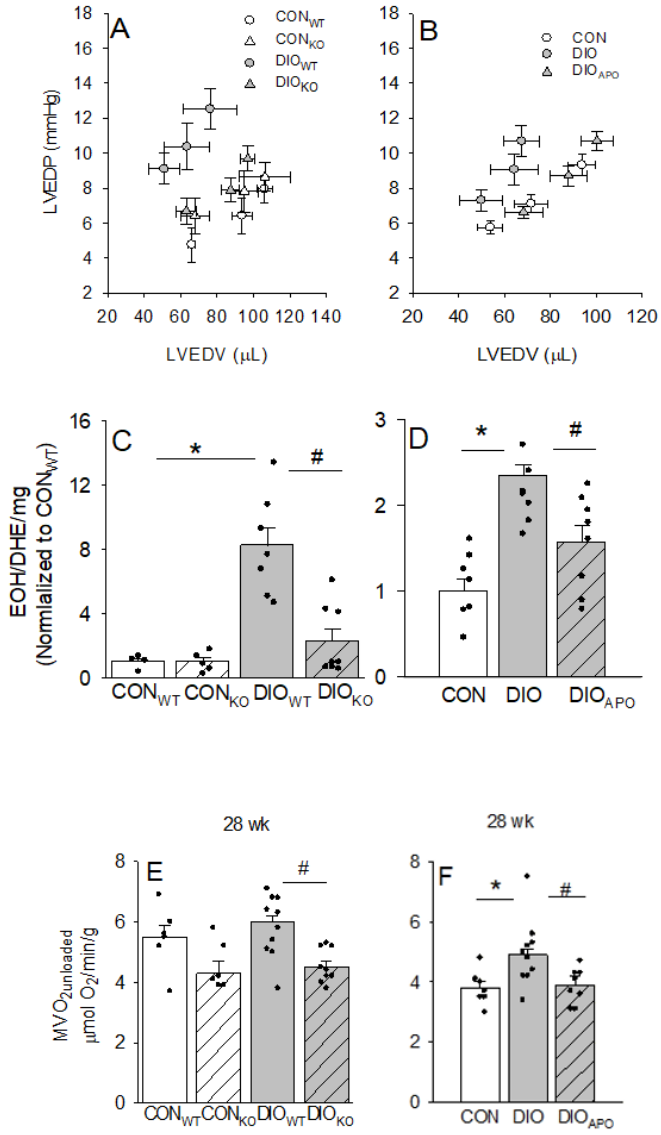

Figure 5: Main findings in paper I. **A-B**: Steady state left ventricular end-diastolic volumes (LVEDV) and pressures (LVEDP) at three different workloads (preload: 4.6 and 8 mmHg and afterload: 50mmHg). **C-D**: Reactive oxygen species-product hydroxyethidium (EOH) per dihydroethidium (DHE) consumed in cardiac tissue. **E-F**: Myocardial oxygen consumption in mechanically unloaded hearts ($MVO_{2unloaded}$). Diet-induced obese C57Bl/6J mice (DIO), wild type (DIO_{WT}), apocynin-treated (DIO_{APO}), NOX2 knock-out (DIO_{KO}). Lean mice were included as controls (CON, CON_{WT} and CON_{KO}). Data are expressed as single values and mean ± SEM *p <0.05 CON vs. DIO within same genotype, # $p < 0.05$ DIO_{WT} vs. DIO_{KO} and DIO vs. DIO_{APO}.

Paper II. Overexpression of NOX2 Exacerbates AngII-Mediated Cardiac Dysfunction and Metabolic Remodelling

Synne S. Hansen* and Tina M. Pedersen*, Julie Marin, Neoma T. Boardman, Ajay M. Shah, Ellen Aasum and Anne D. Hafstad. *Antioxidant* 2022; 11, 143; doi.org/10.3390/antiox11010143 ePub: 2022 January 10.

One of the detrimental effects of AngII in development of HF has been shown to be associated with its activation of NOX2 and subsequently oxidative stress. To study the direct effects of AngII on the heart, mice were treated with a non-pressor dose (50 ng/kg/min, $AngII_{50}$) and a slow pressor dose (400ng/kg/min, $AngII_{400}$). To further elucidate the role of NOX2, we included mice with a cardiomyocyte specific overexpression of NOX2 (csNOX2 TG).

Main findings

- $AngII_{50}$- and $AngII_{400}$-treatments did neither influence body-weight development nor induce systemic changes in non-TG mice. There was a minor increase in mean arterial blood pressure following $AngII_{400}$-treatment in csNOX2 TG mice.
- While $AngII_{50}$-treatment did not induce LV structural or functional changes, $AngII_{400}$-treatment induced hypertrophy without evident LV dysfunction.
- In csNOX2 TG mice, $AngII_{400}$-treatment induced an eccentric cardiac hypertrophy and caused *in vivo* systolic as well as diastolic LV dysfunction.
- In csNOX2 TG mice, $AngII_{400}$-treatment induced a metabolic switch with increased myocardial glucose oxidation rates and a tendency towards reduced palmitate oxidation rates. A similar switch was not evident following $AngII_{50}$ or $AngII_{400}$-treatments of non-TG animals.
- In csNOX2 TG mice, $AngII_{400}$-treatment led to a reduction in basal- and ROX rates in samples of ventricular tissue, indicating altered mitochondrial function.

- Interestingly, although hearts from the $AngII_{50}$-treatment group displayed decreased mechanical efficiency, as well as a borderline significant increase in $MVO_{2unloaded}$, this was not evident following $AngII_{400}$-treatment in neither non-TG nor csNOX2 TG mice.

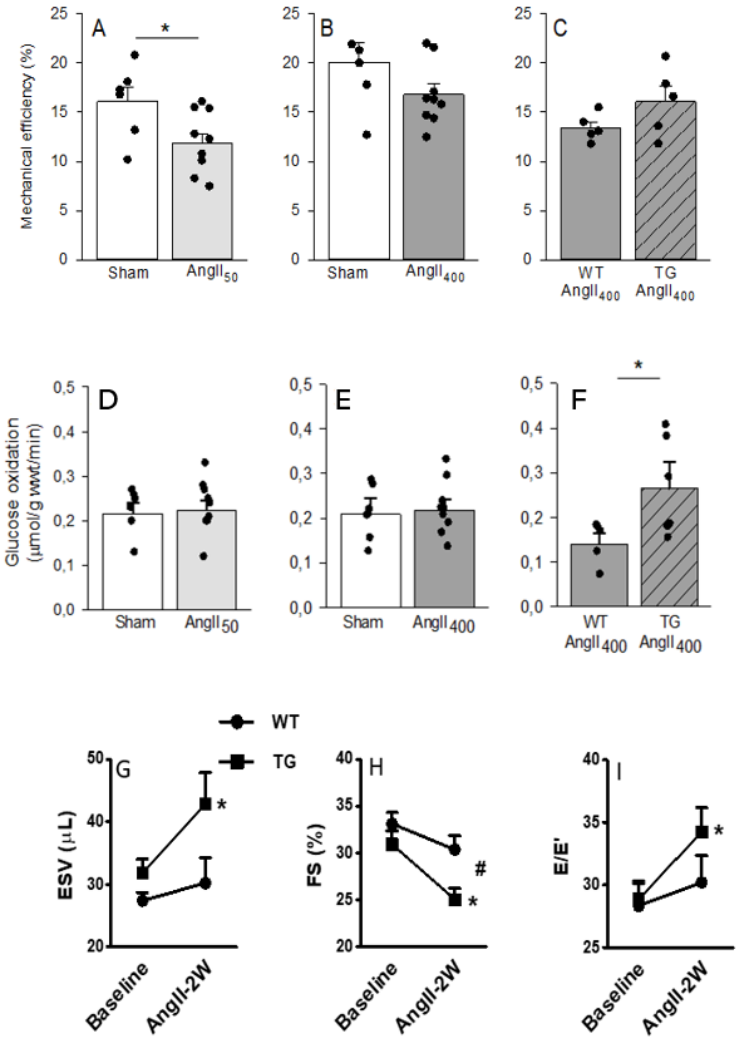

Figure 6. Main findings in paper II. **A-C**: Left ventricular (LV) mechanical efficiency and **D-F**: myocardial glucose oxidation rates measured in isolated perfused hearts from C57BL/6J, wild-type (WT) and csNOX2 transgenic (TG) mice treated for two weeks with micro-osmotic pumps containing either saline (sham), 50 or 400ng/kg/min angiotensin II ($AngII_{50}$ and $AngII_{400}$) **G**: LV End-Systolic Volume (ESV), **H**: LV Fractional Shortening (FS) and **I**: ratio of velocity of early LV filling to early diastolic mitral annular velocity (E/E), measured with echocardiography. Data are presented as single values and mean ± SEM of n=4-7. *p < 0.05 vs. sham or WT, #p < 0.05 vs. baseline.

Paper III. Hydrolyzed Wax Ester from Calanus Oil Protects H9c2 Cardiomyoblasts from Palmitate-Induced lipotoxicity

Synne S. Hansen[1]*, Kirsten M. Jansen[1]*, Kenneth B. Larsen, Anne D. Hafstad, Ragnar L. Olsen, Terje S. Larsen and Ellen Aasum. *Manuscript*

Palmitate is the most abundant dietary FA; however, an excessive load of palmitate is known to cause lipotoxicity in cardiomyoblasts. Dietary supplementation with a marine oil derived from the crustacean Calanus Finmarchicus has previously been found to reduce inflammation [83] and improve post-ischemic cardiac recovery [84] in DIO mice. To examine whether this supplementation could have a direct protective effect on cardiomyoblasts, H9c2 cells subjected to palmitate-induced nutritional stress were co-incubated with WE_H from Calanus oil.

Main findings

- Palmitate-treatment (100 μM) led to approximately 80% cell death in H9c2 cells after 20 hours which was abolished by co-treating with WE_H (10 μM).
- Palmitate-treatment induced ER stress in H9c2 cells, seen as increased expression as well as nuclear translocation of ER stress marker CHOP, which was also markedly reduced by co-treating with WE_H.
- Palmitate-treatment caused impaired autophagic flux, seen as a reduction in the accumulation of autophagosome marker LC3B and selective autophagy receptor p62, which was partly restored by co-treating with WE_H.
- WE_H did not affect the palmitate uptake in the H9c2 cells or inhibit palmitate-induced ROS production.

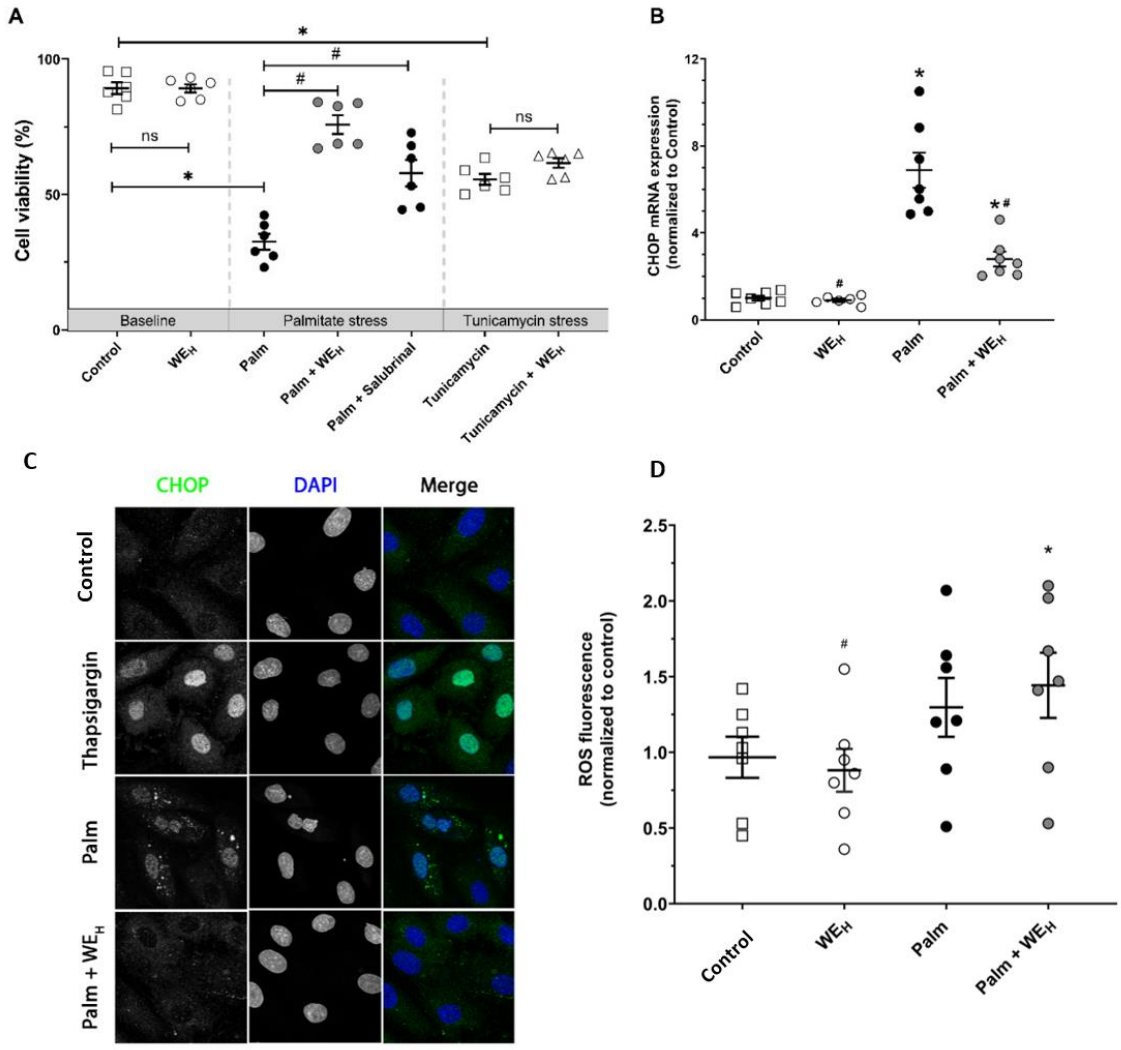

Figure 7: Main findings in paper III. **A-C**: Effect of hydrolysed wax ester (WE_H) from Calanus oil and ER stress inhibition and induction in H9c2 cells. The cells were incubated with 100 μM palmitate (Palm) and 10 μM WE_H. Ethanol treated cells were included as controls. **A**: Cell viability assessed with Live Cell Images following 20-hour incubation with Palm and WE_H. Cells were also incubated in the presence of 60 μM salubrinal (ER stress inhibitor) or 2.5 μg/mL tunicamycin (ER stress inducer) as indicated. **B**: The mRNA expression of the CHOP gene in cells incubated with Palm and WE_H for 6 hours. **C:** The nuclear translocation of CHOP in cells incubated with Palm and WE_H for 15 hours. Cells were also incubated in the presence of 1 μM thapsigargin (ER stress inducer) as positive controls. **D:** ROS measurement in cells treated for 6 hours with Palm, WE_H or a combination of the two with redox sensitive probe, DFCDA. Data are single values and mean ± SEM. * $p<0.05$ vs. control; # $p<0.05$ vs palm.

General discussion

The pathophysiology behind the development of HF is multifactorial and complex. Oxidative stress is suggested to be a central component in the development of HF, and redox signalling has been shown to influence many of the proposed mechanisms that may lead to inefficient hearts. These include processes related to substrate utilization [123], calcium handling [124] and mitochondrial function [125]. Although the mitochondria is the main producer of ROS in the cardiomyocyte, the NOXs are among the major ROS-producing enzymes, and these enzymes have been shown to be involved in the pathogenesis of several types of HF [54]. One aim in this thesis was therefor to investigate the role of NOX2 in obesity-induced ventricular dysfunction, as well as changes in cardiac energetics and metabolism.

Models of obesity-induced heart failure

Paper I include DIO mice models fed either HFD or WD for a total of 28 weeks. Both diets resulted in obesity with insulin resistance and increased adipose inflammations as previously reported [14,21]. In accordance with these studies, we also confirmed cardiometabolic phenotype with increased reliance on FAO, oxidative stress, inefficiency, and development of a mild dysfunction. Our data also confirms previous reports showing that a switch towards increased myocardial FAO precedes the development of LV dysfunction in obese models [30,32,53]. While HFD produced mainly a diastolic dysfunction [21,83], WD produced an additional systolic dysfunction [14]. The WD contains a high content of fructose which has been shown to be especially detrimental in development of obesity due to leptin resistance [126]. Although the direct effects of elevated leptin on the heart is still not fully elucidated, it has been suggested to cause both increased inflammation and elevated FAO, as well as contribute to structural remodelling in the heart [127].

The effects of NOX2 inhibition on myocardial oxidative stress in obesity

In line with previous studies [14,19,21,65] , both HFD and WD caused increased cardiac oxidative stress. Although an increase in NOX4 activity has been reported in in diabetes-induced HF [75], we did not find any increase in H_2O_2 assessed by ethidium which is the main product of NOX4 [54]. This indicates that NOX4 was not a central producer of oxidative stress in our model, which also corroborates with the literature where increased NOX2 activity is reported to be found in cardiac tissue from both obese, type I [60,61] and type II diabetic models [64,65].

The cardiac superoxide production was reduced in both the DIO_{KO} and DIO_{APO}, which is in line with other chronic animal studies of obesity and diabetes using different strategies to reduce NOX2 activity in the heart [64,65]. Interestingly, the obesity-induced increase in mitochondrial ROS production was abolished following apocynin-treatment although this compound in theory should specifically reduce the NOX2 activity in the plasma membrane. Reduced mitochondrial ROS production following apocynin-treatment might be a consequence of inhibiting the NOX2-mediated ROS-induced ROS-release, which has previously been described in models of high lipid load [63], as well as hyperglycaemic stress [57]. In our study we found that both ablation and inhibition of NOX2 improved LV function in DIO mice, results that are in coherence with previous studies linking reduced NOX2 activity to attenuation of LV dysfunction in obese and diabetic models [64,128].

The effects of NOX2 inhibition on obesity-induced myocardial oxygen wasting

In the present thesis we were able to demonstrate a role for NOX2 in obesity-induced mechanical inefficiency, as hearts from DIO_{KO} and DIO_{APO} mice showed increase efficiency, accompanied by a reduced $MVO_{2unloaded}$. Although obesity is known to cause reduced cardiac mechanical efficiency [14,20,21,129], and to increased MVO_2 for non-mechanical processes such as BM and ECC [14,21]. The exact mechanisms behind oxygen wasting effects of obesity and diabetes are not fully elucidated. Increased FA

load and the dependency on FAO has been considered as key contributors to the pathogenesis [14,20,63,129], as lipids are known to induce intracellular effects that may increase oxygen costs of ATP-production due to high FAO [63], increased mitochondrial uncoupling [20,125] as well as induction of futile cycling [130]. The cardiac metabolic switch towards increased FAO seen in DIO mice following 18 weeks of WD was not affected by NOX2 inhibition although the mechanical efficiency was improved at this time-point. This implies that the improved mechanical efficiency and oxygen-sparing effects of reduced NOX2 activity were not linked to altered myocardial FAO.

Increased MVO_2 has been proposed to be associated with impaired mitochondrial function in obesity which could partly explain increased MVO_{2BM}. In the present thesis we found a mild mitochondrial dysfunction with a tendency of decreased respiratory capacity and signs of decreased mitochondrial coupling in DIO mice, which is in line with the findings of several other studies [14,20,63]. It should be noted that apocynin-treatment improved respiratory coupling ratio in mitochondria from DIO_{APO} mice, which could be linked to a reduced ROS-mediated activation of mitochondrial uncoupling proteins [125] and consequently reduced MVO_{2BM}.

Although not addressed in the current study, obesity and diabetes are associated with impaired myocardial calcium handling, including increased calcium leak through the ryanodine receptor (RyR) [17,62,131,132], altered activity through Ca^{2+}-ATPase2 [17] and activation of Ca^{2+}/Calmodulin-dependent protein kinase (CaMKII) [62]. Impaired calcium handling is likely to contribute to the observed obesity-induced increase in MVO_{2ECC} [34,35]. NOX2 inhibition and ablation reduced MVO_{2ECC} in hearts of both DIO_{KO} and DIO_{APO} which might be linked to improved calcium handling as NOX2 inhibition has previously been shown to alter cellular calcium handling by reducing the leak of calcium through the RyR [62,124], as well as to impact CaMKII activity [62].

Are the beneficial effects of reducing myocardial NOX2 activity related to systemic changes?

The effects we observed in the heart following NOX2 ablation and/or inhibition could either be direct effects or be secondary to systemic effects. Although Costford and colleagues [94] reported adverse effect in diet-induced obese NOX2 KO mice, NOX2 ablation and inhibition has generally been demonstrated to have beneficial effects on obesity-induced systemic changes [95,133-135]. The systemic changes in DIO_{KO} and DIO_{APO} were very subtle and thus were not likely to have any major direct impact on the pathophysiology of the heart. Obesity is however also associated with increased activation of the RAAS. Unfortunately, plasma levels of AngII or aldosterone were not measured in this study, and we can therefore not exclude potential systemic effects of these hormones on the heart. In hearts from a model of type 2 diabetes (*db*/*db* mice), elevated levels of NOX2 and $p22^{phox}$ have been shown to be attenuated by the AngII receptor blocker candesartan, which was accompanied by reduced cardiac superoxide levels and fibrosis [77].

Systemic changes in a model of angiotensin II-induced heart failure

Although AngII plays an important role in development of HF by inducing hypertension, it has also been shown to have direct effects on the cardiomyocyte [7,136,137], including being a potent activator of NOX2 [77,138]. In paper II, the aim was to investigate the direct cardiac effects of AngII, and mice were therefore treated with very low doses of AngII (50 or 400 ng/kg/min, $AngII_{50}$ and $AngII_{400}$) to avoid the comorbidities associated with hypertension. We also examined a TG model with cardiomyocyte-specific NOX2 overexpression to investigate whether increased NOX2 activity would aggravate the cardiac effects of AngII-treatment.

$AngII_{50}$- and $AngII_{400}$-treatment did not influence body weight development, confirming that these doses did not cause cachexia [103] which has previously been

reported following high pressor doses of AngII [139]. The slow pressor $AngII_{400}$ dose resulted in a subtle increase in blood pressure following two weeks of treatment in both csNOX2 TG and non-TG mice. However, the magnitude (1-3%) of the increase in blood pressure is not likely to be relevant in terms of cardiac remodelling. The American College of Cardiology and the American Heart Association have developed clinical guidelines for hypertension, where stage 1 hypertension is defined as being > 130-139 mmHg systolic and/or > 80-89 mmHg diastolic pressure [140]. This is an approximate increase of 10% above the normal range. In addition, they state that most patients (70%) who display stage 1 hypertension do not qualify for drug therapy. The fact that $AngII_{400}$ did cause cardiac hypertrophy, support a direct hypertrophic effect of AngII on the heart independent of hypertension [102,141].

Direct effects of angiotensin II on cardiac metabolism and function

Interestingly, the non-pressor dose ($AngII_{50}$) caused mechanical inefficiency, primarily due to increased MVO_2 as cardiac function was not affected. Similar to our findings in paper I, changes in substrate utilization did not seem to play a role in this oxygen wasting effect as $AngII_{50}$ was not associated with altered myocardial substrate oxidation rates. It has previously been reported that a similar treatment (a non-pressure dose of AngII) induced mitochondrial uncoupling in skeletal muscle in mice, which could suggest an impact of $AngII_{50}$ on mitochondrial efficiency [103]. Mitochondrial uncoupling could potentially increase MVO_2 for several processes in the cardiomyocyte. Although not significant, we also found a borderline ($p=0.08$) increase in $MVO_{2unloaded}$ following $AngII_{50}$-treatment. Moreover, there was also a trend towards increased oxygen consumption in the basal and the ROX respiration states measured in the LV tissue samples. It should be noted however that these experiments were performed on previously frozen tissue which may impact mitochondrial integrity and consequently processes such as uncoupling of the mitochondrial membranes.

Despite indications of increased MVO_2 and myocardial remodelling, we found, to our surprise, that increasing the dose to $AngII_{400}$ did not lead to impairment in mechanical efficiency in isolated perfused hearts from neither non-TG nor csNOX2 TG mice. This might indicate a transient oxygen wasting effect of AngII-treatment in the myocardium preceding LV remodelling. Previous studies examining the cardiac functional consequence of treatment with low doses of AngII have shown varied results, where both increased [68], unaltered [103] or impaired [46,51] LV function have been reported. Although we could not find signs of reduced LV function using neither $AngII_{50}$ nor $AngII_{400}$ in non-TG mice, the $AngII_{400}$-treated csNOX2 TG mice did displayed signs of eccentric hypertrophy with both diastolic and systolic LV dysfunction, in agreement with a previous study using the same strain of TG mice [68]. Our data therefore support the notion that oxidative stress is a causative factor in AngII-mediated HF [7].

The effect of increasing NOX2 activity on metabolic remodelling in angiotensin II-induced heart failure

Although several studies have shown that interventions to prevent or reverse a shift of substrate utilization is beneficial in terms of impeding or regressing the progression of HF [26], it is still unclear whether substrate utilization *per se* causes adverse effects. Interestingly, the csNOX2 TG mice showed signs of cardiac metabolic remodelling with a switch towards increased dependency on glucose oxidation for energy production. Downregulation of myocardial FAO and accelerated glucose oxidation have previously been reported in several types of HF, including; pacing-induced HF [142], idiopathic dilated cardiomyopathy [143], following myocardial infarction [144] and in AngII-induced HF [48,49]. The switch towards glucose utilization is regarded as a remodelling towards a more foetal metabolic phenotype [16] and it has been suggested to be an adaptive change, as glucose is a more efficient substrate compared to FA. However, a complete switch

from only glucose oxidation to only FAO should only cause a 12% increased MVO_2 [145], suggesting other mechanisms to be important in determining cardiac efficiency. Although not a significant finding in paper II, impaired myocardial FAO is a consistent finding in several forms of HF [16], and it is believed to contribute to the spiralling deterioration of energy production and the consequent energy deficiency observed in end-stage failing heart [146].

Although we did not find impaired efficiency in the $AngII_{400}$-treated csNOX2 TG mice, we cannot exclude that these hearts are energy deficient. In cardiac tissue from $AngII_{400}$-treated csNOX2 TG mice, we observed signs of reduced oxidative capacity including reduced oxygen consumption rate (OCR) for basal and ROX, although OCR through complex I and complex II did not seem to be impaired. Although these data are hard to interpret, they could suggest that cardiac mitochondria are somewhat more efficient in these $AngII_{400}$-treated csNOX2 TG mice at this timepoint, or that they are in a transitional state towards impaired oxidative capacity with reduced ATP-production. Mechanistic studies have indeed shown that myocardial ROS is associated with reduced mitochondrial ATP-production [52].

Our findings of myocardial metabolic remodelling in the AngII-treated csNOX2 TG mice fits well with the reported findings of long term AngII-exposure in TG mice with cardiac-specific overexpression of angiotensinogen. In this study, mice showed an age-specific decline in protein expression of enzymes involved in FAO (mCPT-1 and MCAD), increased mRNA expression of glucose transporters (*glut 1*) and reduced myocardial FAO rates [47]. In coherence with our findings, the metabolic remodelling in this study did not occur until the animals also displayed signs of HF [47]. Our results suggest that cardiac remodelling due to AngII-stimulation is aggravated by elevated NOX2-induced signalling and elevated myocardial ROS. This is in support of another study by Pellieux and co-workers who described the AngII-mediated decrease in myocardial FAO rates to be attenuated by inhibition of ROS

production [48]. Although the mechanisms behind the metabolic remodelling in AngII-induced HF are not known, we found subtle transcriptional mRNA changes in contrast to the overt long-term metabolic reprogramming of *cpt-1* and *mcad* mRNA observed by Pellieux [47]. However, changes of protein levels are not always in coherence with the regulation of mRNA levels of metabolic enzymes [47] and post-translational changes may indeed also alter enzymatic activity, thus affecting metabolic fluxes. Although not extensively studied in HF, metabolic enzymes can be post-translational redox-regulated [147], and cardiac-specific NOX4-induced elevation of H_2O_2 have been shown to induce metabolic remodelling also in the absence of cardiac stressors [73].

The protective role of poly-unsaturated fatty acids in cardiac lipotoxicity

Excessive circulating FAs may have adverse effects on the myocardium. Lipotoxicity is evident following both acute, and long-term cardiac exposure to high lipids. The mechanisms leading to adverse effects may include accumulation of lipid intermediates [27,148] which can cause disturbances in cellular functions including oxidative stress [66,148,149], apoptosis[66,149], ER stress [27,45,66] and impaired autophagic flux [45,150]. The increased accumulation of lipid intermediates has been linked to the activation of PKC, NOX2 and oxidative stress [62,63]. These adverse effects of FAs are particularly linked to saturated FAs, such as palmitate, which is the most common saturated long-chain FA. Unsaturated FA, as well as PUFAs are less toxic and may even induce cardioprotective effects [84,151,152], however, the underlying mechanisms are not clear. Supplementation of the PUFA-rich Calanus oil and WE from calanus oil have been shown to improve insulin resistance, reduce abdominal fat and adipose tissue inflammation [83,153], and improved LV ischemic recovery in DIO mice [84]. The aim of paper II was therefore to investigate a potential protective effect of a WE_H on lipotoxicity in palmitate exposed H9c2 cardiomyoblasts.

In line with the notion of the cardioprotective effects of Calanus [84] we did indeed observe a very potent protective effect of WE_H in terms of completely abolishing the palmitate-induced cell death after 20 h of palmitate exposure. This supports previous claims that unsaturated FAs and PUFAs exhibit protective properties against palmitate-induced apoptosis in cells [154]. Our data also show WE_H to exhibit protective properties in reducing palmitate-induced ER stress and restoring impaired autophagic flux. These results could support the potential value of restoring normal autophagic activity as a treatment of lipotoxic cardiomyopathy, as suggested by Park et. al. [45].

Similar to previously reports [19,27,62,66,148], palmitate caused a significant increase in endogenous ROS. As palmitate-induced ROS and ER stress have previously been shown to be reduced by inhibition of NOX2 [63,66], and PUFA has been suggested to have ROS scavenging antioxidant properties [80], we were surprised to find that co-treatment with WE_H did not influence ROS production in palmitate-treated cells. Interestingly, data from cells treated with the WE_H alone showed a borderline significant decrease in ROS compared to vehicle cells which might indicate a slight ROS scavenging effect of WE_H, as previously described [80].

Although we have yet to unravel the exact mechanism behind the protective effect of WE_H, we are currently exploring some options. Unsaturated FAs seems to be more efficiently oxidized compared to saturated FAs which might explain why it appears to have no negative impact on the cardiomyocyte [148]. Thus, we can speculate that the WE_H may increase the overall FAO thereby reducing the accumulation of toxic lipid intermediates. Lipid droplets (LDs) consist of neutral lipid deposit, surrounded by monolayer of amphipathic lipids that create a stable emulsion consisting mainly of triglycerides [155]. Incubation with unsaturated FA markedly increases LD formation, in contrast to this, cells incubated with saturated FA show hardly any cytosolic LDs [154]. The formation of LDs inhibit sequestration of FAs [156] and it is

reason to believe that this is one of the protective effects of unsaturated FAs in palmitate-treated cells. For this reason, in future studies we want to investigate both the effect of WE_H on substrate oxidation as well as the effect on LD formation in palmitate-treated cells.

Concluding remarks

Although metabolic remodelling is well established in HF, the underlying mechanisms, and the consequence of this remain ambiguous. In this thesis, we were able to show that NOX2 play an important role in both nutritional and hormonal cardiac stress, by affecting cardiac energetics. This effect was found to precede changes in myocardial substrate utilization, ventricular remodelling, and the impairment of ventricular function. While inhibiting NOX2 was found to attenuate obesity-induced impairment of LV efficiency and function, increased NOX2 signaling aggravated the detrimental effects of AngII-treatment with regard to LV function and metabolic remodelling. Although impaired efficiency preceded the development of ventricular dysfunction in AngII-induced HF, altered substrate utilization did not occur before impaired cardiac function, contrasting metabolic remodelling that is observed during obesity-induced HF. Signs of impaired oxidative capacity in AngII-mediated HF, and a trend towards increased oxidative capacity following NOX2 inhibition in obesity-induced HF support the notion that oxidative stress plays a role in the transition to an energy-depleted heart. Although we were not able to measure the energetic status of these hearts, energetic imbalance limits the contractile reserve, leading to contractile dysfunction and the loss of inotropic reserve in HF.

In clinical trials, preventing oxidative stress utilizing exogenous antioxidants as therapeutic treatments of cardiovascular diseases have been largely unsuccessful [157,158]. Targeting specific NOXs has therefore been suggested as a potential treatment [159-161]. However, the NOX-inhibitors currently available are non-specific

and not isoform-selective, and in addition, many of them have been shown to act as ROS scavengers [161,162]. Consequently, long-term treatments may inhibit the beneficial effects of NOXs in terms of redox signaling. As Elbatreek and colleagues reflect on in their review [162], reducing NOX activity might be more appropriate in acute disease versus its use in preventative measures. In summary, optimization of the current NOX inhibitors, improving isoform selectivity, in addition to more clinical trials are necessary before NOX-inhibition can be considered as a treatment option.

The wax-esters from Calanus oil exhibited profound protective effects in terms of cell survival, ER stress and autophagic flux in a cardiomyoblast model of palmitate-induced lipotoxicity. This did not seem to be mediated through reduced oxidative stress as we had anticipated. A cell model of nutritional-induced HF is however very different from obesity-induced HF in animal models and patients, making it hard to compare exact pathophysiological mechanisms. More research is needed to reveal the full mechanisms involved in the cardioprotective effects, of this oil.

References

1. Bui, A.L.; Horwich, T.B.; Fonarow, G.C. Epidemiology and risk profile of heart failure. *Nature Reviews Cardiology* **2011**, *8*, 30.
2. Ho, K.K.; Pinsky, J.L.; Kannel, W.B.; Levy, D. The epidemiology of heart failure: the Framingham Study. *Journal of the American College of Cardiology* **1993**, *22*, A6-A13.
3. Roger, V.L. Epidemiology of heart failure. *Circulation Research* **2013**, *113*, 646-659.
4. Francis, G.S. Pathophysiology of chronic heart failure. *The American Journal of Medicine* **2001**, *110*, 37-46.
5. Kemp, C.D.; Conte, J.V. The pathophysiology of heart failure. *Cardiovascular Pathology* **2012**, *21*, 365-371.
6. Kumar, V.; Abbas, A.K.; Fausto, N.; Aster, J.C. *Robbins and Cotran pathologic basis of disease, professional edition e-book*; Elsevier health sciences: 2014.
7. Zablocki, D.; Sadoshima, J. Angiotensin II and oxidative stress in the failing heart. *Antioxidants & Redox Signaling* **2013**, *19*, 1095-1109.
8. Kenchaiah, S.; Evans, J.C.; Levy, D.; Wilson, P.W.; Benjamin, E.J.; Larson, M.G.; Kannel, W.B.; Vasan, R.S. Obesity and the risk of heart failure. *New England Journal of Medicine* **2002**, *347*, 305-313.
9. Verma, S.; Hussain, M.E. Obesity and diabetes: an update. *Diabetes & Metabolic Syndrome: Clinical Research & Reviews* **2017**, *11*, 73-79.
10. Hossain, P.; Kawar, B.; El Nahas, M. Obesity and diabetes in the developing world—a growing challenge. *New England Journal of Medicine* **2007**, *356*, 213-215.
11. Swinburn, B.A.; Sacks, G.; Hall, K.D.; McPherson, K.; Finegood, D.T.; Moodie, M.L.; Gortmaker, S.L. The global obesity pandemic: shaped by global drivers and local environments. *The Lancet* **2011**, *378*, 804-814.
12. Gollmer, J.; Zirlik, A.; Bugger, H. Established and emerging mechanisms of diabetic cardiomyopathy. *Journal of Lipid and Atherosclerosis* **2019**, *8*, 26-47.
13. Rubler, S.; Dlugash, J.; Yuceoglu, Y.Z.; Kumral, T.; Branwood, A.W.; Grishman, A. New type of cardiomyopathy associated with diabetic glomerulosclerosis. *American Journal of Cardiology* **1972**, *30*, 595-602.
14. Hafstad, A.D.; Lund, J.; Hadler-Olsen, E.; Höper, A.C.; Larsen, T.S.; Aasum, E. High-and moderate-intensity training normalizes ventricular function and mechanoenergetics in mice with diet-induced obesity. *Diabetes* **2013**, *62*, 2287-2294.
15. How, O.-J.; Aasum, E.; Severson, D.L.; Chan, W.A.; Essop, M.F.; Larsen, T.S. Increased myocardial oxygen consumption reduces cardiac efficiency in diabetic mice. *Diabetes* **2006**, *55*, 466-473.
16. Stanley, W.C.; Recchia, F.A.; Lopaschuk, G.D. Myocardial substrate metabolism in the normal and failing heart. *Physiological Reviews* **2005**, *85*, 1093-1129.
17. Belke, D.D.; Swanson, E.A.; Dillmann, W.H. Decreased sarcoplasmic reticulum activity and contractility in diabetic db/db mouse heart. *Diabetes* **2004**, *53*, 3201-3208.
18. Xu, J.; Wang, G.; Wang, Y.; Liu, Q.; Xu, W.; Tan, Y.; Cai, L. Diabetes-and angiotensin II-induced cardiac endoplasmic reticulum stress and cell death: metallothionein protection. *Journal of cellular and molecular medicine* **2009**, *13*, 1499-1512.
19. Jaishy, B.; Zhang, Q.; Chung, H.S.; Riehle, C.; Soto, J.; Jenkins, S.; Abel, P.; Cowart, L.A.; Van Eyk, J.E.; Abel, E.D. Lipid-induced NOX2 activation inhibits autophagic flux by impairing lysosomal enzyme activity. *Journal of Lipid Research* **2015**, *56*, 546-561.
20. Boudina, S.; Sena, S.; Theobald, H.; Sheng, X.; Wright, J.J.; Hu, X.X.; Aziz, S.; Johnson, J.I.; Bugger, H.; Zaha, V.G. Mitochondrial energetics in the heart in obesity-related diabetes: direct evidence for increased uncoupled respiration and activation of uncoupling proteins. *Diabetes* **2007**, *56*, 2457-2466.

21. Lund, J.; Hafstad, A.D.; Boardman, N.T.; Rossvoll, L.; Rolim, N.P.; Ahmed, M.S.; Florholmen, G.; Attramadal, H.; Wisløff, U.; Larsen, T.S. Exercise training promotes cardioprotection through oxygen-sparing action in high fat-fed mice. *American Journal of Physiology-Heart and Circulatory Physiology* **2015**, *308*, 823-829.
22. Hansen, S.S.; Aasum, E.; Hafstad, A.D. The role of NADPH oxidases in diabetic cardiomyopathy. *Biochimica et Biophysica Acta (BBA)-Molecular Basis of Disease* **2018**, *1864*, 1908-1913.
23. Aasum, E. Myocardial energetics and efficiency. *Heart Metabolism* **2011**, *53*, 4.
24. Randle, P.J. Regulatory interactions between lipids and carbohydrates: the glucose fatty acid cycle after 35 years. *Diabetes/Metabolism Reviews* **1998**, *14*, 263-283.
25. Lopaschuk, G.D.; Ussher, J.R.; Folmes, C.D.; Jaswal, J.S.; Stanley, W.C. Myocardial fatty acid metabolism in health and disease. *Physiological Reviews* **2010**, *90*, 207-258.
26. Doenst, T.; Nguyen, T.D.; Abel, E.D. Cardiac metabolism in heart failure: implications beyond ATP production. *Circulation Research* **2013**, *113*, 709-724.
27. Haffar, T.; Berube-Simard, F.; Bousette, N. Impaired fatty acid oxidation as a cause for lipotoxicity in cardiomyocytes. *Biochemical and Biophysical Research Communications* **2015**, *468*, 73-78, doi:10.1016/j.bbrc.2015.10.162.
28. Abdelmagid, S.A.; Clarke, S.E.; Nielsen, D.E.; Badawi, A.; El-Sohemy, A.; Mutch, D.M.; Ma, D.W. Comprehensive profiling of plasma fatty acid concentrations in young healthy Canadian adults. *PloS One* **2015**, *10*, e0116195.
29. Neubauer, S.; Horn, M.; Cramer, M.; Harre, K.; Newell, J.B.; Peters, W.; Pabst, T.; Ertl, G.; Hahn, D.; Ingwall, J.S. Myocardial phosphocreatine-to-ATP ratio is a predictor of mortality in patients with dilated cardiomyopathy. *Circulation* **1997**, *96*, 2190-2196.
30. Buchanan, J.; Mazumder, P.K.; Hu, P.; Chakrabarti, G.; Roberts, M.W.; Yun, U.J.; Cooksey, R.C.; Litwin, S.E.; Abel, E.D. Reduced cardiac efficiency and altered substrate metabolism precedes the onset of hyperglycemia and contractile dysfunction in two mouse models of insulin resistance and obesity. *Endocrinology* **2005**, *146*, 5341-5349.
31. Mazumder, P.K.; O'Neill, B.T.; Roberts, M.W.; Buchanan, J.; Yun, U.J.; Cooksey, R.C.; Boudina, S.; Abel, E.D. Impaired cardiac efficiency and increased fatty acid oxidation in insulin-resistant ob/ob mouse hearts. *Diabetes* **2004**, *53*, 2366-2374.
32. Peterson, L.R.; Waggoner, A.D.; Schechtman, K.B.; Meyer, T.; Gropler, R.J.; Barzilai, B.; Dávila-Román, V.G. Alterations in left ventricular structure and function in young healthy obese women: assessment by echocardiography and tissue Doppler imaging. *Journal of the American College of Cardiology* **2004**, *43*, 1399-1404.
33. How, O.-J.; Larsen, T.; Hafstad, A.; Khalid, A.; Myhre, E.; Murray, A.; T. Boardman, N.; Cole, M.; Clarke, K.; Severson, D. Rosiglitazone treatment improves cardiac efficiency in hearts from diabetic mice. *Archives of Physiology and Biochemistry* **2007**, *113*, 211-220.
34. Boardman, N.; Hafstad, A.D.; Larsen, T.S.; Severson, D.L.; Aasum, E. Increased O2 cost of basal metabolism and excitation-contraction coupling in hearts from type 2 diabetic mice. *American Journal of Physiology-Heart and Circulatory Physiology* **2009**, *296*, 1373-1379.
35. Boardman, N.T.; Larsen, T.S.; Severson, D.L.; Essop, M.F.; Aasum, E. Chronic and acute exposure of mouse hearts to fatty acids increases oxygen cost of excitation-contraction coupling. *American Journal of Physiology-Heart and Circulatory Physiology* **2011**, *300*, 1631-1636.
36. Finck, B.N.; Lehman, J.J.; Leone, T.C.; Welch, M.J.; Bennett, M.J.; Kovacs, A.; Han, X.; Gross, R.W.; Kozak, R.; Lopaschuk, G.D. The cardiac phenotype induced by PPARα overexpression mimics that caused by diabetes mellitus. *The Journal of Clinical Investigation* **2002**, *109*, 121-130.
37. Fillmore, N.; Mori, J.; Lopaschuk, G. Mitochondrial fatty acid oxidation alterations in heart failure, ischaemic heart disease and diabetic cardiomyopathy. *British Journal of Pharmacology* **2014**, *171*, 2080-2090.

38. How, O.-J.; Aasum, E.; Kunnathu, S.; Severson, D.L.; Myhre, E.S.; Larsen, T.S. Influence of substrate supply on cardiac efficiency, as measured by pressure-volume analysis in ex vivo mouse hearts. *American Journal of Physiology-Heart and Circulatory Physiology* **2005**, *288*, 2979-2985.
39. Dalgas, C.; Povlsen, J.A.; Løfgren, B.; Erichsen, S.B.; Bøtker, H.E. Effects of fatty acids on cardioprotection by pre-ischaemic inhibition of the malate–aspartate shuttle. *Clinical and Experimental Pharmacology and Physiology* **2012**, *39*, 878-885.
40. Gambert, S.; Vergely, C.; Filomenko, R.; Moreau, D.; Bettaieb, A.; Opie, L.H.; Rochette, L. Adverse effects of free fatty acid associated with increased oxidative stress in postischemic isolated rat hearts. *Molecular and Cellular Biochemistry* **2006**, *283*, 147-152.
41. Zou, L.; Li, X.; Wu, N.; Jia, P.; Liu, C.; Jia, D. Palmitate induces myocardial lipotoxic injury via the endoplasmic reticulum stress-mediated apoptosis pathway. *Molecular Medicine Reports* **2017**, *16*, 6934-6939.
42. Makrecka-Kuka, M.; Liepinsh, E.; Murray, A.J.; Lemieux, H.; Dambrova, M.; Tepp, K.; Puurand, M.; Käämbre, T.; Han, W.H.; de Goede, P. Altered mitochondrial metabolism in the insulin-resistant heart. *Acta Physiologica* **2020**, *228*, e13430.
43. Unger, R.H.; Orci, L. Diseases of liporegulation: new perspective on obesity and related disorders. *The FASEB Journal* **2001**, *15*, 312-321.
44. Liang, Q.; Kobayashi, S. Mitochondrial quality control in the diabetic heart. *Journal of Molecular and Cellular Cardiology* **2016**, *95*, 57-69.
45. Park, M.; Sabetski, A.; Kwan Chan, Y.; Turdi, S.; Sweeney, G. Palmitate induces ER stress and autophagy in H9c2 cells: implications for apoptosis and adiponectin resistance. *Journal of Cellular Physiology* **2015**, *230*, 630-639.
46. Mori, J.; Zhang, L.; Oudit, G.Y.; Lopaschuk, G.D. Impact of the renin–angiotensin system on cardiac energy metabolism in heart failure. *Journal of Molecular and Cellular Cardiology* **2013**, *63*, 98-106.
47. Pellieux, C.; Aasum, E.; Larsen, T.S.; Montessuit, C.; Papageorgiou, I.; Pedrazzini, T.; Lerch, R. Overexpression of angiotensinogen in the myocardium induces downregulation of the fatty acid oxidation pathway. *Journal of Molecular and Cellular Cardiology* **2006**, *41*, 459-466.
48. Pellieux, C.; Montessuit, C.; Papageorgiou, I.; Lerch, R. Angiotensin II downregulates the fatty acid oxidation pathway in adult rat cardiomyocytes via release of tumour necrosis factor-α. *Cardiovascular Research* **2009**, *82*, 341-350.
49. Choi, Y.S.; de Mattos, A.B.M.; Shao, D.; Li, T.; Nabben, M.; Kim, M.; Wang, W.; Tian, R.; Kolwicz Jr, S.C. Preservation of myocardial fatty acid oxidation prevents diastolic dysfunction in mice subjected to angiotensin II infusion. *Journal of Molecular and Cellular Cardiology* **2016**, *100*, 64-71.
50. Mori, J.; Alrob, O.A.; Wagg, C.S.; Harris, R.A.; Lopaschuk, G.D.; Oudit, G.Y. ANG II causes insulin resistance and induces cardiac metabolic switch and inefficiency: a critical role of PDK4. *American Journal of Physiology-Heart and Circulatory Physiology* **2013**, *304*, 1103-1113.
51. Mori, J.; Basu, R.; McLean, B.A.; Das, S.K.; Zhang, L.; Patel, V.B.; Wagg, C.S.; Kassiri, Z.; Lopaschuk, G.D.; Oudit, G.Y. Agonist-induced hypertrophy and diastolic dysfunction are associated with selective reduction in glucose oxidation: a metabolic contribution to heart failure with normal ejection fraction. *Circulation: Heart Failure* **2012**, *5*, 493-503.
52. Tsutsui, H.; Kinugawa, S.; Matsushima, S. Oxidative stress and heart failure. *American Journal of Physiology-Heart and Circulatory Physiology* **2011**.
53. Hafstad, A.D.; Nabeebaccus, A.A.; Shah, A.M. Novel aspects of ROS signalling in heart failure. *Basic Research in Cardiology* **2013**, *108*, 1-11.
54. Zhang, M.; Perino, A.; Ghigo, A.; Hirsch, E.; Shah, A.M. NADPH oxidases in heart failure: poachers or gamekeepers? *Antioxidants & Redox Signaling* **2013**, *18*, 1024-1041.

55. Lassègue, B.; San Martín, A.; Griendling, K.K. Biochemistry, physiology, and pathophysiology of NADPH oxidases in the cardiovascular system. *Circulation Research* **2012**, *110*, 1364-1390.
56. Zorov, D.B.; Juhaszova, M.; Sollott, S.J. Mitochondrial ROS-induced ROS release: an update and review. *Biochimica et Biophysica Acta (BBA)-Bioenergetics* **2006**, *1757*, 509-517.
57. Balteau, M.; Tajeddine, N.; De Meester, C.; Ginion, A.; Des Rosiers, C.; Brady, N.R.; Sommereyns, C.; Horman, S.; Vanoverschelde, J.-L.; Gailly, P. NADPH oxidase activation by hyperglycaemia in cardiomyocytes is independent of glucose metabolism but requires SGLT1. *Cardiovascular Research* **2011**, *92*, 237-246.
58. Balteau, M.; Van Steenbergen, A.; Timmermans, A.D.; Dessy, C.; Behets-Wydemans, G.; Tajeddine, N.; Castanares-Zapatero, D.; Gilon, P.; Vanoverschelde, J.-L.; Horman, S. AMPK activation by glucagon-like peptide-1 prevents NADPH oxidase activation induced by hyperglycemia in adult cardiomyocytes. *American Journal of Physiology-Heart and Circulatory Physiology* **2014**, *307*, 1120-1133.
59. Huynh, K.; Kiriazis, H.; Du, X.-J.; Love, J.E.; Gray, S.P.; Jandeleit-Dahm, K.A.; McMullen, J.R.; Ritchie, R.H. Targeting the upregulation of reactive oxygen species subsequent to hyperglycemia prevents type 1 diabetic cardiomyopathy in mice. *Free Radical Biology and Medicine* **2013**, *60*, 307-317.
60. Nishio, S.; Teshima, Y.; Takahashi, N.; Thuc, L.C.; Saito, S.; Fukui, A.; Kume, O.; Fukunaga, N.; Hara, M.; Nakagawa, M. Activation of CaMKII as a key regulator of reactive oxygen species production in diabetic rat heart. *Journal of Molecular and Cellular Cardiology* **2012**, *52*, 1103-1111.
61. Shen, E.; Li, Y.; Li, Y.; Shan, L.; Zhu, H.; Feng, Q.; Arnold, J.M.O.; Peng, T. Rac1 is required for cardiomyocyte apoptosis during hyperglycemia. *Diabetes* **2009**, *58*, 2386-2395.
62. Joseph, L.C.; Avula, U.M.R.; Wan, E.Y.; Reyes, M.V.; Lakkadi, K.R.; Subramanyam, P.; Nakanishi, K.; Homma, S.; Muchir, A.; Pajvani, U.B. Dietary saturated fat promotes arrhythmia by activating NOX2 (NADPH Oxidase 2). *Circulation: Arrhythmia and Electrophysiology* **2019**, *12*, e007573.
63. Joseph, L.C.; Barca, E.; Subramanyam, P.; Komrowski, M.; Pajvani, U.; Colecraft, H.M.; Hirano, M.; Morrow, J.P. Inhibition of NAPDH oxidase 2 (NOX2) prevents oxidative stress and mitochondrial abnormalities caused by saturated fat in cardiomyocytes. *PloS one* **2016**, *11*, e0145750.
64. Fukuda, M.; Nakamura, T.; Kataoka, K.; Nako, H.; Tokutomi, Y.; Dong, Y.-F.; Yasuda, O.; Ogawa, H.; Kim-Mitsuyama, S. Ezetimibe ameliorates cardiovascular complications and hepatic steatosis in obese and type 2 diabetic db/db mice. *Journal of Pharmacology and Experimental Therapeutics* **2010**, *335*, 70-75.
65. Gharib, M.; Tao, H.; Fungwe, T.V.; Hajri, T. Cluster differentiating 36 (CD36) deficiency attenuates obesity-associated oxidative stress in the heart. *PloS one* **2016**, *11*, e0155611.
66. Yang, L.; Guan, G.; Lei, L.; Liu, J.; Cao, L.; Wang, X. Oxidative and endoplasmic reticulum stresses are involved in palmitic acid-induced H9c2 cell apoptosis. *Bioscience Reports* **2019**, *39*.
67. Brand, S.; Amann, K.; Schupp, N. Angiotensin II-induced hypertension dose-dependently leads to oxidative stress and DNA damage in mouse kidneys and hearts. *Journal of Hypertension* **2013**, *31*, 333-344.
68. Zhang, M.; Prosser, B.L.; Bamboye, M.A.; Gondim, A.N.; Santos, C.X.; Martin, D.; Ghigo, A.; Perino, A.; Brewer, A.C.; Ward, C.W. Contractile function during angiotensin-II activation: increased Nox2 activity modulates cardiac calcium handling via phospholamban phosphorylation. *Journal of the American College of Cardiology* **2015**, *66*, 261-272.
69. Seshiah, P.N.; Weber, D.S.; Rocic, P.; Valppu, L.; Taniyama, Y.; Griendling, K.K. Angiotensin II stimulation of NAD (P) H oxidase activity: upstream mediators. *Circulation Research* **2002**, *91*, 406-413.

70. Prosser, B.L.; Ward, C.W.; Lederer, W. X-ROS signaling: rapid mechano-chemo transduction in heart. *Science* **2011**, *333*, 1440-1445.
71. Zhang, M.; Brewer, A.C.; Schröder, K.; Santos, C.X.; Grieve, D.J.; Wang, M.; Anilkumar, N.; Yu, B.; Dong, X.; Walker, S.J. NADPH oxidase-4 mediates protection against chronic load-induced stress in mouse hearts by enhancing angiogenesis. *Proceedings of the National Academy of Sciences* **2010**, *107*, 18121-18126.
72. Santos, C.X.; Hafstad, A.D.; Beretta, M.; Zhang, M.; Molenaar, C.; Kopec, J.; Fotinou, D.; Murray, T.V.; Cobb, A.M.; Martin, D. Targeted redox inhibition of protein phosphatase 1 by Nox4 regulates eIF 2α-mediated stress signaling. *The EMBO journal* **2016**, *35*, 319-334.
73. Nabeebaccus, A.; Hafstad, A.; Zoccarato, A.; Eykyn, T.; West, J.; Griffin, J.; Mayr, M.; Shah, A. C Nox4-dependent Reprogramming of Glucose Metabolism and Fatty Acid Oxidation Facilitates Cardiac Adaption to Chronic Pressure-Overload. **2016**.
74. Sciarretta, S.; Volpe, M.; Sadoshima, J. NOX4 regulates autophagy during energy deprivation. *Autophagy* **2014**, *10*, 699-701.
75. Kuroda, J.; Ago, T.; Matsushima, S.; Zhai, P.; Schneider, M.D.; Sadoshima, J. NADPH oxidase 4 (Nox4) is a major source of oxidative stress in the failing heart. *Proceedings of the National Academy of Sciences* **2010**, *107*, 15565-15570.
76. Li, J.; Zhu, H.; Shen, E.; Wan, L.; Arnold, J.M.O.; Peng, T. Deficiency of rac1 blocks NADPH oxidase activation, inhibits endoplasmic reticulum stress, and reduces myocardial remodeling in a mouse model of type 1 diabetes. *Diabetes* **2010**, *59*, 2033-2042.
77. Fukuda, M.; Nakamura, T.; Kataoka, K.; Nako, H.; Tokutomi, Y.; Dong, Y.-F.; Ogawa, H.; Kim-Mitsuyama, S. Potentiation by candesartan of protective effects of pioglitazone against type 2 diabetic cardiovascular and renal complications in obese mice. *Journal of Hypertension* **2010**, *28*, 340-352.
78. Zinkevich, N.S.; Gutterman, D.D. ROS-induced ROS release in vascular biology: redox-redox signaling. *American Journal of Physiology-Heart and Circulatory Physiology* **2011**, *301*, 647-653.
79. Kimura, S.; Zhang, G.-X.; Nishiyama, A.; Shokoji, T.; Yao, L.; Fan, Y.-Y.; Rahman, M.; Suzuki, T.; Maeta, H.; Abe, Y. Role of NAD (P) H oxidase-and mitochondria-derived reactive oxygen species in cardioprotection of ischemic reperfusion injury by angiotensin II. *Hypertension* **2005**, *45*, 860-866.
80. Richard, D.; Kefi, K.; Barbe, U.; Bausero, P.; Visioli, F. Polyunsaturated fatty acids as antioxidants. *Pharmacological Research* **2008**, *57*, 451-455.
81. Zhang, Y.; Yang, X.; Shi, H.; Dong, L.; Bai, J. Effect of α-linolenic acid on endoplasmic reticulum stress-mediated apoptosis of palmitic acid lipotoxicity in primary rat hepatocytes. *Lipids in Health and Disease* **2011**, *10*, 122, doi:10.1186/1476-511x-10-122.
82. Pedersen, A.M.; Vang, B.; Olsen, R.L. Oil from Calanus finmarchicus—composition and possible use: a review. *Journal of Aquatic Food Product Technology* **2014**, *23*, 633-646.
83. Höper, A.C.; Salma, W.; Khalid, A.M.; Hafstad, A.D.; Sollie, S.J.; Raa, J.; Larsen, T.S.; Aasum, E. Oil from the marine zooplankton Calanus finmarchicus improves the cardiometabolic phenotype of diet-induced obese mice. *British Journal of Nutrition* **2013**, *110*, 2186-2193, doi:10.1017/s0007114513001839.
84. Jansen, K.M.; Moreno, S.; Garcia-Roves, P.M.; Larsen, T.S. Dietary Calanus oil recovers metabolic flexibility and rescues postischemic cardiac function in obese female mice. *American Journal of Physiology-Heart and Circulatory Physiology* **2019**, *317*, 290-299.
85. Abdurrachim, D.; Ciapaite, J.; Wessels, B.; Nabben, M.; Luiken, J.J.; Nicolay, K.; Prompers, J.J. Cardiac diastolic dysfunction in high-fat diet fed mice is associated with lipotoxicity without impairment of cardiac energetics in vivo. *Biochimica et Biophysica Acta (BBA)-Molecular and Cell Biology of Lipids* **2014**, *1841*, 1525-1537.

86. Collins, S.; Martin, T.L.; Surwit, R.S.; Robidoux, J. Genetic vulnerability to diet-induced obesity in the C57BL/6J mouse: physiological and molecular characteristics. *Physiology & Behavior* **2004**, *81*, 243-248.
87. Nicholson, A.; Reifsnyder, P.C.; Malcolm, R.D.; Lucas, C.A.; MacGregor, G.R.; Zhang, W.; Leiter, E.H. Diet-induced obesity in Two C57BL/6 substrains with intact or mutant nicotinamide nucleotide transhydrogenase (Nnt) gene. *Obesity* **2010**, *18*, 1902-1905.
88. Zeng, H.; Vaka, V.R.; He, X.; Booz, G.W.; Chen, J.X. High-fat diet induces cardiac remodelling and dysfunction: assessment of the role played by SIRT 3 loss. *Journal of Cellular and Molecular Medicine* **2015**, *19*, 1847-1856.
89. Burke, S.J.; Batdorf, H.M.; Burk, D.H.; Noland, R.C.; Eder, A.E.; Boulos, M.S.; Karlstad, M.D.; Jason Collier, J. db/db mice exhibit features of human type 2 diabetes that are not present in weight-matched C57BL/6J mice fed a western diet. *Journal of Diabetes Research* **2017**, *2017*.
90. Pedersen, T.M.; Boardman, N.T.; Hafstad, A.D.; Aasum, E. Isolated perfused working hearts provide valuable additional information during phenotypic assessment of the diabetic mouse heart. *PLoS One* **2018**, *13*, e0204843, doi:10.1371/journal.pone.0204843.
91. Prpic, V.; Watson, P.M.; Frampton, I.C.; Sabol, M.A.; Jezek, G.E.; Gettys, T.W. Differential mechanisms and development of leptin resistance in A/J versus C57BL/6J mice during diet-induced obesity. *Endocrinology* **2003**, *144*, 1155-1163.
92. Surwit, R.S.; Kuhn, C.M.; Cochrane, C.; McCubbin, J.A.; Feinglos, M.N. Diet-induced type II diabetes in C57BL/6J mice. *Diabetes* **1988**, *37*, 1163-1167.
93. Matthews, D.R.; Hosker, J.; Rudenski, A.; Naylor, B.; Treacher, D.; Turner, R. Homeostasis model assessment: insulin resistance and β-cell function from fasting plasma glucose and insulin concentrations in man. *Diabetologia* **1985**, *28*, 412-419.
94. Costford, S.R.; Castro-Alves, J.; Chan, K.L.; Bailey, L.J.; Woo, M.; Belsham, D.D.; Brumell, J.H.; Klip, A. Mice lacking NOX2 are hyperphagic and store fat preferentially in the liver. *American Journal of Physiology-Endocrinology and Metabolism* **2014**, *306*, 1341-1353.
95. Meng, R.; Zhu, D.-L.; Bi, Y.; Yang, D.-H.; Wang, Y.-P. Apocynin improves insulin resistance through suppressing inflammation in high-fat diet-induced obese mice. *Mediators of Inflammation* **2010**, *2010*.
96. Bedard, K.; Krause, K.-H. The NOX family of ROS-generating NADPH oxidases: physiology and pathophysiology. *Physiological Reviews* **2007**, *87*, 245-313.
97. Stolk, J.; Hiltermann, T.; Dijkman, J.; Verhoeven, A. Characteristics of the inhibition of NADPH oxidase activation in neutrophils by apocynin, a methoxy-substituted catechol. *American Journal of Respiratory Cell and Molecular Biology* **1994**, *11*, 95-102.
98. Heumüller, S.; Wind, S.; Barbosa-Sicard, E.; Schmidt, H.H.; Busse, R.; Schröder, K.; Brandes, R.P. Apocynin is not an inhibitor of vascular NADPH oxidases but an antioxidant. *Hypertension* **2008**, *51*, 211-217.
99. Ellmark, S.H.; Dusting, G.J.; Ng Tang Fui, M.; Guzzo-Pernell, N.; Drummond, G.R. The contribution of Nox4 to NADPH oxidase activity in mouse vascular smooth muscle. *Cardiovascular Research* **2005**, *65*, 495-504.
100. Hauck, L.; Grothe, D.; Billia, F. p21CIP1/WAF1-dependent inhibition of cardiac hypertrophy in response to Angiotensin II involves Akt/Myc and pRb signaling. *Peptides* **2016**, *83*, 38-48.
101. Zhang, Y.; Yan, H.; Guang, G.-c.; Deng, Z.-r. Overexpressed connective tissue growth factor in cardiomyocytes attenuates left ventricular remodeling induced by angiotensin II perfusion. *Clinical and Experimental Hypertension* **2017**, *39*, 168-174.
102. Zhong, J.; Basu, R.; Guo, D.; Chow, F.L.; Byrns, S.; Schuster, M.; Loibner, H.; Wang, X.-h.; Penninger, J.M.; Kassiri, Z. Angiotensin-converting enzyme 2 suppresses pathological hypertrophy, myocardial fibrosis, and cardiac dysfunction. *Circulation* **2010**, *122*, 717-728.

103. Inoue, N.; Kinugawa, S.; Suga, T.; Yokota, T.; Hirabayashi, K.; Kuroda, S.; Okita, K.; Tsutsui, H. Angiotensin II-induced reduction in exercise capacity is associated with increased oxidative stress in skeletal muscle. *American Journal of Physiology-Heart and Circulatory Physiology* **2012**, *302*, 1202-1210.
104. Kawada, N.; Imai, E.; Karber, A.; Welch, W.J.; Wilcox, C.S. A mouse model of angiotensin II slow pressor response: role of oxidative stress. *Journal of the American Society of Nephrology* **2002**, *13*, 2860-2868.
105. Simon, G.; Abraham, G.; Cserep, G. Pressor and subpressor angiotensin II administration two experimental models of hypertension. *American Journal of Hypertension* **1995**, *8*, 645-650.
106. Luther, J.M.; Fogo, A.B. Under pressure—how to assess blood pressure in rodents: tail-cuff? *Kidney International* **2019**, *96*, 34-36.
107. Neely, J.; Liebermeister, H.; Morgan, H. Effect of pressure development on membrane transport of glucose in isolated rat heart. *American Journal of Physiology-Legacy Content* **1967**, *212*, 815-822.
108. Olejnickova, V.; Novakova, M.; Provaznik, I. Isolated heart models: cardiovascular system studies and technological advances. *Medical & Biological Engineering & Computing* **2015**, *53*, 669-678.
109. Barr, R.L.; Lopaschuk, G.D. Methodology for measuring in vitro/ex vivo cardiac energy metabolism. *Journal of Pharmacological and Toxicological Methods* **2000**, *43*, 141-152.
110. Suga, H. Total mechanical energy of a ventricle model and cardiac oxygen consumption. *American Journal of Physiology-Heart and Circulatory Physiology* **1979**, *236*, 498-505.
111. Aasum, E.; Hafstad, A.D.; Larsen, T.S. Changes in substrate metabolism in isolated mouse hearts following ischemia-reperfusion. In *Biochemistry of Diabetes and Atherosclerosis*; Springer: 2003; pp. 97-103.
112. Garedew, A.; Hütter, E.; Haffner, B.; Gradl, P.; Gradl, L.; Jansen-Dürr, P.; Gnaiger, E. High-resolution respirometry for the study of mitochondrial function in health and disease. The OROBOROS Oxygraph-2k. In Proceedings of the Proceedings of the 11th Congress of the European Shock Society, Vienna, Austria (H Redl, ed) Bologna, Italy: Medimond International Proceedings, 2005; pp. 107-111.
113. Palmer, J.W.; Tandler, B.; Hoppel, C.L. Biochemical properties of subsarcolemmal and interfibrillar mitochondria isolated from rat cardiac muscle. *Journal of Biological Chemistry* **1977**, *252*, 8731-8739.
114. Acin-Perez, R.; Benador, I.Y.; Petcherski, A.; Veliova, M.; Benavides, G.A.; Lagarrigue, S.; Caudal, A.; Vergnes, L.; Murphy, A.N.; Karamanlidis, G. A novel approach to measure mitochondrial respiration in frozen biological samples. *The EMBO Journal* **2020**, *39*, e104073.
115. Osto, C.; Benador, I.Y.; Ngo, J.; Liesa, M.; Stiles, L.; Acin-Perez, R.; Shirihai, O.S. Measuring mitochondrial respiration in previously frozen biological samples. *Current Protocols in Cell Biology* **2020**, *89*, e116.
116. Kimes, B.; Brandt, B. Properties of a clonal muscle cell line from rat heart. *Experimental Cell Research* **1976**, *98*, 367-381.
117. Pereira, S.L.; Ramalho-Santos, J.; Branco, A.F.; Sardao, V.A.; Oliveira, P.J.; Carvalho, R.A. Metabolic remodeling during H9c2 myoblast differentiation: relevance for in vitro toxicity studies. *Cardiovascular Toxicology* **2011**, *11*, 180-190.
118. Witek, P.; Korga, A.; Burdan, F.; Ostrowska, M.; Nosowska, B.; Iwan, M.; Dudka, J. The effect of a number of H9C2 rat cardiomyocytes passage on repeatability of cytotoxicity study results. *Cytotechnology* **2016**, *68*, 2407-2415.
119. Spector, A.A. Fatty acid binding to plasma albumin. *Journal of Lipid Research* **1975**, *16*, 165-179.

120. Laurindo, F.R.; Fernandes, D.C.; Santos, C.X. Assessment of superoxide production and NADPH oxidase activity by HPLC analysis of dihydroethidium oxidation products. *Methods in Enzymology* **2008**, *441*, 237-260.
121. Vandesompele, J.; De Preter, K.; Pattyn, F.; Poppe, B.; Van Roy, N.; De Paepe, A.; Speleman, F. Accurate normalization of real-time quantitative RT-PCR data by geometric averaging of multiple internal control genes. *Genome Biology* **2002**, *3*, research0034. 0031.
122. Baertschi, B.; Gyger, M. Ethical considerations in mouse experiments. *Current Protocols in Mouse Biology* **2011**, *1*, 155-167.
123. Nabeebaccus, A.; Zhang, M.; Shah, A.M. NADPH oxidases and cardiac remodelling. *Heart Failure Reviews* **2011**, *16*, 5-12.
124. Donoso, P.; Finkelstein, J.P.; Montecinos, L.; Said, M.; Sánchez, G.; Vittone, L.; Bull, R. Stimulation of NOX2 in isolated hearts reversibly sensitizes RyR2 channels to activation by cytoplasmic calcium. *Journal of Molecular and Cellular Cardiology* **2014**, *68*, 38-46.
125. Echtay, K.S.; Roussel, D.; St-Pierre, J.; Jekabsons, M.B.; Cadenas, S.; Stuart, J.A.; Harper, J.A.; Roebuck, S.J.; Morrison, A.; Pickering, S. Superoxide activates mitochondrial uncoupling proteins. *Nature* **2002**, *415*, 96-99.
126. Shapiro, A.; Mu, W.; Roncal, C.; Cheng, K.-Y.; Johnson, R.J.; Scarpace, P.J. Fructose-induced leptin resistance exacerbates weight gain in response to subsequent high-fat feeding. *American Journal of Physiology-Regulatory, Integrative and Comparative Physiology* **2008**, *295*, 1370-1375.
127. Sweeney, G. Cardiovascular effects of leptin. *Nature Reviews Cardiology* **2010**, *7*, 22-29.
128. Roe, N.; Thomas, D.; Ren, J. Inhibition of NADPH oxidase alleviates experimental diabetes-induced myocardial contractile dysfunction. *Diabetes, Obesity and Metabolism* **2011**, *13*, 465-473.
129. Cole, M.A.; Murray, A.J.; Cochlin, L.E.; Heather, L.C.; McAleese, S.; Knight, N.S.; Sutton, E.; Abd Jamil, A.; Parassol, N.; Clarke, K. A high fat diet increases mitochondrial fatty acid oxidation and uncoupling to decrease efficiency in rat heart. *Basic Research in Cardiology* **2011**, *106*, 447-457.
130. Myrmel, T.; Forsdahl, K.; Larsen, T.S. Triacylglycerol metabolism in hypoxic, glucose-deprived rat cardiomyocytes. *Journal of molecular and cellular cardiology* **1992**, *24*, 855-868.
131. Kuster, G.M.; Lancel, S.; Zhang, J.; Communal, C.; Trucillo, M.P.; Lim, C.C.; Pfister, O.; Weinberg, E.O.; Cohen, R.A.; Liao, R. Redox-mediated reciprocal regulation of SERCA and Na+–Ca2+ exchanger contributes to sarcoplasmic reticulum Ca2+ depletion in cardiac myocytes. *Free Radical Biology and Medicine* **2010**, *48*, 1182-1187.
132. Stølen, T.O.; Høydal, M.A.; Kemi, O.J.; Catalucci, D.; Ceci, M.; Aasum, E.; Larsen, T.; Rolim, N.; Condorelli, G.; Smith, G.L. Interval training normalizes cardiomyocyte function, diastolic Ca2+ control, and SR Ca2+ release synchronicity in a mouse model of diabetic cardiomyopathy. *Circulation Research* **2009**, *105*, 527-536.
133. Meng, R.; Zhu, D.-L.; Bi, Y.; Yang, D.-H.; Wang, Y.-P. Anti-oxidative effect of apocynin on insulin resistance in high-fat diet mice. *Annals of Clinical & Laboratory Science* **2011**, *41*, 236-243.
134. Pepping, J.K.; Freeman, L.R.; Gupta, S.; Keller, J.N.; Bruce-Keller, A.J. NOX2 deficiency attenuates markers of adiposopathy and brain injury induced by high-fat diet. *American Journal of Physiology-Endocrinology and Metabolism* **2013**, *304*, 392-404.
135. Du, J.; Fan, L.M.; Mai, A.; Li, J.M. Crucial roles of N ox2-derived oxidative stress in deteriorating the function of insulin receptors and endothelium in dietary obesity of middle-aged mice. *British Journal of Pharmacology* **2013**, *170*, 1064-1077.
136. Domenighetti, A.A.; Wang, Q.; Egger, M.; Richards, S.M.; Pedrazzini, T.; Delbridge, L.M. Angiotensin II–mediated phenotypic cardiomyocyte remodeling leads to age-dependent cardiac dysfunction and failure. *Hypertension* **2005**, *46*, 426-432.

137. Mazzolai, L.; Nussberger, J.r.; Aubert, J.-F.; Brunner, D.B.; Gabbiani, G.; Brunner, H.R.; Pedrazzini, T. Blood pressure–independent cardiac hypertrophy induced by locally activated renin-angiotensin system. *Hypertension* **1998**, *31*, 1324-1330.
138. Dikalov, S.I.; Nazarewicz, R.R.; Bikineyeva, A.; Hilenski, L.; Lassegue, B.; Griendling, K.K.; Harrison, D.G.; Dikalova, A.E. Nox2-induced production of mitochondrial superoxide in angiotensin II-mediated endothelial oxidative stress and hypertension. *Antioxidants & Redox Signaling* **2014**, *20*, 281-294.
139. Sugiyama, M.; Yamaki, A.; Furuya, M.; Inomata, N.; Minamitake, Y.; Ohsuye, K.; Kangawa, K. Ghrelin improves body weight loss and skeletal muscle catabolism associated with angiotensin II-induced cachexia in mice. *Regulatory Peptides* **2012**, *178*, 21-28.
140. Flack, J.M.; Adekola, B. Blood pressure and the new ACC/AHA hypertension guidelines. *Trends in Cardiovascular Medicine* **2020**, *30*, 160-164.
141. Glenn, D.J.; Cardema, M.C.; Ni, W.; Zhang, Y.; Yeghiazarians, Y.; Grapov, D.; Fiehn, O.; Gardner, D.G. Cardiac steatosis potentiates angiotensin II effects in the heart. *American Journal of Physiology-Heart and Circulatory Physiology* **2015**, *308*, 339-350.
142. Osorio, J.C.; Stanley, W.C.; Linke, A.; Castellari, M.; Diep, Q.N.; Panchal, A.R.; Hintze, T.H.; Lopaschuk, G.D.; Recchia, F.A. Impaired myocardial fatty acid oxidation and reduced protein expression of retinoid X receptor-α in pacing-induced heart failure. *Circulation* **2002**, *106*, 606-612.
143. Dávila-Román, V.G.; Vedala, G.; Herrero, P.; De Las Fuentes, L.; Rogers, J.G.; Kelly, D.P.; Gropler, R.J. Altered myocardial fatty acid and glucose metabolism in idiopathic dilated cardiomyopathy. *Journal of the American College of Cardiology* **2002**, *40*, 271-277.
144. Ussher, J.R.; Wang, W.; Gandhi, M.; Keung, W.; Samokhvalov, V.; Oka, T.; Wagg, C.S.; Jaswal, J.S.; Harris, R.A.; Clanachan, A.S. Stimulation of glucose oxidation protects against acute myocardial infarction and reperfusion injury. *Cardiovascular Research* **2012**, *94*, 359-369.
145. Opie, L.; Lopaschuk, G. Fuels: aerobic and anaerobic metabolism. *Heart physiology: from cell to circulation. Lippincott Williams & Wilkins, Philadelphia* **2004**, 306-354.
146. Ingwall, J.S.; Weiss, R.G. Is the failing heart energy starved? On using chemical energy to support cardiac function. *Circulation research* **2004**, *95*, 135-145.
147. Wang, S.-B.; Murray, C.I.; Chung, H.S.; Van Eyk, J.E. Redox regulation of mitochondrial ATP synthase. *Trends in cardiovascular medicine* **2013**, *23*, 14-18.
148. Haffar, T.; Akoumi, A.; Bousette, N. Lipotoxic palmitate impairs the rate of β-oxidation and citric acid cycle flux in rat neonatal cardiomyocytes. *Cellular Physiology and Biochemistry* **2016**, *40*, 969-981.
149. Wei, C.D.; Li, Y.; Zheng, H.Y.; Tong, Y.Q.; Dai, W. Palmitate induces H9c2 cell apoptosis by increasing reactive oxygen species generation and activation of the ERK1/2 signaling pathway. *Molecular Medicine Reports* **2013**, *7*, 855-861.
150. Park, S.; Oh, T.S.; Kim, S.; Kim, E.K. Palmitate-induced autophagy liberates monounsaturated fatty acids and increases Agrp expression in hypothalamic cells. *Anim Cells Syst (Seoul)* **2019**, *23*, 384-391, doi:10.1080/19768354.2019.1696407.
151. Zhu, B.Q.; Sievers, R.E.; Sun, Y.P.; Morse-Fisher, N.; Parmley, W.W.; Wolfe, C.L. Is the reduction of myocardial infarct size by dietary fish oil the result of altered platelet function? *American Heart Journal* **1994**, *127*, 744-755, doi:10.1016/0002-8703(94)90540-1.
152. Yang, B.C.; Saldeen, T.G.; Bryant, J.L.; Nichols, W.W.; Mehta, J.L. Long-term dietary fish oil supplementation protects against ischemia-reperfusion-induced myocardial dysfunction in isolated rat hearts. *American Heart Journal* **1993**, *126*, 1287-1292, doi:10.1016/0002-8703(93)90524-d.
153. Höper, A.C.; Salma, W.; Sollie, S.J.; Hafstad, A.D.; Lund, J.; Khalid, A.M.; Raa, J.; Aasum, E.; Larsen, T.S. Wax esters from the marine copepod Calanus finmarchicus reduce diet-

induced obesity and obesity-related metabolic disorders in mice. *The Journal of nutrition* **2014**, *144*, 164-169, doi:10.3945/jn.113.182501.
154. Soumura, M.; Kume, S.; Isshiki, K.; Takeda, N.; Araki, S.-i.; Tanaka, Y.; Sugimoto, T.; Chin-Kanasaki, M.; Nishio, Y.; Haneda, M. Oleate and eicosapentaenoic acid attenuate palmitate-induced inflammation and apoptosis in renal proximal tubular cell. *Biochemical and Biophysical Research Communications* **2010**, *402*, 265-271.
155. Alsabeeh, N.; Chausse, B.; Kakimoto, P.A.; Kowaltowski, A.J.; Shirihai, O. Cell culture models of fatty acid overload: problems and solutions. *Biochimica et Biophysica Acta (BBA)-Molecular and Cell Biology of Lipids* **2018**, *1863*, 143-151.
156. Han, J.; Kaufman, R.J. The role of ER stress in lipid metabolism and lipotoxicity. *Journal of Lipid Research* **2016**, *57*, 1329-1338.
157. Bjelakovic, G.; Nikolova, D.; Gluud, L.L.; Simonetti, R.G.; Gluud, C. Mortality in randomized trials of antioxidant supplements for primary and secondary prevention: systematic review and meta-analysis. *Jama* **2007**, *297*, 842-857.
158. Miller III, E.R.; Pastor-Barriuso, R.; Dalal, D.; Riemersma, R.A.; Appel, L.J.; Guallar, E. Meta-analysis: high-dosage vitamin E supplementation may increase all-cause mortality. *Annals of internal medicine* **2005**, *142*, 37-46.
159. Gorin, Y.; Block, K. Nox as a target for diabetic complications. *Clinical science* **2013**, *125*, 361-382.
160. Teixeira, G.; Szyndralewiez, C.; Molango, S.; Carnesecchi, S.; Heitz, F.; Wiesel, P.; Wood, J. Therapeutic potential of NADPH oxidase 1/4 inhibitors. *British Journal of Pharmacology* **2017**, *174*, 1647-1669.
161. Altenhöfer, S.; Radermacher, K.A.; Kleikers, P.W.; Wingler, K.; Schmidt, H.H. Evolution of NADPH oxidase inhibitors: selectivity and mechanisms for target engagement. *Antioxidants & Redox Signaling* **2015**, *23*, 406-427.
162. Elbatreek, M.H.; Mucke, H.; Schmidt, H.H. NOX inhibitors: from bench to naxibs to bedside. In *Reactive Oxygen Species*; Springer: 2020; pp. 145-168.

Review:

The Role of NADPH Oxidases in Diabetic Cardiomyopathy

BBA - Molecular Basis of Disease 1864 (2018) 1908–1913

Contents lists available at ScienceDirect

BBA - Molecular Basis of Disease

journal homepage: www.elsevier.com/locate/bbadis

The role of NADPH oxidases in diabetic cardiomyopathy☆

Synne S. Hansen, Ellen Aasum, Anne D. Hafstad*

Cardiovascular Research Group, Department of Medical Biology, Faculty of Health Sciences, UIT-The Arctic University of Tromsø, N-9037 Tromsø, Norway

ARTICLE INFO

Keywords:
NADPH oxidases
Diabetic cardiomyopathy
Oxidative stress
Metabolism
Obesity and insulin resistance

ABSTRACT

Systemic changes during diabetes such as high glucose, dyslipidemia, hormonal changes and low grade inflammation, are believed to induce structural and functional changes in the cardiomyocyte associated with the development of diabetic cardiomyopathy. One of the hallmarks of the diabetic heart is increased oxidative stress. NADPH-oxidases (NOXs) are important ROS-producing enzymes in the cardiomyocyte mediating both adaptive and maladaptive changes in the heart. NOXs have been suggested as a therapeutic target for several diabetic complications, but their role in diabetic cardiomyopathy is far from elucidated. In this review we aim to provide an overview of the current knowledge regarding the understanding of how NOXs influences cardiac adaptive and maladaptive processes in a "diabetic milieu". This article is part of a Special issue entitled Cardiac adaptations to obesity, diabetes and insulin resistance, edited by Professors Jan F.C. Glatz, Jason R.B. Dyck and Christine Des Rosiers.

1. Introduction

The worldwide incidence of diabetes mellitus (DM) is increasing rapidly due to lifestyle changes. Patients with DM are two to four times more likely to develop cardiovascular disease (CVD) like high blood pressure, coronary artery disease and heart failure (HF), and have three times higher overall mortality rate compared to those without DM [1]. Diabetic cardiomyopathy is considered as left ventricular dysfunction in the absence of significant coronary or hypertensive disease [2].The development of this cardiomyopathy is multifactorial and complex and remains to be completely understood. Hallmarks of diabetes such as high blood sugar (hyperglycemia), dyslipidemia, hyperinsulinemia, activation of the Renin-Angiotensin-System (RAS) and a chronic low-grade inflammation, are believed to trigger a range of structural and functional changes at the cellular level in the diabetic heart (Fig. 1). Accordingly, these hearts exhibit a range of features including oxidative stress, altered metabolism, mitochondrial dysfunction, fibrosis, apoptosis, increased ER stress, impaired autophagy, inflammation and altered calcium handling.

NADPH oxidases (NOXs) are a family of enzymes whose primary function is to produce reactive oxygen species (ROS). They were first recognized as ROS-generating enzymes in professional phagocytes, playing an extremely important role in the mechanisms of host defense against infectious agents. NOXs are also believed to be a major source of ROS in different organs. Many of the systemic changes in diabetes are known activators of NOXs [3], and NOXs have therefore been suggested as a therapeutic target for diabetic complications (as reviewed by Gorin and Block [4]). However, studies undertaking the role of NOXs report both detrimental and protective effects of different NOX isoforms in the cardiovascular system [5,6], and the role of NOXs in diabetic cardiomyopathy is far from elucidated. The aim of the present review, is to provide an overview of the current knowledge regarding the understanding of how NOXs influences cardiac adaptive and maladaptive processes in a "diabetic milieu".

1.1. Cardiac redox-signaling and oxidative stress

In response to specific stimuli (acute, transient or sustained), reactive oxygen- and nitrogen species (RONS) are produced through various enzymes in cardiomyocytes (Fig. 2). Under physiological conditions, RONS are known to play key roles in different signaling pathways through their oxidation of specific targets, so-called redox signaling [7,8]. However, following increased activation of RONS-producing enzymes and/or impairment of endogenous antioxidant capacity, oxidative stress may occur [9]. Hence, redox signaling comes in

Abbreviations: AGEs, advanced glycation end-products; RAGE, AGE receptors; Ang II, angiotensin II; CaMKII, Ca^{2+}/calmodulin-dependent protein kinase II; DATS, diallyl trisulfide; ER, endoplasmic reticulum; eNOS and nNOS, endothelial and neuronal nitric oxide synthase; FA, fatty acid; GLUT, glucose transporter; Gly-BSA, glycated BSA; HF, heart failure; HG, high glucose; NOX, NADPH-oxidase; NCX, Na^{+}-Ca^{2+} exchanger; MAO, monoamine oxidase; Plin-5, perilipin 5; PKC, protein kinase C; RAS, Renin-Angiotensin-System; ROS, reactive oxygen species; RONS, reactive oxygen- and nitrogen species; SR, sarcoplasmic reticulum; SGLT, sodium-glucose cotransporter; XO, xanthine oxidase

☆ This article is part of a Special issue entitled Cardiac adaptations to obesity, diabetes and insulin resistance, edited by Professors Jan F.C. Glatz, Jason R.B. Dyck and Christine Des Rosiers.

* Corresponding author.
E-mail address: anne.hafstad@uit.no (A.D. Hafstad).

http://dx.doi.org/10.1016/j.bbadis.2017.07.025
Received 30 May 2017; Received in revised form 19 July 2017; Accepted 21 July 2017
Available online 25 July 2017

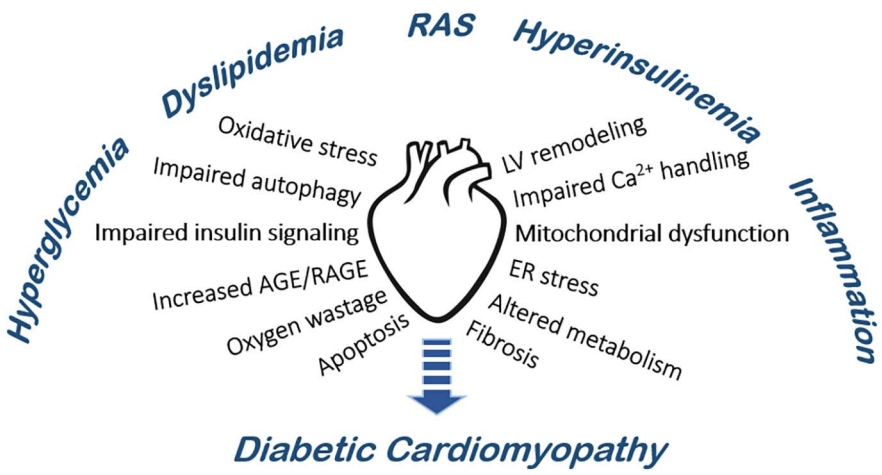

Fig. 1. A range of systemic changes in diabetes such as hyperglycemia, dyslipidemia, increased activation of the Renin-Angiotensin-System (RAS), hyperinsulinemia and a chronic low grade inflammation are believed to lead to cellular changes in cardiomyocyte and consequently the development of diabetic cardiomyopathy. Advanced glycation end-products (AGE), AGE receptors (RAGE), endoplasmic reticulum (ER).

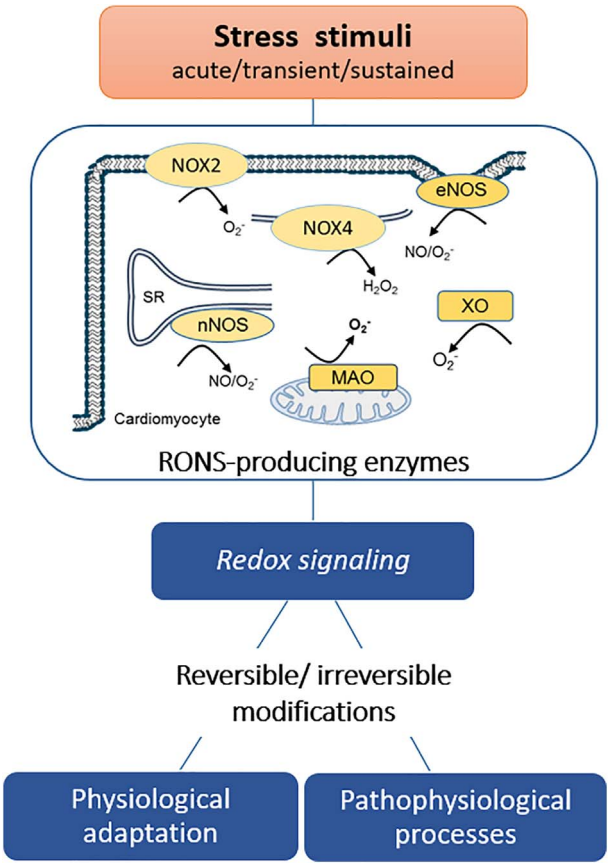

Fig. 2. In response to various stimuli, several enzyme systems in the cardiomyocyte produce reactive oxygen- and nitrogen species (RONS). These enzymes (NADPH oxidase (NOX), endothelial and neuronal nitric oxide synthase (eNOS and nNOS), monoamine oxidase (MAO), xanthine oxidase (XO)) can through redox signaling mediate reversible or irreversible modification leading to physiological adaptive or pathophysiological processes. Sarcoplasmic reticulum (SR).

"different flavors" where reversible modification may transiently change protein activity involved in physiological adaptations, while irreversible oxidations may lead to pathophysiological processes such as in HF [10] (Fig. 2). A vast amount of clinical and experimental studies support increased oxidative damage in diabetic hearts [11–13].

1.2. NADPH oxidases in the heart

Of the seven mammalian NOX isoforms (Nox1–5 and Duox1–2), NOX2 and NOX4 are expressed in the heart [5]. Both isoforms exist as a heterodimeric flavocytochrome with a p22phox subunit, but they differ in their structure, activation, subcellular localization, type of ROS produced as well as in the specific signaling pathways they induce [14]. NOX2 activation requires the recruitment of several cytosolic subunits (p47phox, p67phox, p40phox and Rac1) which bind to the flavocytochrome to induce production of mainly superoxide. NOX4 on the other hand, is situated at internal membranes such as the endoplasmic reticulum (ER) and the mitochondria, is constitutively active, produces hydrogen peroxide and is mainly transcriptionally regulated [5]. Interestingly, these two enzymes have been shown to have distinct physiological and pathophysiological roles in the heart. In response to physiological stressors, NOX2 have been reported to be involved in stretch-induced calcium release, EC-coupling, and preconditioning [15–17]. NOX4 have been shown to play important roles in endogenous detoxifying responses [18], angiogenesis [19], ER-stress and protein unfolding stress response [20], substrate utilization [21] and in mediating metabolic stress responses [22]. Following different types of sustained stress, NOX2-dependent signaling promotes several detrimental processes in cardiac pathology, including cardiomyocyte hypertrophy, contractile dysfunction, arrhythmia, interstitial fibrosis, cell death, and cardiac rupture after myocardial infarction as reviewed by Zhang et al. [3]. In contrast, in the setting of chronic hemodynamic stress, NOX4 have been shown to mediate protective effects such as adaptive remodeling with better preserved function and reduced hypertrophy [19,23].

2. Hyperglycemia and NOX activity in the diabetic heart

Elevated glucose (hyperglycemia) is an important risk factor for developing cardiovascular disease. In addition to generating pyruvate for oxidation, elevated plasma levels of glucose may also affect non-oxidative pathways including the polyolhexosamine biosynthetic pathway, protein kinase C (PKC) activation and production of advanced glycation end-products (AGEs). There are growing evidence that hyperglycemia can induce NOX activity through various pathways in the heart (Fig. 3).

2.1. NOX2 activation by glycated proteins

Both intracellular and extracellular lipids and protein exposed to high levels of sugars may undergo glycosylation. Zhang and co-workers [24] found glycated BSA (Gly-BSA) to induce ROS production and increase NOX2 activity in cardiomyocytes. They also reported that the activation of NOX2 was PKC-dependent and associated with translocation of the nuclear factor κB (NF-κB) to the nucleus. Interestingly neither NOX4, xanthine oxidase (XO), nitric oxide synthase (NOS) nor

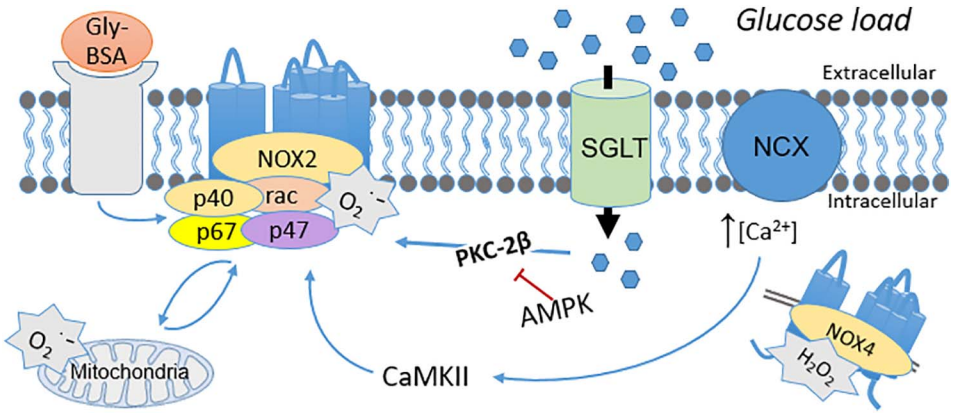

Fig. 3. Schematic diagram of proposed mechanisms for NADPH oxidase (NOX) activation in cardiomyocytes exposed to high glucose (HG) load. HG load through the Sodium-glucose cotransporter (SGLT) leads to activation of protein kinase C-2 β (PKC), recruitment of catalytic subunits and consequently increased production of NOX2-derived superoxide. HG-induced elevation in intracellular Ca^{2+} ($[Ca^{2+}]$) activates Ca^{2+}/calmodulin-dependent protein kinase II (CaMKII) and consequently increases NOX2 activity. Activation results in NOX2 superoxide ($O_2^{\cdot -}$) production, which promotes mitochondrial ROS production in a positive feedback loop. NOX4 has also been shown to be activated by HG through unknown mechanisms. NOX2, but not NOX4 activity is increased following stimulation of glycated BSA (Gly-BSA). AMP-activated protein kinase (AMPK), Na^{+}-Ca^{2+} exchanger (NCX).

mitochondrial ROS, seemed to a play role in this process. Although AGEs may be important in the pathogenesis of diabetic cardiomyopathy [25], there is no direct evidence of AGE-induced NOX activation in diabetic hearts. Circumstantial evidence, however, suggests that increased AGE accumulation and AGE receptor (RAGE) expression in diabetic hearts are coupled with increased expression of NOX2 and its catalytic subunits [26].

2.2. NOX-activation by acute high glucose exposure

A vast amount of cell studies have demonstrated glucose-toxicity to be mediated through NOX2 activation. Exposing cardiomyocytes to a high glucose (HG) media enhance protein expression of NOX2 and its catalytic subunits [27–29], induce translocation of catalytic subunits to the cell membrane [28,30,31], and increase overall NOX2 activity [32–34]. Multiple interventions to inhibit NOX2 activity have clearly demonstrated abrogation of HG-induced elevation of ROS in cardiomyocytes [30,33–35]. NOX2 inhibition also ameliorates the detrimental cellular effects of HG, as indicted by improved insulin signaling [30,33], increased endogenous antioxidant capacity [33], reduced apoptosis/cell death [27,28,32,34,36] and increased cardiomyocyte contractility [29]. Although less studied, HG-induced increase in NOX4 expression has also been reported in cardiomyocytes [37,38]. Transfecting cultured cardiomyocytes with dominant negative NOX4 was able to reduce HG-increased expression of fetal gene program [37], suggesting NOX4 to play a role in HG-induced detrimental effects in cardiomyocytes.

2.3. NOX-activation by chronic high glucose exposure

Animal studies also report increased NOX activity in hearts following chronic hyperglycemia. Increased cardiac NOX2 activity has been found in hearts from both type I [26,27,34–36,38–43] and type II [42,44,45]diabetic models. Furthermore strategies to directly reduce NOX2 activity in diabetic hearts have been shown to abolish many of the detrimental changes associated with diabetes. Reduced NOX2 activity in streptozotocin-induced diabetic hearts following cardiac specific knock down of the catalytic subunit Rac1 was associated with reduced cardiac oxidative stress [34,39], ameliorated diabetes-induced collagen deposition, decreased inflammation [39], reduced markers of apoptosis [34] and reduced ER-stress [39]. These beneficial cellular effects were accompanied by reduced myocardial remodeling and improved cardiac function [34,39]. Using a therapeutic approach, long term treatment with the NOX2 inhibitor apocynin has also been able to ameliorate many of the diabetes-induced adverse cellular effects and improve systolic and diastolic ventricular function [34,39,43,46]. Increased expression of NOX4 has also been reported in hearts from diabetic models [37,38,47,48], and anti-diabetic treatments and exercise have been shown to normalize this expression [38,48]. Maalouf et al. demonstrated direct cardiac effect of NOX4 inhibition as administration of antisense NOX4 oligonucleotides (NOX4-AS) decreased diabetes-induced cardiac ROS production associated with improved mechanical function [37]. Surprisingly, diabetes was not associated with a change in NOX2 activity or expression in this study, a finding that is commonly reported [27,34–36,38–45].

Several signaling pathways may mediate the HG-induced activation of NOX2 (Fig. 3). Phosphorylation of p47phox and consequent translocation to the plasma membrane is known to be catalyzed by several types of PKCs in neutrophils [49]. HG can activate PKC-β2 in cardiac caveolae [50], and in line with this, a PKC-β2-inhibitor was shown to reduce the HG-induced p47phox translocation [31]. Balteau and coworkers [30] reported that inhibition of glucose uptake through glucose transporter 1 and 4 (GLUT1 and GLUT 4) did not affect HG-induced ROS production, and that the HG-induced NOX2 activation and consequent ROS production could be mimicked by using non-metabolizable glucose-analogs. They therefore suggested that glucose transport through the sodium-glucose cotransporter (SGLT) is responsible for the activation of NOX2, and not glucose utilization per se. In a follow-up study [31] they found that AMP-activated protein kinase (AMPK) activity could inhibited HG-induced NOX2 activity by blocking the PKC-β2 pathway and the subsequent translocation of p47phox to the membrane. In the same study, p47phox was shown to translocate to caveoline-3 and that disruption of the caveolar structure prevented HG-induced ROS. Together, these data strengthen the notion of a HG-induced signalosome located in cardiac caveolae.

A cross-talk between other ROS-producing enzymes and NOX activity has been suggested following acute HG-exposure in cardiomyocytes. Both inhibition of either mitochondrial superoxide or NOX2 was found to prevent HG-induced ROS [36]. Chronic antioxidant supplementation using diallyl trisulfide (DATS) [27], coenzyme Q10 [40,41], mito-TEMPO [36] or *N*-acetyl-L-cysteine (NAC) [42] has also been shown to reduce myocardial NOX2 expression and activation in diabetes, resulting in ameliorated morphological remodeling and improved ventricular function. Cardiac specific knock-down of cardiac Rac1 also reduced mitochondrial superoxide production [34,39], suggesting that NOX2 could contribute to mitochondrial ROS in hyperglycemic hearts. Furthermore, apocynin has also been suggested to limit diabetes-induced eNOS uncoupling in cardiomyocytes [43]. Together, these studies clearly suggest an interaction between different ROS sources in the cardiomyocyte where NOX2 activity in the diabetic heart may both modify and be modified by other ROS-producing enzymes.

3. Dyslipidemia and NOX activation in the diabetic heart

In addition to elevated glucose, diabetes is associated with dyslipidemia where both elevated fatty acid (FA) uptake and oxidation is believed to induce cardiac lipotoxicity. Growing evidence suggests that

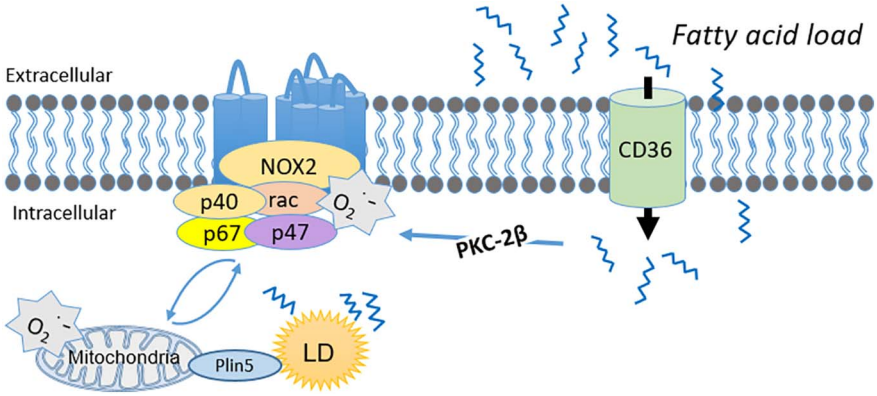

Fig. 4. Schematic diagram of proposed mechanisms for NADPH oxide (NOX) activation in cardiomyocytes exposed to saturated fatty acids (FA). Transport of FA through CD36 leads to activation of protein kinase C-2 β (PKC-2β), which promotes recruitment of NOX2 catalytic subunits and activation of NOX2. This activation results in superoxide ($O_2\cdot^-$) production, which consequently promotes mitochondrial ROS production in a positive feedback loop. Lipid droplets (LD) release FA in to the cytosol and are transported into the mitochondria with assistance from perilipin 5 (Plin5). FA released from the LDs promotes NOX2 activation.

exposure to a high lipid load result in activation of NOX2 [42,44,45,51,52] (Fig. 4).

3.1. NOX activation by acute lipid load

Cardiomyocytes exposed to the saturated FA, palmitate, exhibit increased levels of p47phox in the membrane and elevated ROS production [51,52]. Oleate, an unsaturated FA did not increase superoxide production, suggesting that this effect is not a general effect of a FA load, but rather a result of high levels of saturated FA [51]. In a NOX2 KO model, high levels of palmitate did not induce higher levels of ROS, mitochondrial dysfunction [51,52] or sarcoplasmic reticulum calcium-leak [52]. In agreement with this, NOX2 inhibitors (apocynin and gp91 ds-tat) and SiRNA-mediated depletion of p47phox prevented palmitate-induced ROS formation [52]. Interestingly, NOX2 inhibition also restored lysosome acidification and enzyme activity as well as reduced autophagosome accumulation in palmitate-treated cardiomyocytes [51]. In contrast, inhibiting NOS, another known source of ROS, had minimal effect on palmitate-induced ROS formation [52].

Both PKC activation and ROS-induced ROS-release are proposed to mediate the palmitate-induced NOX2 activation in cardiomyocytes, as inhibition of PKC prevented palmitate-induced NOX2-derived ROS production [51,52]. Furthermore, mitochondrial ROS seems to be an important contribution to the total ROS levels induced by elevated palmitate levels, as mito-TEMPO eliminated the palmitate-induced ROS formation in cardiomyocytes. Interestingly the palmitate induced ROS production from NOX2 seemed to precede palmitate induced mitochondrial ROS production [52].

3.2. NOX activation by chronic dyslipidemia

The palmitate-induced activity of NOX2 is supported by studies on animal models of obesity and diabetes. First, lipid lowering treatment has been shown to lower the NOX-dependent ROS production in obese and diabetic animals [44,45]. Treating Diabetic *db/db* mice with a cholesterol-lowering drug, resulted in reduced NOX2 activity in the heart, which could have contributed to the attenuation of oxidative stress [45]. In addition silencing of the FA-transporter CD36 decreased NOX2-dependent ROS production in hearts from *ob/ob* mice. This was accompanied by prevention of cardiac steatosis, as well as increased insulin sensitivity and glucose utilization in the heart [44]. Perilipin 5 (Plin5) is essential to protect lipid droplets in the cardiomyocyte. It is abundantly expressed in the heart and is thought to stabilize lipid droplets by preventing accumulation of lipotoxic intermediates. Interestingly, Kuramoto and colleagues found that the suppression of myocardial lipid droplet accumulation in diabetic Plin5-KO mice was associated with attenuation of diabetes-induced cardiac dysfunction. These hearts, which were protected against functional remodeling, and also exhibited decreased assembly of NOX2, reduced membrane translocation of PKC-2β and lower levels of ROS [42].

4. Activation of NOX by the renin-angiotensin system (RAS) in the diabetic heart

Angiotensin II (Ang II) is a well-known activator of NOXs, that has been shown mediate a range of pathological cardiac changes such as fibrosis, apoptosis and hypertrophy [3,8]. Huynh and colleagues [40] reported that the ACE-inhibitor ramipril was effective in preventing diabetes-induced upregulation of p47phox, p22phox and NOX2 expression together with reduced NOX2 driven myocardial superoxide production. This was accompanied by reduced apoptosis, fibrosis and hypertrophic gene expression. Also, blocking AT1 with candesartan in *db/db* mice ameliorated NOX2 and p22phox expression, superoxide content and macrophage infiltration in the heart [53]. In cardiomyocytes, the use of an Ang II type 1 (AT_1) antagonist could ameliorate HG-induced increase in p47phox expression and prevent HG-induced abnormalities [29]. Thus, the increased RAS activity in diabetes most likely supports the interplay between Ang II and NOX activity in the diabetic heart.

5. Impaired calcium handling and NOX activation in the diabetic heart

Alteration in calcium handling and the excitation-contraction coupling machinery is profound in the diabetic heart [54]. Although not clearly demonstrated, impaired cardiac calcium handling has been suggested to modulate NOX activity. Exposure to HG was shown to increase intracellular calcium ($[Ca^{2+}]_i$) through the sodium-calcium exchanger (NCX) in cardiomyocytes. This consequently increased Ca^{2+}/calmodulin-dependent protein kinase II CaMKII activation which was associated with increased NOX2 activation [35]. Inhibition of CaMKII activity reduced NOX2 activity and ROS production in diabetic hearts, indicating a link between activated CaMKII and the activation of NOX2 [35]. Conversely, CaMKII and other calcium handling proteins are redox sensitive and their activity may consequently be altered by NOXs [55]. It is tempting to speculate that some of the observed beneficial effects on ventricular function following NOX2 inhibition could be mediated through improved calcium handling in diabetic hearts. Apocynin treatment did however fail to alter diabetes-induced effects on protein expression of sarcoplasmic reticulum ATPase as well as phospholamban phosphorylation in type 1 diabetic hearts, despite improved contractile properties [43]. However, restoring the optimal redox state for intracellular Ca^{2+}-handling proteins, may very well not be reflected in the overall protein expression levels.

6. Gaps in current knowledge and future perspectives

The current knowledge regarding the role of NOXs in diabetic cardiomyopathy is mostly from animal- and cell studies, as there are few clinical studies. Increased NOX activity accompanied by translocation of p47phox to the cardiomyocyte sarcolemma has however been

reported in failing human myocardium [56]. NOX-derived ROS has also been suggested to be involved in the development of vascular disease in diabetic patients [57]. All though ROS seem to play a major role in the pathology of cardiovascular diseases, clinical trials with general exogenous antioxidant treatments have been largely unsuccessful in terms of preventing or treating such diseases [58,59]. Specific-ROS-producing enzymes like the NOXs have therefore emerged as potential therapeutic targets, as recently reviewed by several groups [4,60,61]. However, a major challenge with the development of NOX inhibitors is that they are often un-specific and not isoform selective, they also may exhibit general ROS-scavenging properties [61]. In addition, NOXs also have important validated physiological functions which need to be sustained. Mutations in humans leaving a dysfunctional NOX2 protein leads to chronic granulomatous disease and NOX2 KO mice display impaired immune defense against pathogens [62]. Therefore, complete abrogation of NOX2 activity does not seem to be an acceptable therapeutic approach. In contrast, genetic deletion of NOX4 has revealed no spontaneous pathologies and a dual NOX1/4 inhibitor have been tested in the clinic with good tolerability [60]. However, the role of NOX4 in pathology is controversial as indicated by studies both reporting beneficial [19] and detrimental [63] effects of NOX4 in experimental HF. One factor that can explain these discrepancies is the severity of the HF applied in the different studies, where NOX4 may mediate beneficial effects through increased angiogenesis in the progression of a less severe HF. This topic is not studied in different animal models of diabetes where the progression to diabetic cardiomyopathy may vary greatly. Therefore there is a still a need for more understanding of the individual roles of NOX homologues in molecular mechanisms and signaling cascades in pursuing potential therapeutic interventions.

7. Conclusion

Significant progress has been made to elucidating the role of NOXs in diabetic cardiomyopathy. Anti-diabetic treatments and correction of dyslipidemia are associated with both reduced NOX2 and NOX4 activity in the heart, suggesting diabetes-induced systemic activators of NOXs. Cell studies clearly suggest a detrimental role for increased NOX2 activity following exposure to high glucose, elevated glycated proteins, dyslipidemia and increased activity of RAS. Also, reducing NOX2 activity in chronic models of diabetes, through NOX2 inhibition/deletion consistently reports to be associated with amelioration of adverse cardiac effects. The role of NOX4 in diabetic cardiomyopathy is however less elucidated, but studies so far suggest NOX4 to mediate adverse effects. Several studies indicate a marked complexity in the activation of NOXs which present a challenge when studying the role of these enzymes. Certain activators of NOXs also seem to be targets of NOX-induced redox modulation, creating feedback-loops and potential amplifying signaling cycles. Although cell and animal studies clearly suggest a role for NOXs in some of the pathological processes, there is still the need for more understanding of the individual role of NOX homologues in the progression of diabetic cardiomyopathy.

Transparency Document

The Transparency document associated with this article can be found, in online version.

Acknowledgements

Funding was provided by the Novo Nordisk Foundation (NNF13OC0005765 and NNF14OC0010235), the Norwegian Health Association (6682) (fellowship to ADH) and the UiT-The Arctic University of Norway (fellowship to SSH). The contribution from Dr. Neoma T Boardman is greatly appreciated.

References

[1] W.B. Kannel, M. Hjortland, W.P. Castelli, Role of diabetes in congestive heart failure: the Framingham study, Am. J. Cardiol. 34 (1974) 29–34.
[2] F.S. Fein, E.H. Sonnenblick, Diabetic cardiomyopathy, Cardiovasc. Drugs Ther. 8 (1994) 65–73.
[3] M. Zhang, A. Perino, A. Ghigo, E. Hirsch, A.M. Shah, NADPH oxidases in heart failure: poachers or gamekeepers? Antioxid. Redox Signal. 18 (2013) 1024–1041.
[4] Y. Gorin, K. Block, Nox as a target for diabetic complications, Clin. Sci. 125 (2013) 361–382.
[5] B. Lassègue, A. San Martín, K.K. Griendling, Biochemistry, physiology, and pathophysiology of NADPH oxidases in the cardiovascular system, Circ. Res. 110 (2012) 1364–1390.
[6] L. Gao, G.E. Mann, Vascular NAD (P) H oxidase activation in diabetes: a double-edged sword in redox signalling, Cardiovasc. Res. 82 (2009) 9–20.
[7] C.X. Santos, N. Anilkumar, M. Zhang, A.C. Brewer, A.M. Shah, Redox signaling in cardiac myocytes, Free Radic. Biol. Med. 50 (2011) 777–793.
[8] J.R. Burgoyne, H. Mongue-Din, P. Eaton, A.M. Shah, Redox signaling in cardiac physiology and pathology, Circ. Res. 111 (2012) 1091–1106.
[9] W. Dröge, Free radicals in the physiological control of cell function, Physiol. Rev. 82 (2002) 47–95.
[10] A.D. Hafstad, A.A. Nabeebaccus, A.M. Shah, Novel aspects of ROS signalling in heart failure, Basic Res. Cardiol. 108 (2013) 359.
[11] E.J. Anderson, A.P. Kypson, E. Rodriguez, C.A. Anderson, E.J. Lehr, P.D. Neufer, Substrate-specific derangements in mitochondrial metabolism and redox balance in the atrium of the type 2 diabetic human heart, J. Am. Coll. Cardiol. 54 (2009) 1891–1898.
[12] F. Giacco, M. Brownlee, Oxidative stress and diabetic complications, Circ. Res. 107 (2010) 1058–1070.
[13] V. Ramakrishna, R. Jailkhani, Oxidative stress in non-insulin-dependent diabetes mellitus (NIDDM) patients, Acta Diabetol. 45 (2008) 41–46.
[14] N. Anilkumar, R. Weber, M. Zhang, A. Brewer, A.M. Shah, Nox4 and nox2 NADPH oxidases mediate distinct cellular redox signaling responses to agonist stimulation, Arterioscler. Thromb. Vasc. Biol. 28 (2008) 1347–1354.
[15] B.L. Prosser, C.W. Ward, W. Lederer, X-ROS signaling: rapid mechano-chemo transduction in heart, Science 333 (2011) 1440–1445.
[16] M. Zhang, B.L. Prosser, M.A. Bamboye, A.N. Gondim, C.X. Santos, D. Martin, A. Ghigo, A. Perino, A.C. Brewer, C.W. Ward, Contractile function during angiotensin-II activation, J. Am. Coll. Cardiol. 66 (2015) 261–272.
[17] R.M. Bell, A.C. Cave, S. Johar, D.J. Hearse, A.M. Shah, M.J. Shattock, Pivotal role of NOX-2-containing NADPH oxidase in early ischemic preconditioning, FASEB J. 19 (2005) 2037–2039.
[18] A.C. Brewer, T.V. Murray, M. Arno, M. Zhang, N.P. Anilkumar, G.E. Mann, A.M. Shah, Nox4 regulates Nrf2 and glutathione redox in cardiomyocytes in vivo, Free Radic. Biol. Med. 51 (2011) 205–215.
[19] M. Zhang, A.C. Brewer, K. Schröder, C.X. Santos, D.J. Grieve, M. Wang, N. Anilkumar, B. Yu, X. Dong, S.J. Walker, NADPH oxidase-4 mediates protection against chronic load-induced stress in mouse hearts by enhancing angiogenesis, Proc. Natl. Acad. Sci. 107 (2010) 18121–18126.
[20] C.X. Santos, A.D. Hafstad, M. Beretta, M. Zhang, C. Molenaar, J. Kopec, D. Fotinou, T.V. Murray, A.M. Cobb, D. Martin, Targeted redox inhibition of protein phosphatase 1 by Nox4 regulates eIF2α-mediated stress signaling, EMBO J. 35 (2016) 319–334.
[21] A. Nabeebaccus, A. Hafstad, A. Zoccarato, T. Eykyn, J. West, J. Griffin, M. Mayr, A. Shah, C Nox4-dependent reprogramming of glucose metabolism and fatty acid oxidation facilitates cardiac adaption to chronic pressure-overload, Heart 102 (2016) A146.
[22] S. Sciarretta, M. Volpe, J. Sadoshima, NOX4 regulates autophagy during energy deprivation, Autophagy 10 (2014) 699–701.
[23] S. Matsushima, J. Kuroda, T. Ago, P. Zhai, Y. Ikeda, S. Oka, G.-H. Fong, R. Tian, J. Sadoshima, Broad suppression of NADPH oxidase activity exacerbates ischemia/reperfusion injury through inadvertent downregulation of hypoxia-inducible factor-1α and upregulation of peroxisome proliferator–activated receptor-α, Circ. Res. 112 (2013) 1135–1149.
[24] M. Zhang, A.L. Kho, N. Anilkumar, R. Chibber, P.J. Pagano, A.M. Shah, A.C. Cave, Glycated proteins stimulate reactive oxygen species production in cardiac myocytes, Circulation 113 (2006) 1235–1243.
[25] R. Candido, J.M. Forbes, M.C. Thomas, V. Thallas, R.G. Dean, W.C. Burns, C. Tikellis, R.H. Ritchie, S.M. Twigg, M.E. Cooper, A breaker of advanced glycation end products attenuates diabetes-induced myocardial structural changes, Circ. Res. 92 (2003) 785–792.
[26] W. Yu, J. Wu, F. Cai, J. Xiang, W. Zha, D. Fan, S. Guo, Z. Ming, C. Liu, Curcumin alleviates diabetic cardiomyopathy in experimental diabetic rats, PLoS One 7 (2012) e52013.
[27] W.-W. Kuo, W.-J. Wang, C.-Y. Tsai, C.-L. Way, H.-H. Hsu, L.-M. Chen, Diallyl trisufide (DATS) suppresses high glucose-induced cardiomyocyte apoptosis by inhibiting JNK/NFκB signaling via attenuating ROS generation, Int. J. Cardiol. 168 (2013) 270–280.
[28] K.H. Tsai, W.J. Wang, C.W. Lin, P. Pai, T.Y. Lai, C.Y. Tsai, W.W. Kuo, NADPH oxidase-derived superoxide anion-induced apoptosis is mediated via the JNK-dependent activation of NF-κB in cardiomyocytes exposed to high glucose, J. Cell. Physiol. 227 (2012) 1347–1357.
[29] J.R. Privratsky, L.E. Wold, J.R. Sowers, M.T. Quinn, J. Ren, AT1 blockade prevents glucose-induced cardiac dysfunction in ventricular myocytes, Hypertension 42 (2003) 206–212.

[30] M. Balteau, N. Tajeddine, C. de Meester, A. Ginion, C. Des Rosiers, N.R. Brady, C. Sommereyns, S. Horman, J.-L. Vanoverschelde, P. Gailly, NADPH oxidase activation by hyperglycaemia in cardiomyocytes is independent of glucose metabolism but requires SGLT1, Cardiovasc. Res. 92 (2011) 237–246.
[31] M. Balteau, A. Van Steenbergen, A.D. Timmermans, C. Dessy, G. Behets-Wydemans, N. Tajeddine, D. Castanares-Zapatero, P. Gilon, J.-L. Vanoverschelde, S. Horman, AMPK activation by glucagon-like peptide-1 prevents NADPH oxidase activation induced by hyperglycemia in adult cardiomyocytes, Am. J. Phys. Heart Circ. Phys. (2014) (ajpheart. 00210.02014).
[32] Y. Li, Y. Li, Q. Feng, M. Arnold, T. Peng, Calpain activation contributes to hyperglycaemia-induced apoptosis in cardiomyocytes, Cardiovasc. Res. (2009) cvp189.
[33] D. Joseph, C. Kimar, B. Symington, R. Milne, M.F. Essop, The detrimental effects of acute hyperglycemia on myocardial glucose uptake, Life Sci. 105 (2014) 31–42.
[34] E. Shen, Y. Li, Y. Li, L. Shan, H. Zhu, Q. Feng, J.M.O. Arnold, T. Peng, Rac1 is required for cardiomyocyte apoptosis during hyperglycemia, Diabetes 58 (2009) 2386–2395.
[35] S. Nishio, Y. Teshima, N. Takahashi, L.C. Thuc, S. Saito, A. Fukui, O. Kume, N. Fukunaga, M. Hara, M. Nakagawa, Activation of CaMKII as a key regulator of reactive oxygen species production in diabetic rat heart, J. Mol. Cell. Cardiol. 52 (2012) 1103–1111.
[36] R. Ni, T. Cao, S. Xiong, J. Ma, G.-C. Fan, J.C. Lacefield, Y. Lu, S. Le Tissier, T. Peng, Therapeutic inhibition of mitochondrial reactive oxygen species with mito-TEMPO reduces diabetic cardiomyopathy, Free Radic. Biol. Med. 90 (2016) 12–23.
[37] R.M. Maalouf, A.A. Eid, Y.C. Gorin, K. Block, G.P. Escobar, S. Bailey, H.E. Abboud, Nox4-derived reactive oxygen species mediate cardiomyocyte injury in early type 1 diabetes, Am. J. Phys. Cell Phys. 302 (2012) C597–C604.
[38] Z. Guo, W. Qi, Y. Yu, S. Du, J. Wu, J. Liu, Effect of exenatide on the cardiac expression of adiponectin receptor 1 and NADPH oxidase subunits and heart function in streptozotocin-induced diabetic rats, Diabetol. Metab. Syndr. 6 (2014) 29.
[39] J. Li, H. Zhu, E. Shen, L. Wan, J.M.O. Arnold, T. Peng, Deficiency of rac1 blocks NADPH oxidase activation, inhibits endoplasmic reticulum stress, and reduces myocardial remodeling in a mouse model of type 1 diabetes, Diabetes 59 (2010) 2033–2042.
[40] K. Huynh, H. Kiriazis, X.-J. Du, J.E. Love, S.P. Gray, K.A. Jandeleit-Dahm, J.R. McMullen, R.H. Ritchie, Targeting the upregulation of reactive oxygen species subsequent to hyperglycemia prevents type 1 diabetic cardiomyopathy in mice, Free Radic. Biol. Med. 60 (2013) 307–317.
[41] M.J. De Blasio, K. Huynh, C. Qin, S. Rosli, H. Kiriazis, A. Ayer, N. Cemerlang, R. Stocker, X.-J. Du, J.R. McMullen, Therapeutic targeting of oxidative stress with coenzyme Q 10 counteracts exaggerated diabetic cardiomyopathy in a mouse model of diabetes with diminished PI3K (p110α) signaling, Free Radic. Biol. Med. 87 (2015) 137–147.
[42] K. Kuramoto, F. Sakai, N. Yoshinori, T.Y. Nakamura, S. Wakabayashi, T. Kojidani, T. Haraguchi, F. Hirose, T. Osumi, Deficiency of a lipid droplet protein, perilipin 5, suppresses myocardial lipid accumulation, thereby preventing type 1 diabetes-induced heart malfunction, Mol. Cell. Biol. 34 (2014) 2721–2731.
[43] N. Roe, D. Thomas, J. Ren, Inhibition of NADPH oxidase alleviates experimental diabetes-induced myocardial contractile dysfunction, Diabetes. Obes. Metab. 13 (2011) 465–473.
[44] M. Gharib, H. Tao, T.V. Fungwe, T. Hajri, Cluster differentiating 36 (CD36) deficiency attenuates obesity-associated oxidative stress in the heart, PLoS One 11 (2016) e0155611.
[45] M. Fukuda, T. Nakamura, K. Kataoka, H. Nako, Y. Tokutomi, Y.-F. Dong, O. Yasuda, H. Ogawa, S. Kim-Mitsuyama, Ezetimibe ameliorates cardiovascular complications and hepatic steatosis in obese and type 2 diabetic db/db mice, J. Pharmacol. Exp. Ther. 335 (2010) 70–75.
[46] D.R. Gonzalez, A.V. Treuer, G. Lamirault, V. Mayo, Y. Cao, R.A. Dulce, J.M. Hare, NADPH oxidase-2 inhibition restores contractility and intracellular calcium handling and reduces arrhythmogenicity in dystrophic cardiomyopathy, Am. J. Physiol. Heart Circ. Physiol. 307 (2014) H710–H721.
[47] P.K. Mishra, N. Tyagi, U. Sen, I.G. Joshua, S.C. Tyagi, Synergism in hyperhomocysteinemia and diabetes: role of PPAR gamma and tempol, Cardiovasc. Diabetol. 9 (2010) 49.
[48] M.F. da Silva, A.J. Natali, E. da Silva, G.J. Gomes, B.G. Teodoro, D.N. Cunha, L.R. Drummond, F.R. Drummond, A.G. Moura, F.G. Belfort, Attenuation of Ca2 + homeostasis, oxidative stress, and mitochondrial dysfunctions in diabetic rat heart: insulin therapy or aerobic exercise? J. Appl. Physiol. 119 (2015) 148–156.
[49] A. Fontayne, P.M.-C. Dang, M.-A. Gougerot-Pocidalo, J. El Benna, Phosphorylation of p47phox sites by PKC α, βII, δ, and ζ: effect on binding to p22phox and on NADPH oxidase activation, Biochemistry 41 (2002) 7743–7750.
[50] S. Lei, H. Li, J. Xu, Y. Liu, X. Gao, J. Wang, K.F. Ng, W.B. Lau, X.-l. Ma, B. Rodrigues, Hyperglycemia-induced protein kinase C β2 activation induces diastolic cardiac dysfunction in diabetic rats by impairing caveolin-3 expression and Akt/eNOS signaling, Diabetes 62 (2013) 2318–2328.
[51] B. Jaishy, Q. Zhang, H.S. Chung, C. Riehle, J. Soto, S. Jenkins, P. Abel, L.A. Cowart, J.E. Van Eyk, E.D. Abel, Lipid-induced NOX2 activation inhibits autophagic flux by impairing lysosomal enzyme activity, J. Lipid Res. 56 (2015) 546–561.
[52] L.C. Joseph, E. Barca, P. Subramanyam, M. Komrowski, U. Pajvani, H.M. Colecraft, M. Hirano, J.P. Morrow, Inhibition of NAPDH oxidase 2 (NOX2) prevents oxidative stress and mitochondrial abnormalities caused by saturated fat in cardiomyocytes, PLoS One 11 (2016) e0145750.
[53] M. Fukuda, T. Nakamura, K. Kataoka, H. Nako, Y. Tokutomi, Y.-F. Dong, H. Ogawa, S. Kim-Mitsuyama, Potentiation by candesartan of protective effects of pioglitazone against type 2 diabetic cardiovascular and renal complications in obese mice, J. Hypertens. 28 (2010) 340–352.
[54] D.D. Belke, W.H. Dillmann, Altered cardiac calcium handling in diabetes, Curr. Hypertens. Rep. 6 (2004) 424–429.
[55] G.M. Kuster, S. Lancel, J. Zhang, C. Communal, M.P. Trucillo, C.C. Lim, O. Pfister, E.O. Weinberg, R.A. Cohen, R. Liao, Redox-mediated reciprocal regulation of SERCA and Na + –Ca2 + exchanger contributes to sarcoplasmic reticulum Ca2 + depletion in cardiac myocytes, Free Radic. Biol. Med. 48 (2010) 1182–1187.
[56] C. Heymes, J.K. Bendall, P. Ratajczak, A.C. Cave, J.-L. Samuel, G. Hasenfuss, A.M. Shah, Increased myocardial NADPH oxidase activity in human heart failure, J. Am. Coll. Cardiol. 41 (2003) 2164–2171.
[57] T.J. Guzik, S. Mussa, D. Gastaldi, J. Sadowski, C. Ratnatunga, R. Pillai, K.M. Channon, Mechanisms of increased vascular superoxide production in human diabetes mellitus, Circulation 105 (2002) 1656–1662.
[58] G. Bjelakovic, D. Nikolova, L.L. Gluud, R.G. Simonetti, C. Gluud, Mortality in randomized trials of antioxidant supplements for primary and secondary prevention: systematic review and meta-analysis, JAMA 297 (2007) 842–857.
[59] E.R. Miller, R. Pastor-Barriuso, D. Dalal, R.A. Riemersma, L.J. Appel, E. Guallar, Meta-analysis: high-dosage vitamin E supplementation may increase all-cause mortality, Ann. Intern. Med. 142 (2005) 37–46.
[60] G. Teixeira, C. Szyndralewiez, S. Molango, S. Carnesecchi, F. Heitz, P. Wiesel, J.M. Wood, Therapeutic potential of NADPH oxidase 1/4 inhibitors, Br. J. Pharmacol. 174 (2017) 1647–1669.
[61] S. Altenhöfer, K.A. Radermacher, P.W. Kleikers, K. Wingler, H.H. Schmidt, Evolution of NADPH oxidase inhibitors: selectivity and mechanisms for target engagement, Antioxid. Redox Signal. 23 (2015) 406–427.
[62] J.D. Pollock, D.A. Williams, M.A. Gifford, L.L. Li, X. Du, J. Fisherman, S.H. Orkin, C.M. Doerschuk, M.C. Dinauer, Mouse model of X-linked chronic granulomatous disease, an inherited defect in phagocyte superoxide production, Nat. Genet. 9 (1995) 202–209.
[63] J. Kuroda, T. Ago, S. Matsushima, P. Zhai, M.D. Schneider, J. Sadoshima, NADPH oxidase 4 (Nox4) is a major source of oxidative stress in the failing heart, Proc. Natl. Acad. Sci. 107 (2010) 15565–15570.

Paper I:

NADPH Oxidase 2 Mediates Myocardial Oxygen Wasting in Obesity

antioxidants

MDPI

Article

NADPH Oxidase 2 Mediates Myocardial Oxygen Wasting in Obesity

Anne D. Hafstad [1,*], Synne S. Hansen [1], Jim Lund [1], Celio X. C. Santos [2], Neoma T. Boardman [1], Ajay M. Shah [2] and Ellen Aasum [1]

[1] Cardiovascular Research Group, Department of Medical Biology, Faculty of Health Sciences, UIT—The Arctic University of Norway, 9019 Tromsø, Norway; synne.s.hansen@uit.no (S.S.H.); jim.lund@ri.se (J.L.); neoma.boardman@uit.no (N.T.B.); ellen.aasum@uit.no (E.A.)

[2] School of Cardiovascular Medicine & Sciences, King's College London British Heart Foundation Centre of Excellence, London SE5 9NU, UK; celioxcs@yahoo.com.br (C.X.C.S.); ajay.shah@kcl.ac.uk (A.M.S.)

* Correspondence: anne.hafstad@uit.no

Received: 17 December 2019; Accepted: 17 February 2020; Published: 19 February 2020

Abstract: Obesity and diabetes are independent risk factors for cardiovascular diseases, and they are associated with the development of a specific cardiomyopathy with elevated myocardial oxygen consumption (MVO_2) and impaired cardiac efficiency. Although the pathophysiology of this cardiomyopathy is multifactorial and complex, reactive oxygen species (ROS) may play an important role. One of the major ROS-generating enzymes in the cardiomyocytes is nicotinamide adenine dinucleotide phosphate (NADPH) oxidase 2 (NOX2), and many potential systemic activators of NOX2 are elevated in obesity and diabetes. We hypothesized that NOX2 activity would influence cardiac energetics and/or the progression of ventricular dysfunction following obesity. Myocardial ROS content and mechanoenergetics were measured in the hearts from diet-induced-obese wild type (DIO_{WT}) and global NOK2 knock-out mice (DIO_{KO}) and in diet-induced obese C57BL/6J mice given normal water (DIO) or water supplemented with the NOX2-inhibitor apocynin (DIO_{APO}). Mitochondrial function and ROS production were also assessed in DIO and DIO_{APO} mice. This study demonstrated that ablation and pharmacological inhibition of NOX2 both improved mechanical efficiency and reduced MVO_2 for non-mechanical cardiac work. Mitochondrial ROS production was also reduced following NOX2 inhibition, while cardiac mitochondrial function was not markedly altered by apocynin-treatment. Therefore, these results indicate a link between obesity-induced myocardial oxygen wasting, NOX2 activation, and mitochondrial ROS.

Keywords: obesity; ROS; NADPH-oxidase; myocardial oxygen consumption; metabolism; cardiac efficiency

1. Introduction

Obesity, insulin resistance, and diabetes are independent risk factors for heart failure [1], and they are associated with a distinct diabetic cardiomyopathy independent of coronary heart disease or hypertension [2]. The pathophysiology behind this type of cardiomyopathy is far from elucidated, but increased oxidative stress is suggested to play an essential role [3,4]. A major non-mitochondrial source of ROS in cardiomyocytes are NADPH oxidases (NOXs). NOX2 is one of the main isoforms in the cardiomyocyte and several potent activators of NOX2, such as hyperglycemia, hyperlipidemia, angiotensin II, and cytokines [5,6], are known to be elevated in animals models of obesity and diabetes [7]. Experimental studies have demonstrated NOX2 upregulation in terms of gene expression, protein levels, and activity in the left ventricle of both type I [8–11] and type II [12–14] diabetic models. Pharmacological and genetic strategies for reducing NOX2 activity have also been associated with

amelioration of oxidative stress and other factors that are believed to contribute to the development of diabetic cardiomyopathy, including fibrosis, ER stress markers, autophagy, and inflammation, in combination with improved ventricular function [7].

Important hallmarks of diabetic cardiomyopathy are altered myocardial metabolism with increased fatty acid oxidation [15–17], energy imbalance [15,18], impaired mechanoenergetic properties [19], and increased myocardial oxygen consumption (MVO_2) [20]. The underlying mechanisms for the increase in MVO_2 are not fully elucidated, but they may be linked to the increased fatty acid load [19] or oxidation [21], impaired calcium handing [22], and/or mitochondrial dysfunction [23,24].

Whether increased NOX2-mediated signalling might influence obesity/diabetes-induced impairments in myocardial metabolism and/or efficiency is not known. However, NOX2-signalling has been shown to influence many of the same factors that are believed to contribute to myocardial oxygen wasting in obesity/diabetes. These include changes in mitochondrial function and ROS production [25], as well as altered activity of calcium-handling proteins and impaired calcium homeostasis [26–29]. In accordance with this, we have also shown an association between cardiac tissue ROS-content and MVO_2 in the hearts from diet-induced obese mice [23], suggesting a role for ROS in myocardial oxygen wasting. Based on this, we hypothesize that genetic ablation and the pharmacological inhibition of NOX2 may attenuate obesity-induced oxygen wasting in the myocardium.

2. Materials and Methods

2.1. Animals

Global NOX2 knock-out mice (NOX2 KO) and their wild-type littermates (WT) on a C57BL/6J background, which were originally obtained from a colony established at King's College, London, UK, were bred locally. Five weeks old, male NOX2 KO mice (n = 16) and their wild-type male littermates (WT, n = 14) were fed a high a fat diet (HFD; 60% kcal from fat, TestDiet, London, UK) for 28 weeks, resulting in diet-induced obese mice (DIO_{KO} and DIO_{WT}, respectively). Age matched WT (n = 7) and NOX2 KO (n = 7) mice that were fed a standard control diet served as lean controls (CON_{WT} and CON_{KO}).

In another cohort of animals, obesity was induced in male C57BL/6J mice (Charles River Laboratories, n = 42) by feeding them a Western, palatable diet for 18 or 28 weeks (WD, 35% kcal from fat, TestDiet, London UK) starting at the age of 5–6 weeks. After seven weeks on this diet, the mice were divided into two weight-matched groups receiving either normal water (DIO, n = 23) or water supplemented with the NOX2 inhibitor; 2.4 g/L apocynin ($DIO_{APO,}$ n = 19 [30]) for the rest of the feeding periods. The age-matched mice were fed a standard control diet (CON, n = 22). Another subset of mice (DIO, DIO_{APO} and CON, 6–7 mice per group) were included to study mitochondrial function.

The experiments were designed according to the guidelines from the Federation of European Laboratory Animal Science Associations (FELASA), EU animal research directive (86/609/EEC), Council of Europe (ETS 123), and the EU directive (2010/63/ EU). The local authority of the National Animal Research Authority in Norway approved the ethical protocols (FOTS id: 4772 and 3946). The 3R's (Replacement, Reduction, and Refinement) have specifically been addressed when designing the study. All mice received chow *ad libitum*, free access to drinking water, and they were housed at 23 °C.

2.2. Plasma Parameters

To test glucose tolerance, blood was collected from the saphenous vein in fasted (4 h) animals and measured (glucometer, FreeStyle Lite, Alameda, CA) before (0 min.) and 15, 30, 60, 120 min. after administration of a glucose solution (1.3 g/kg body wt i.p.). Plasma free fatty acids (FFA) were analyzed using a commercial kit (NEFA-HR, Wako, Germany) and insulin was analyzed using ELISA kits (DRG Diagnostics, Germany). Insulin resistance was evaluated while using the homeostatic model assessment for quantifying insulin resistance (HOMA). This was calculated from the product of fasting blood glucose and insulin (μU/mL), and then divided by 22.5 [31].

2.3. Isolated Heart Perfusions

The isolated hearts were perfused with a modified KHB buffer supplemented with 0.5 mM palmitate bound to 3% BSA. Myocardial glucose and fatty acid oxidation rates were measured in isolated perfused working hearts, while using radio-labelled isotopes [15]. Stroke work (SW) and parameters of left ventricular (LV) function were assessed by a 1.0 F micromanometer-conductance catheter. Myocardial oxygen consumption (MVO_2) was measured using fiber-optic oxygen probes, as previously described [19]. The relationship between cardiac work and MVO_2 was used to evaluate mechanical efficiency [19]. MVO_2 was also measured in unloaded, retrograde-perfused hearts before ($MVO_{2\ unloaded}$) and after KCl-arrest, to measure oxygen cost for basal metabolism ($MVO_{2\ BM}$). Based on these measurements, we also calculated the oxygen consumption for processes related to excitation-contraction coupling ($MVO_{2\ ECC}$) [20].

2.4. Assessment of ROS Production in Myocardial Tissue

ROS production was assessed while using the dihydroethidium-high pressure liquid chromatography (DHE-HPLC) method, as described before [32]. Briefly, fresh LV tissue (58.7 ± 2.5 mg) was incubated with 100 µM DHE in PBS containing 100µM DTPA for 30 min. at 37 °C. The samples were quickly washed with PBS/DTPA, resuspended in cold acetonitrille and sonicated (3 × 8 W, 5 sec). The homogenates were centrifuged at 13,000 rpm for 10 min. and the supernatant collected in a new tube and dried under vacuum while using a SpeedVacuum (ThermoScientific). The dried pellet was frozen at −80 °C and further resuspended in PBS/DTPA and then injected into a HPLC system (Dionex, UltiMate 3000, London, UK). DHE was monitored by ultraviolet absorption at 245 nm and either hydroxyethidium (EOH) and ethidium (E) were monitored by fluorescence detection with excitation 510 nm and emission 595 nm. Here, the DHE-derived products are expressed as ratios of EOH and E per DHE consumed per gram of wet weight tissue.

2.5. Mitochondrial Function and ROS Production

In a follow-up study, we sought to investigate the mitochondrial effects of NOX2 inhibition by apocynin treatment of C57BL/6J fed a WD for 28 weeks (CON, DIO, and DIO_{APO} mice). Isolated cardiac mitochondria were obtained from freshly harvested LV tissue while using a slight modification of the method of Palmer et al. [33], and mitochondrial function was measured in an oxygraph (Oxygraph 2k, Oroboros Instruments, Austria). The experiments were performed using malate (2.5 mM), glutamate (5mM) and pyruvate (10mM, PG), or malate (2.5 mM) and palmityol-carnitine (10mM, PC) as substrates. Mitochondrial leak state was determined before ADP addition (Leak). A saturated amount of ADP was then added to induce maximal mitochondrial respiration capacity (OXPHOS). Cytochrome C was added to the chambers (10 µM) to evaluate the integrity of mitochondrial membranes. H_2O_2 production was also assessed in respiring mitochondria while using Amplex UltraRed (AmR, 10 µM) dye. The reaction of H_2O_2 and AmR was catalyzed by horseradish peroxidase (10 uU) to produce a red fluorescent compound (recorded by the Fluo LED2-Module in Oxygraph 2k). The AUR signal was calibrated during the protocols using a fixed amount of H_2O_2 (10 µM). Exogenous SOD (5 µM) was added to reduce any remaining O_2^- to H_2O_2. The rates of respiration and ROS production were adjusted to protein content and experiments were performed at 37 °C.

2.6. Real-Time Quantitative PCR

RNA was isolated from perirenal white adipose tissue (PWAT), stored in Allprotect Tissue Reagent, and then measured using the RNeasy Lipid Tissue Mini Kit protocol (Qiagen, Hilden, Germany). The liver samples were stored in RNA later (Qiagen, Hilden, Germany) at −20 °C until the isolation of RNA by RNeasy Fibrous Mini Kit protocol with a small modification (the Proteinase K step was removed). The RNA concentration and purity were determined using spectrophotometry (NanoDrop 2000, Thermo Fisher, Waltham, MA, USA). 200 ng (PWAT) or 1000 ng (liver) of RNA was

reverse-transcribed into cDNA while using High Capacity cDNA Reverse Transcription Kit (Thermo Fisher, Waltham, MA, USA). Real-time PCR was performed in a LightCycler®96 System (Roche, Basel, Switzerland), where we pipetted 5 ng (PWAT) or 12.5 ng (liver) of cDNA and FastStart Essential DNA Green Master (Roche, Basel, Switzerland). Our target genes were Tumor necrosis factor-alpha (*Tnfα*) and NOX2 (*Nox2*). *Tnfα* (NM_013693.3) forward primer: CAT-CTT-CTC-AAA-ATT-CGA-GTG-ACA-A and reversed primer: TGG-GAG-TAG-ACA-AGG-TAC-AAC-CC. *Nox2* (NM_007807.5) forward primer: TGAATGCCAGAGTCGGGATT and reversed primer: CCC-CCT-TCA-GGG-TTC-TTG-ATT-T. The target gene expression levels were normalized to hypoxanthine phosphoribosyltransferase 1 (*Hprt1*, NM_013556.2) detected by forward primer: TCC-TCC-TCA-GAC-CGC-TTT-T and reverse primer: CCT-GGT-TCA-TCA-TCG-CTA-ATC. The stability of the housekeeping gene was determined by geNorm [34].

2.7. Statistical Analysis

The data are expressed as mean ± SEM. Differences between groups were analysed using a One-Way ANOVA. A post-hoc test (Holm-Sidak method) was used with multiple comparisons between groups when using different genotypes (CON_{WT}, CON_{KO}, DIO_{WT} and DIO_{KO}) and comparison against a control (DIO) when using the same genotype (CON, DIO and DIO_{APO}). The overall significance level was set to $p < 0.05$. The differences between diets within the same genotype and differences between genotypes within the same diet are indicated within the tables and figures.

3. Results

3.1. Effect of NOX2 Ablation and Inhibition on Obesity, Glucose Tolerance and Inflammatory Status

Obesity promotes a low-grade chronic inflammation, which is associated with insulin resistance in mice. Therefore, we assessed both insulin resistance and a marker of hepatic and adipose tissue inflammation. Following 28 weeks on a HFD, DIO_{WT} and DIO_{KO} displayed similar gain in body-weight, PWAT, and liver weight when compared to their respective lean genotypes (CON_{WT} and CON_{KO}, Table 1). An analysis of liver and white adipose tissue also showed increased hepatic and PWAT mRNA expression of NOX2 and the inflammatory marker TNFα (Table 1) in DIO_{WT} mice. Knocking down NOX2 did not reduce the hepatic expression of *tnfα* following obesity in DIO_{KO} compared to DIO_{WT} mice (Table 1). However, PWAT *tnfα* expression was significantly reduced in DIO_{KO} mice (Table 1), suggesting reduced adipose inflammation. The plasma levels of glucose and FFA were not different between groups, while fasted plasma insulin and HOMA-indexes were elevated in DIO_{WT} as compared to CON_{WT}. Although there was also a trend towards reduced HOMA-IR in DIO_{KO} when compared to CON_{KO}, this did not reach statistical significance.

Apocynin was added to the drinking water in order to reduce NOX2 activity in obese C57BL/6J mice to further study the effects of NOX2-activity in obesity. We used two time-points, 18 and 28 weeks of western diet (WD) feeding, in order to follow the development of obesity and systemic effects of NOX2 inhibition. In the first six weeks of apocynin treatment, body weight gain was significantly lower in DIO_{APO} when compared to untreated DIO mice (data not shown), but, at the 18 week time-point, there were no measurable effects of apocynin-treatment on obesity, liver, or PWAT weight (Table 2). However, there was an increased glucose tolerance and reduced levels of circulating FFA in DIO_{APO} mice as compared to non-treated DIO mice at this time point (Table 2). Weight gain increased to a similar extent in DIO and DIO_{APO} mice following 28 weeks of WD However, liver weights were reduced by apocynin-treatment (Table 2). Glucose tolerance was not attenuated by apocynin treatment in DIO_{APO} mice and, surprisingly, plasma FFA was not different between groups at this time-point (Table 2).

Table 1. Animal characteristics of wild type (WT) and global NOX2 knock-out (KO), control mice (CON), and diet-induced obese mice (DIO) given an obesogenic diet for 28 weeks.

	CON_{WT} $n = 7–9$	CON_{KO} $n = 7$	DIO_{WT} $n = 10–15$	DIO_{KO} $n = 10–16$
Body weight (g)	35.1 ± 1.8	35.0 ± 1.0	50.8 ± 1.2 *	49.4 ±1.4 *
Heart weight (mg)	158 ± 3	159± 4	177 ± 6 *	183 ± 5 *
PWAT weight (g)	0.70 ± 0.12	0.61 ± 0.04	0.21 ± 15 *	0.22 ± 0.19 *
$Nox2_{PWAT}$	1.0 ± 0.2	n.d.	5.0 ± 1.2 *	n.d.
$Tnf\alpha_{PWAT}$	1.0 ± 0.2	0.7 ± 0.1	10.2 ± 2.6 *	3.0 ± 0.6 *,#
Liver weight (g)	1.7 ± 0.2	1.5 ± 0.1	2.7 ± 0.2 *	2.6 ± 0.2 *
$Nox2_{liver}$	1.0 ± 0.2	n.d.	1.9 ± 0.3 *	n.d.
$Tnf\alpha$ l_{iver}	1.0 ± 0.3	0.9 ± 0.2	2.9 ± 0.4 *	2.8 ± 0.3 *
Plasma FFA_{fed} (μM)	532 ± 112	967 ± 292	835 ± 96	1057 ± 260
Blood glucose $_{fasted}$ (mmol/L)	5.6 ± 0.2	7.0 ± 0.1	6.6 ± 0.5	7.1 ± 0.3
Insulin $_{fasted}$ (μU/mL)	1.7± 0.3	2.1 ± 0.4	6.5 ± 1.5 *	4.5 ± 0.5
HOMA-IR	2 ± 1	3 ± 1	30 ± 13 *	13 ± 3

Blood samples were obtained from n = 5–10 per group. Perirenal white adipose tissue (PWAT), free fatty acids (FFA). The mRNA expression of genes encoding for tumor necrosis factor α (Tnfα) and NADPH oxidase 2 (NOX2), was normalized to the corresponding expression in CON_{WT}. Values are means ± SEM. * $p < 0.05$ CON vs. DIO within the same genotype. # $p < 0.05$ between genotypes in the same diet.

Table 2. Animal characteristics of chow fed controls (CON) and diet-induced obese C57BL/6J mice with or without apocynin treatment (DIO and DIO_{APO}).

18 Weeks of Diet	**CON** $n = 8–11$	**DIO** $n = 8–12$	DIO_{APO} $n = 8–9$
Body weight (g)	30.1 ± 0.4	42.7 ± 1.2 *	40.1 ± 1.8
Heart weight (mg)	134 ± 3	144 ± 4 *	149 ± 6
PWAT weight (g)	0.2 ± 0.2	1.0 ± 0.7 *	0.8 ± 1.1
Liver weight (g)	1.1 ± 0.1	1.7 ± 0.2 *	1.4 ± 0.1
Plasma FFA_{fed} (μM)	638 ± 88	1086 ± 143 *	648 ± 88 #
Blood glucose $_{fasted}$ (mM)	4.7 ± 0.2	5.1 ± 0.2	4.7 ± 0.1
Glucose tolerance test (AUC)	603 ± 45	945 ± 57 *	761 ± 52 #
28 Weeks of Diet	$n = 8–10$	$n = 8–14$	$n = 8–10$
Body weight (g)	31.6 ± 0.8	49.9 ± 1.2 *	46.5 ± 1.6
Heart weight (mg)	139 ± 4	158 ± 3 *	154 ± 4
PWAT weight (g)	0.4 ± 0.7	1.4 ± 0.6 *	1.2 ± 83
Liver weight (g)	1.1 ± 0.1	2.4 ± 0.2 *	1.8 ± 0.2 #
Plasma FFA_{fed} (μM)	583 ± 44	637 ± 74	655 ± 39
Blood glucose $_{fasted}$ (mM)	5.6 ± 0.3	6.0 ± 0.3	5.8 ± 0.3
Glucose tolerance test (AUC)	747 ± 55	926 ± 50 *	861 ± 67

Blood samples were obtained from 16–22 mice per group (18wk) and 10–14 in per group (28wk). Perirenal white adipose tissue (PWAT), area under curve (AUC). The values are means ± SEM. * $p < 0.05$ CON vs. DIO, # $p < 0.05$ DIO vs. DIO_{APO}.

Together, these data suggest modest systemic effects of both NOX2 ablation and inhibition with a slight increase in glucose tolerance as well as an improved low-grade adipose inflammatory response to diet-induced obesity.

3.2. Effects of Obesity and NOX Inhibition on Myocardial Reactive Oxygen Species

Pieces of left ventricular (LV) tissue were incubated with DHE, and the fluorescence of the products hydroxyethidium (EOH) and ethidium (E) were measured using HPLC, in order to examine whether ablation or inhibition of NOX2 activity could reduce cardiac ROS-content. The EOH product is a specific superoxide-derived DHE product, and was increased in cardiac tissue from both models of obesity following 28 weeks of obesogenic diet when compared to their lean controls. The ablation

and inhibition of NOX2 reduced the EOH product in cardiac tissue following obesity (Figure 1A,B). The ethidium product (which relates to other ROS) was not significantly elevated in ventricular tissue from obese mice or influenced by NOX2 ablation or inhibition (Figure 1C,D).

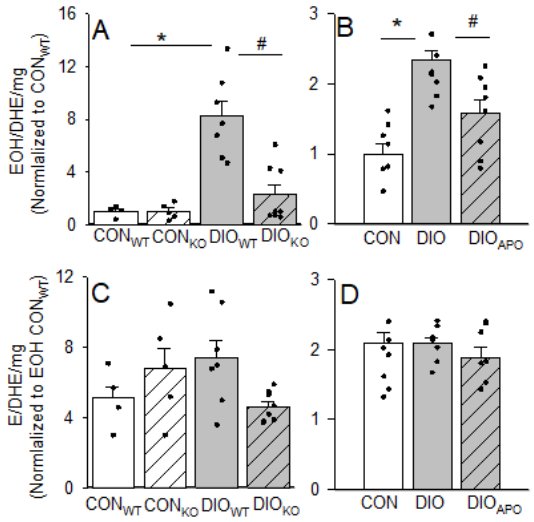

Figure 1. Reactive oxygen species-products hydroxyethidium (EOH) and ethidium (E) per dihydroethidium (DHE) consumed in cardiac tissue from lean controls (CON_{WT} and CON_{KO}) and obese (DIO_{WT} and DIO_{KO}) wild type and NOX2 KO mice fed a high fat diet for 28 weeks (**A**,**C**). Also shown in lean (CON), obese (DIO), and apocynin-treated obese (DIO_{APO}) C57BL/6J mice fed a western diet for 28 weeks (**B**,**D**) n = 4–8 in each group. Values are normalized to EOH in lean controls. Single values and means ± SEM. * $p < 0.05$ CON vs. DIO within same genotype, $^{\#}$ $p < 0.05$ DIO_{WT} vs. DIO_{KO} and DIO vs. DIO_{APO}.

3.3. *Effects of NOX2 Ablation and Inhibition on Ventricular Function*

Twenty-eight weeks of HFD induced LV dysfunction in DIO_{WT} mice. This was mainly a diastolic dysfunction, being illustrated by increased LV end-diastolic pressure (LVEDP) and end-diastolic pressure-volume relationships (EDPVR, Table 3). However, obesity-induced diastolic dysfunction was abrogated in DIO_{KO} mice, as these hearts exhibited reduced LVEDP and EDPVR when compared to DIO_{WT} (Table 3). In addition, the LV relaxation time-constant (Tau) was significantly lower in DIO_{KO} as compared to DIO_{WT} hearts, suggesting improved early LV diastolic function (Table 3). Although the parameters of LV systolic function (such as dP/dt max and Preload Recruitable Stroke Work index, PRSWi) were not significantly different between groups, we found cardiac output to be modestly increased in DIO_{KO} as compared to DIO_{WT} (Table 3).

Eighteen weeks of WD did not induce LV dysfunction in DIO mice, as the parameters of LV function were similar between groups (Table 4). Twenty-eight weeks of WD induced both LV systolic and diastolic dysfunction, being evident as lower cardiac output, reduced dP/dt_{min}, increased relaxation factor (Tau) and EDPVR in DIO when compared to CON hearts (Table 4). Apocynin treatment increased LV systolic and diastolic function in DIO_{APO} mice, evident as increased cardiac output and PRSWi, together with the normalization of EDPVR relationships (Table 4).

Analysis of the relationship between LV end-diastolic pressure (LVEDP) and volume (LVEDV) at three different workloads showed a left and upwards shift of this relationship in DIO hearts following 28 weeks of obesogenic diet (Figure 2A,C), thus suggesting LV concentric remodeling. This was attenuated by both NOX2 ablation ($DIO_{KO,}$ Figure 2A) and by apocynin treatment (DIO_{APO}, Figure 2C). Ventricular volumes and pressures were not different between groups following 18 weeks of WD (Figure 2B).

Table 3. Steady state and load-independent parameters of left-ventricular (LV) function obtained in isolated perfused working hearts from wild type (WT) and global NOX2 knock out (KO) control mice (CON) and diet-induced obese mice (DIO) given an obesogenic diet for 28 weeks.

	CON_{WT} $n = 6$	CON_{KO} $n = 5$	DIO_{WT} $n = 6–11$	DIO_{KO} $n = 8–10$
Cardiac output (mL/min)	11.6 ± 0.6	11.8 ± 0.9	10.9 ± 0.4	12.2 ± 0.2#
Coronary flow (mL/min)	4.0 ± 0.3	3.5 ± 0.3	3.8 ± 0.3	3.7 ± 0.2
Heart rate (bpm)	418 ± 1	408 ± 10	419 ± 7	413 ± 6
dP/dt_{max} (mmHg/sec)	3515 ± 259	3093 ± 126	3785 ± 230	3806 ± 143
dP/dt_{min} (mmHg/sec)	−2982 ± 215	−2611 ± 106	−3134 ± 174	−3230 ± 110
Tau $_{Weiss}$ (msec)	10.8 ± 0.3	11.7 ± 0.3	11.7 ± 0.8	10.4 ± 0.3 #
LVEDP (mmHg)	7.9 ± 0.8	8.6 ± 0.6	12.5 ± 1.2 *	9.7 ± 0.7 #
LVDP (mmHg)	59 ± 2	59 ± 1	65 ± 2	66 ± 2
LVEDV (µL)	105 ± 4	106 ± 13	76 ± 14	97 ± 4
EDPVR (mmHg/µL)	0.12 ± 0.01	0.14 ± 0.01	0.24 ± 0.04 *	0.11 ± 0.01 #
PRSWi	34.0 ± 1.1	28.8 ± 2.1	30.1 ± 2.9	36.7 ± 2.4

Hearts were paced at 10% above intrinsic heart rate. Steady state parameters were obtained at a pre- and afterload of 8 and 50 mmHg, respectively. LV end-diastolic pressure (LVEDP), developed pressure (LVDP) and end-diastolic volume (LVEDV), maximum positive and negative first time derivative of LV pressure (dP/dt_{max} and dP/dt_{min}), LV relaxation time constant (Tau). Load-independent parameters; the slope of LV end-diastolic-pressure-volume relationships (EDPVR) and Preload Recruitable Stroke Work index (PRSWi) were obtained by a temporary preload reduction. Values are means ± SEM. * $p < 0.05$ within the same genotype. # $p < 0.05$ between genotypes in the same diet.

Table 4. Steady state and load-independent parameters of left-ventricular (LV) function obtained in isolated perfused working hearts from chow-fed controls (CON) and diet-induced obese C57BL/6J mice with or without apocynin treatment (DIO and DIO_{APO}).

18 Weeks of Diet	**CON** $n = 8$	**DIO** $n = 6$	DIO_{APO} $n = 6$
Aortic flow (mL/min)	10.8 ± 0.4	10.1 ± 0.6	10.7 ± 0.1
Coronary flow (mL/min)	3.0 ± 0.2	3.3 ± 0.2	3.3 ± 0.3
Heart rate (bpm)	396 ± 11	359 ± 17	399 ± 13
dP/dt_{max} (mmHg/sec)	3749 ± 138	3925 ± 65	3615 ± 159
dP/dt_{min} (mmHg/sec)	−2854 ± 105	−2961 ± 89	−2863 ± 131
Tau $_{Weiss}$ (msec)	11.0 ± 0.6	11.0 ± 0.4	11.3 ± 0.5
LVEDP (mmHg)	7.8 ± 1.1	8.5 ±1.1	9.0 ± 1.8
LVDP (mmHg)	57 ± 2	59 ± 2	57 ± 3
LVEDV (µL)	72 ± 10	58 ± 13	55 ± 14
EDPVR (mmHg/µL)	0.16 ± 0.01	0.19 ± 0.01	0.19 ± 0.04
PRSWi	29.9 ± 1.8	24.4 ± 1.2	27.4 ± 3.3
28 Weeks of Diet	$n = 7$	$n = 9$	$n = 8$
Aortic flow (mL/min)	12.5 ± 0.3	9.4 ± 0.9 *	12.1 ± 0.1 #
Coronary flow (mL/min)	3.2 ± 0.2	3.5 ± 0.2	3.2 ± 0.3
Heart rate (bpm)	434 ± 11	404 ± 9	415 ± 0.8
dP/dt_{max} (mmHg/sec)	3968 ± 50	3697 ± 121 *	3935 ± 92
dP/dt_{min} (mmHg/sec)	−3142 ± 51	−2735 ± 116 *	−2948 ± 68
Tau $_{Weiss}$ (msec)	10.0 ± 0.2	11.3 ± 0.4 *	10.8 ± 0.3
LVEDP (mmHg)	9.3 ± 0.6	10.7 ± 0.9	10.3 ± 0.6
LVDP (mmHg)	59 ± 1	56 ± 1	58 ± 1
LVEDV (µL)	94 ± 6	67 ± 8 *	87 ± 2 #
EDPVR (mmHg/µL)	0.18 ± 0.01	0.30 ± 0.04 *	0.18 ± 0.02 #
PRSWi	28.3 ± 2.7	23.7 ± 2.4	32.4 ± 1.5 #

The hearts were paced at 10% above intrinsic heart rate. Steady state parameters were obtained at a pre- and afterload of 8 and 50 mmHg, respectively. LV end-diastolic pressure (LVEDP), developed pressure (LVDP) and end-diastolic volume (LVEDV), maximum positive and negative first time derivative of LV pressure (dP/dt_{max} and dP/dt_{min}), LV relaxation time constant (Tau). Load-independent parameters including the slope of LV end-diastolic-pressure-volume relationships (EDPVR) and Preload Recruitable Stroke Work index (PRSWi) were obtained by a temporary preload reduction. Values are means ± SEM. * $p < 0.05$ CON vs. DIO. # $p < 0.05$ DIO vs. DIO_{APO}.

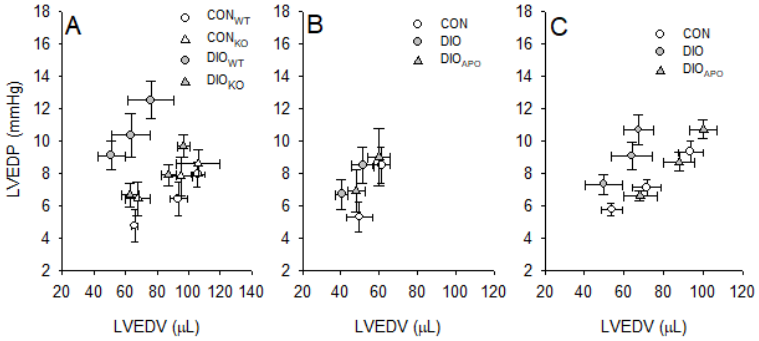

Figure 2. Steady state left ventricular end-diastolic volumes (LVEDV) and pressures (LVEDP) at three different workloads (preload: 4,6 and 8 mmHg and afterload: 50mmHg) from lean controls (CON_{WT} and CON_{KO}) and obese (DIO_{WT} and DIO_{KO}) wild type and NOX2 KO mice fed a high fat diet for 28 weeks (**A**), as well as lean (CON), obese (DIO) and apocynin-treated obese (DIO_{APO}) C57BL/6J mice fed a western diet for 18 (**B**) and 28 weeks (**C**). n = 5–10 per group, the values are mean ± SEM.

3.4. Effects of NOX2 Ablation and Inhibition on Myocardial Energetics

Reduced LV mechanical efficiency (stroke work/MVO_2) in hearts following obesogenic diets has been reported in several studies [23,34]. Here, we observed a trend towards reduced mechanical efficiency in DIO hearts following 18 weeks of WD (Figure 3B), with a significant reduction of LV mechanical efficiency in DIO when compared to CON hearts following 28 weeks of WD (Figure 3C). Ablation and inhibition of NOX2 both significantly increased mechanical efficiency in the hearts from obese mice (Figure 3A–C). The differences in LV mechanical efficiency were due to differences in MVO_2 at the 18-week timepoint (Figure 3E), while both reduced MVO_2 and increased SW seemed to contribute to increased LV mechanical efficiency following NOX2 ablation and inhibition after 28 weeks of obesogenic diets.

Obesity and diabetes have previously also been associated with elevated myocardial oxygen costs for non-mechanical processes ($MVO_{2unloaded}$) [23,35], which includes oxygen consuming processes that are associated with excitation-contraction coupling (ECC) and basal metabolism (BM) to maintain cellular homeostasis [20,23]. In line with the changes in mechanical efficiency, DIO_{KO} hearts also exhibited reduced $MVO_{2unloaded}$ compared to DIO_{WT} hearts when completely unloaded of mechanical work (Figure 4A). This was also found in DIO_{APO} hearts when compared to DIO hearts at both time points (Figure 4B,C). The reduced $MVO_{2unloaded}$ in DIO_{KO} hearts was associated with reduced myocardial oxygen consumption for ECC (MVO_{2ECC}, Figure 4D), and also found in DIO_{APO} after 18 weeks of obesogenic diet (Figure 4E). There were only subtle changes in the MVO_2 for basal metabolism between groups (MVO_{2BM}, Figure 4G,H). At the 28-week time point, both changes in MVO_{2ECC} and MVO_{2BM} (Figure 4F,I) seemed to contribute to a reduced obesity-induced oxygen wasting in unloaded hearts from DIO_{APO} mice.

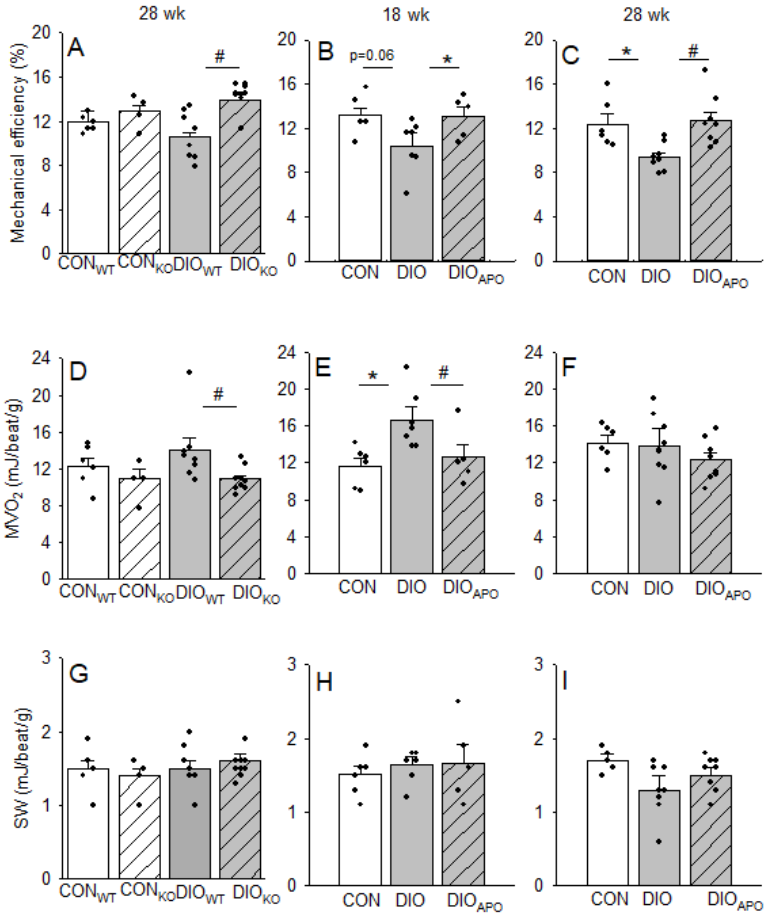

Figure 3. Left ventricular mechanical efficiency (**A**–**C**) expressed as stroke-work (SW, **G**–**I**) relative to myocardial oxygen consumption (**D**–**F**) in hearts from lean controls (CON_{WT} and CON_{KO}) and diet-induced obese (DIO) wild type and NOX2 KO mice (DIO_{WT} and DIO_{KO}) fed a high fat diet for 28 weeks (**A**,**D**,**G**) as well as lean controls (CON) and untreated and apocynin-treated obese C57BL/6J mice (DIO and DIO_{APO}) fed a western diet for 18 weeks (**B**,**E**,**H**) or 28 weeks (**C**,**F**,**I**). Single values and means ± SEM. * $p < 0.05$ CON vs. DIO within same genotype, $^{\#}$ $p < 0.05$ DIO_{WT} vs. DIO_{KO} and DIO vs. DIO_{APO}.

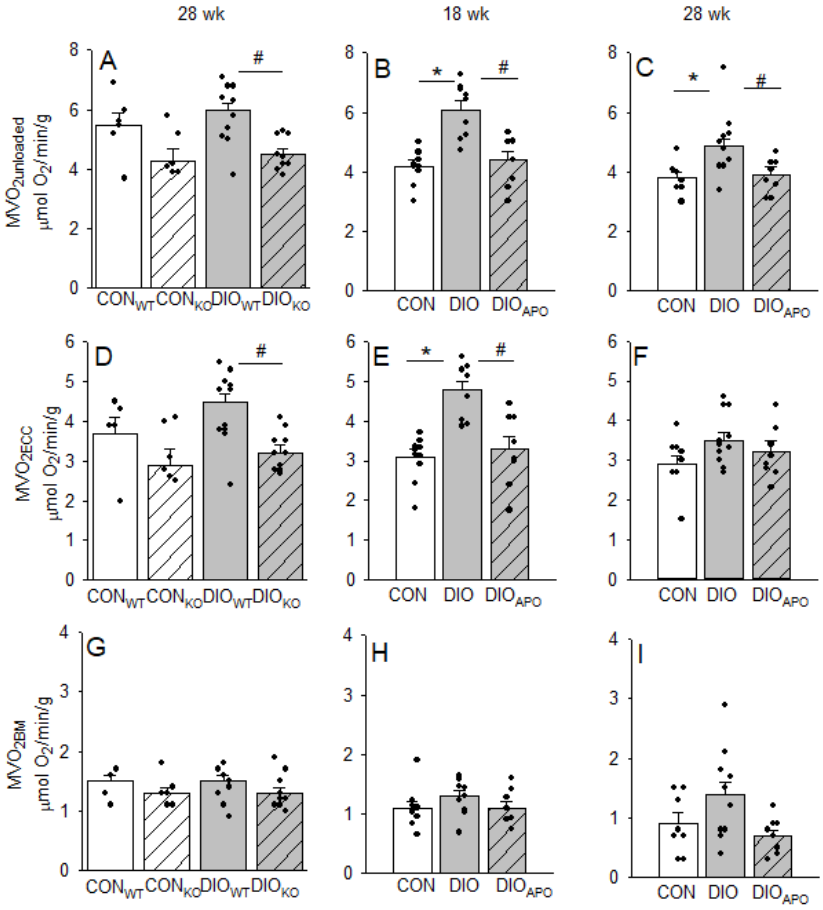

Figure 4. Myocardial oxygen consumption in mechanically unloaded hearts ($MVO_{2unloaded}$, **A**–**C**) and for processes associated with excitation-contraction coupling (MVO_{2ECC}, **D**–**F**) and basal metabolism (MVO_{2BM}, **G**–**I**) that was obtained from lean controls wild-type (CON_{WT}) and NOX2-KO mice (CON_{KO}) and obese mice fed a high fat diet for 28 weeks (DIO_{WT} and DIO_{KO}). (**A**,**D**,**G**). Also shown in lean controls (CON) and untreated and apocynin-treated obese C57BL/6J mice (DIO and DIO_{APO}) that were fed a western diet for 18 weeks (**B**,**E**,**H**) or 28 weeks (**C**,**F**,**I**). Single values and means ± SEM. * $p < 0.05$ within the same genotype, $^{\#}$ $p < 0.05$ between genotypes within the same diet.

3.5. Effects of NOX2 Inhibition on Myocardial Substrate Utilization and Mitochondrial Function

Myocardial glucose oxidation rates were markedly down in DIO as compared to CON hearts following 18 weeks of WD with a concomitant increase in palmitate oxidation rates. We did not find apocynin treatment to alter substrate oxidation rates (Figure 5).

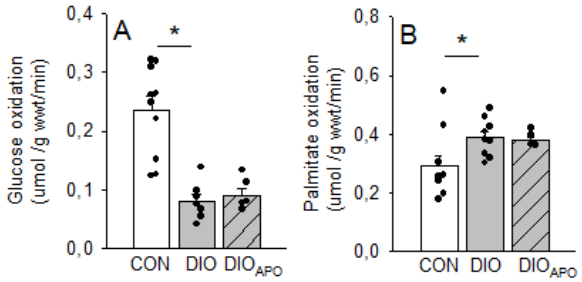

Figure 5. Glucose (**A**) and palmitate (**B**) oxidation rates measured in isolated working hearts from lean controls (CON), diet-induced obese (DIO), and obese apocynin-treated (DIO_{APO}) C57BL/6J mice fed an obesogenic western diet for 18 weeks. Single values and mean ± SEM, * $p < 0.05$ vs. DIO.

We further studied the mitochondrial function in ventricular tissue from CON, DIO, and DIO_{APO} mice that were fed a WD for 28 weeks. The respiration rates were measured while using pyruvate and glutamate (PG) or palmityol-carnitine (PC) as substrates. There were no significant changes in Leak or OXPHOS states when using PG or PC as substrates in isolated cardiac mitochondria (Figure 6A,B,D–E). Respiratory control ratios (OXPHOS/Leak) were not significantly different between groups when using PG as substrates (Figure 6C), but significantly higher in the mitochondria from DIO_{APO} hearts when using PC as substrates. There was also with a borderline difference between CON and DIO ($p = 0.08$, Figure 6F).

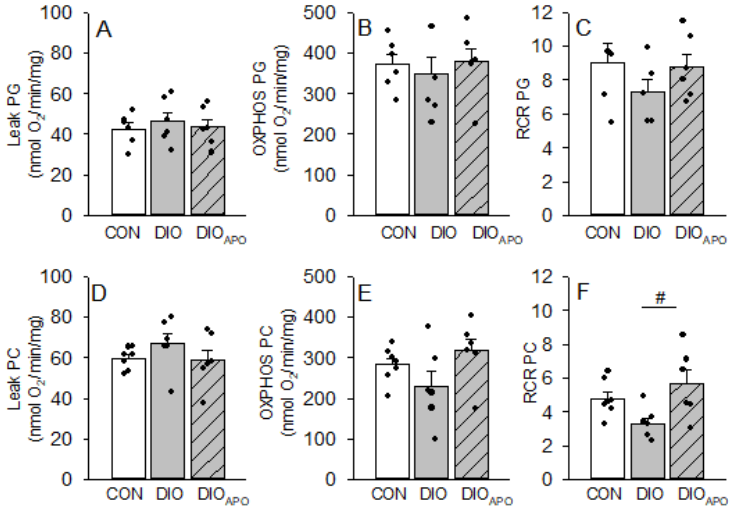

Figure 6. Oxygen fluxes (leak and maximal mitochondrial respiration capacity, OXPHOS) and respiratory coupling ratio (RCR) in isolated cardiac mitochondria using pyruvate and glutamate (PG, **A**–**C**) or palmityol-carnitine as substrates (PC, **D**–**F**). Mitochondria were obtained from lean controls (CON), untreated and apocynin-treated obese C57BL/6J mice (DIO and DIO_{APO}) fed a western diet for 28 weeks. Single values and mean ± SEM, $^{\#}$ $p < 0.05$ DIO vs. DIO_{APO}.

Finally, we assessed ROS production in isolated cardiac mitochondria. When adjusting the ROS production for mass or O_2 flux (respiration rate), we found increased ROS production in the leak state in mitochondria from DIO hearts when using PG and PC as substrates. This obesity-induced ROS production was attenuated following apocynin treatment (DIO_{APO}, Figure 7A,B). Similar results were found for ROS production in the OXPHOS states. In general, the mass-specific ROS production tended to be higher in the leak states than in the OXPHOS state within groups, while mitochondria respiring on PG exhibited higher ROS production than when respiring on PC ($p < 0.001$).

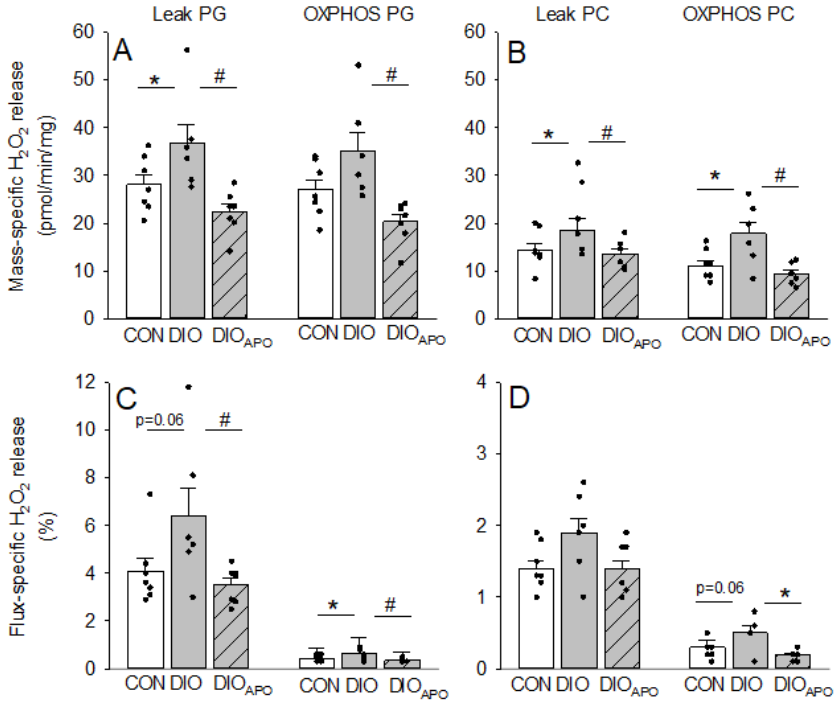

Figure 7. Mass-specific and flux-specific H_2O_2- release from isolated cardiac mitochondria using either pyruvate and glutamate (PG, panel **A** and **C**) or palmityol-carnitine as substrates (PC, panel **B** and **D**) as substrates. Mitochondria were obtained from lean controls (CON) and untreated and apocynin-treated obese C57BL/6J mice (DIO and DIO_{APO}) fed a western diet for 28 weeks. Single values and means ± SEM, * $p < 0.05$ CON versus DIO, # $p < 0.05$ DIO vs. DIO_{APO}.

4. Discussion

In the present study, we only found subtle systemic effects of NOX2-inibition and ablation (KO) on the development of diet-induced obesity. Reduced NOX2-activity tended to improve insulin resistance and transiently reduce plasma lipids. It had little effects in fat depots, but tended to reduce adipose tissue inflammation. However, reduced NOX2 activity did have a marked effect on the development of cardiac dysfunction and the obesity-induced impaired cardiac energetics. For the first time, we were able to demonstrate that the obesity-mediated increase in myocardial oxygen wasting was prevented in both NOX2-KO mice and by NOX2-inhibition with apocynin. We also demonstrated a possible cross-talk between NOX2-activation and mitochondrial ROS-production, as has been previously suggested.

Apocynin-treatment and NOX2-ablation have been associated with reduced obesity in several studies on mice while using different ages, types of obesogenic diets, and feeding periods [30,36–38]. Many studies have also suggested NOX2-derived oxidative stress to be involved in the progression of obesity and pre-diabetes, through impaired glucose tolerance [30,37,39,40], insulin resistance [39], dyslipidemia [37,38,40], and visceral adipose inflammation [30,36]. However, there are discrepancies regarding the systemic effects of NOX2 activity in obesity, with one study also reporting adverse systemic effects, such as hyperphagia, elevated obesity, hepatic steatosis, and inflammation, together with exacerbated insulin resistance in obese NOX2 KO mice [41]. The present study does not show major effects of reduced NOX2 activity on body weight gain while using long term obesogenic diets, but the data do suggest a transient reduction following the start of the apocynin-treatment. This is in line with previous studies using shorter feeding periods and similar apocynin-treatments of DIO mice [30,38]. Additionally, reduced NOX2 activity seemed to improve glucose tolerance, reduce hyperlipidemia, and reduce adipose inflammation following obesity to some degree, in accordance with previous studies [30,36]. We did not find NOX2 ablation to reduce the expression of these inflammatory markers, as previously reported, although obesity in the present study was also associated with increased

hepatic *nox2* gene expression and elevated markers of macrophage infiltration and inflammation in liver [30,38].

Even though the systemic effects of reduced NOX2 activity in obesity were subtle in our hands, the cardiac effects were more profound. Diabetes and obesity have been shown to increase myocardial NOX2 activity with both increased expression and recruitment of catalytic subunits to the plasma membrane and elevated ROS production [8,9,13,14,42,43]. Our data support this by showing elevated levels of EOH in cardiac tissue in DIO mice, which is primarily a product of increased superoxide. Apocynin treatment and the ablation of NOX2 partly normalized superoxide derived EOH, but had no effect on ethidium, suggesting reduced NOX2 activity when compared to reduced NOX4 (which primarily produces H_2O_2). Our results are also in line with previous data showing reduced cardiac NOX2 activity in diabetes and high fat feeding of mice following both the genetic ablation of NOX2 [8,44] and pharmacological treatment with NOX2-inhibitors [8,11].

In line with previous studies from our group using similar mouse strains, the use of a western diet seemed to produce more adverse cardiac effects in terms of inducing LV systolic and diastolic dysfunction [23] when compared to the use of a high fat diet which primarily induced LV diastolic dysfunction [34]. NOX2 knockout and apocynin-treatment both abrogated the development of obesity-induced LV dysfunction. This was evident as improved parameters of diastolic and systolic function and reduced concentric remodeling. Therefore, our results are in accordance with many studies where genetic and pharmacological strategies to reduce NOX2 activity have been associated with attenuation of LV dysfunction, pathological remodeling, in models of diabetes [8,9,11,12], sepsis-induced cardiomyopathy [29], pressure overload [45], and in the aged heart [28].

The present study also confirmed an obesity-mediated impairment of myocardial energetics, as previously reported in similar DIO models [22,23,34]. In accordance with previous studies [23], oxygen wasting processes were induced in the myocardium well before the development of LV dysfunction, as 18 weeks of WD induced elevated MVO_2 for non-mechanical work ($MVO_{2unladed}$) and processes that are associated with excitation-contraction coupling (MVO_{2ECC}) in the absence LV dysfunction. Although not significant, the MVO_2 used for basal metabolism also tended to be increased, however we were not able to reproduce previous studies showing the same decrease in mechanical efficiency or oxygen wasting effects following HFD [23,34,46]. One could speculate that also lean mice on the standard chow are becoming somewhat obese, and that a shorter feeding period in this mouse strain could have produced different results, due to the extensive feeding period.

More importantly, we found that the mechanical efficiency was increased, while $MVO_{2unloaded}$ and MVO_{2ECC} were reduced, suggesting improved cardiac energetics following NOX2 inhibition and ablation. The exact mechanisms behind obesity-induced myocardial oxygen wasting are not clear, but the increase in MVO_{2ECC} suggests that impaired calcium handling is a candidate. Many calcium handling proteins are redox sensitive and their activity may consequently be altered by NOXs [47]. Impaired calcium handling is well documented in diabetic hearts and includes altered sarcoplasmic reticulum Ca^{2+}-ATPase2 (SERCa2) activity [48], elevated intracellular Ca^{2+}-levels, and increased ryanodine receptor 2 (RyR2)-leakage [49]. Recently, Joseph et al. [44] reported profound effects of a short-term saturated high fat diet (SHFD, 4 weeks) of mice on myocardial calcium handling before the development of both obesity and ventricular structural changes. While SHFD induced heart rhythm abnormalities in WT mice, this was absent in NOX2 KO hearts and following apocynin treatment. Additionally, the oxidation of the RYR2 promotes calcium leak and increased calcium sparks, which were also absent in NOX2 KO hearts from mice that were fed a SHFD [44]. Other studies have reported a negative impact of NOX2-derived superoxide following acute exposure to FA load [25] and in other types of heart failure [28]. Our data demonstrating both improved LV function and myocardial energetics may very well be a functional consequence of the improved calcium handling associated with reduced NOX2 activity reported in the studies above. Wall stress has also been suggested to determine myocardial oxygen consumption [50], and it is partly determined by LV pressure. However, concentric remodeling could also reduce wall stress due to decreased LV radius and increased wall

thickness. Although the total LV wall stress was not addressed in the current study, one cannot exclude that attenuated LV remodeling with the reduced LV stiffness observed by NOX2 ablation and inhibition could have contributed to improved mechanical efficiency.

Diabetes and obesity are associated with increased myocardial FA oxidation rates, which is again suggested to contribute to an obligatory increase in myocardial oxygen consumption, as the oxidation of FAs requires more oxygen for the same amount of ATP produced, when compared to glucose. However, there is evidence that the increased O_2 cost for FA oxidation is lacking, and the inhibition of myocardial FA oxidation does not abolish the increase in MVO_2 when hearts are perfused with high FAs [51,52]. Although we also found that increased FA oxidation in DIO hearts is accompanied by increased MVO_2, we did not find the oxygen sparing effect of apocynin treatment to be linked to altered myocardial FA oxidation. This again supports that FA oxidation per se has no major role in altered MVO_2.

Several studies have associated diabetes and obesity with cardiac mitochondrial dysfunction, although there is no complete consensus in the literature [23,24,34]. Elevated, circulating FFA has been suggested to contribute, as an acute FA load to isolated hearts and cardiomyocytes has been shown to impair mitochondrial function [24,25]. The observed transient reduction in circulating FFA following apocynin treatment could very well be a contributor to the observed attenuation of detrimental cardiac effects. Although NOX2 is situated at the sarcolemma, Joseph et al. [25] found that both the inhibition and ablation of NOX2 could attenuate lipid-load induced mitochondrial respiratory dysfunction and mitochondrial ROS-release in cardiomyocytes. Maximal respiratory capacity was not impaired following obesity in cardiac mitochondria in the present study, but apocynin treatment was found to increase mitochondrial coupling. Improved mitochondrial coupling can be beneficial in terms of reducing oxygen-wasting processes for basal metabolism, and, therefore, could contribute to the reduced $MVO_{2unloaded}$ observed following NOX2 ablation and inhibition in the present study. Although apocynin has been reported to exhibit direct antioxidant properties in vascular systems [53], it is extensively used as an inhibitor of myocardial NOX2 activity in many studies. Our data also support reduced myocardial NOX2 activity to be associated with reduced cardiac mitochondrial ROS release [25,54]. The apocynin-mediated reduction in ROS could contribute to the improved mitochondrial coupling in mitochondria from these hearts, as ROS have been shown to activate mitochondrial uncoupling proteins [55].

5. Conclusions

In line with previous studies on other models of heart failure, this study demonstrates that ablation and inhibition of NOX2 both attenuated obesity-induced left ventricular remodeling and dysfunction. Reduced NOX2 activity was also associated with improved myocardial energetics that could be attributed to decreased myocardial oxygen consumption for non-mechanical work, including processes that are associated with excitation-contraction coupling. Myocardial substrate utilization and mitochondrial respiratory capacity was not profoundly affected by NOX2 inhibition, but obesity-induced mitochondrial ROS production was abrogated.

Author Contributions: Conceptualization, A.D.H., J.L. and E.A.; Data curation, A.D.H., S.S.H. and J.L.; Formal analysis, A.D.H., S.S.H., C.X.C.S., N.T.B. and E.A.; Funding acquisition, A.D.H. and E.A.; Investigation, A.D.H., S.S.H., J.L. and C.X.C.S.; Methodology, A.D.H., S.S.H., J.L., C.X.C.S., N.T.B., A.M.S. and E.A.; Project administration, A.D.H., J.L. and E.A.; Resources, A.D.H., A.M.S. and E.A.; Supervision, A.D.H. and E.A.; Visualization, A.D.H.; Writing—original draft, A.D.H. and S.S.H.; Writing—review & editing, A.D.H., N.T.B., A.M.S. and E.A. All authors have read and agreed to the published version of the manuscript.

Funding: This research was funded by The Norwegian Health Association (fellowship to ADH, 6682) the Novo Nordisk Foundation (NNF13OC0005765 and NNF14OC0010235, to EA), and the UiT-The Arctic University of Norway (fellowship to SSH and publication charges of the article). AMS is supported by the British Heart Foundation.

Acknowledgments: The contributions from Trine Lund, Thomas Andersen, Hege Hagerup, Victoria Steinsund and Knut Steines are greatly appreciated.

Conflicts of Interest: The authors declare no conflict of interest.

References

1. Kannel, W.B.; Hjortland, M.; Castelli, W.P. Role of diabetes in congestive heart failure: The Framingham study. *Am. J. Cardiol.* **1974**, *34*, 29–34. [CrossRef]
2. Fein, F.S.; Sonnenblick, E.H. Diabetic cardiomyopathy. *Cardiovasc. Drugs Ther.* **1994**, *8*, 65–73. [CrossRef] [PubMed]
3. Anderson, E.J.; Kypson, A.P.; Rodriguez, E.; Anderson, C.A.; Lehr, E.J.; Neufer, P.D. Substrate-specific derangements in mitochondrial metabolism and redox balance in the atrium of the type 2 diabetic human heart. *J. Am. Coll. Cardiol.* **2009**, *54*, 1891–1898. [CrossRef] [PubMed]
4. Giacco, F.; Brownlee, M. Oxidative stress and diabetic complications. *Circ. Res.* **2010**, *107*, 1058–1070. [CrossRef] [PubMed]
5. Anilkumar, N.; Weber, R.; Zhang, M.; Brewer, A.; Shah, A.M. Nox4 and nox2 NADPH oxidases mediate distinct cellular redox signaling responses to agonist stimulation. *Arterioscler. Thromb. Vasc. Biol.* **2008**, *28*, 1347–1354. [CrossRef] [PubMed]
6. Nabeebaccus, A.; Zhang, M.; Shah, A.M. NADPH oxidases and cardiac remodelling. *Heart Fail. Rev.* **2011**, *16*, 5–12. [CrossRef] [PubMed]
7. Hansen, S.S.; Aasum, E.; Hafstad, A.D. The role of NADPH oxidases in diabetic cardiomyopathy. *Biochim. Biophys. Acta Mol. Basis Dis.* **2018**, *1864*, 1908–1913. [CrossRef]
8. Shen, E.; Li, Y.; Li, Y.; Shan, L.; Zhu, H.; Feng, Q.; Arnold, J.M.O.; Peng, T. Rac1 is required for cardiomyocyte apoptosis during hyperglycemia. *Diabetes* **2009**, *58*, 2386–2395. [CrossRef] [PubMed]
9. Li, J.; Zhu, H.; Shen, E.; Wan, L.; Arnold, J.M.O.; Peng, T. Deficiency of rac1 blocks NADPH oxidase activation, inhibits endoplasmic reticulum stress, and reduces myocardial remodeling in a mouse model of type 1 diabetes. *Diabetes* **2010**, *59*, 2033–2042. [CrossRef] [PubMed]
10. Nishio, S.; Teshima, Y.; Takahashi, N.; Thuc, L.C.; Saito, S.; Fukui, A.; Kume, O.; Fukunaga, N.; Hara, M.; Nakagawa, M. Activation of CaMKII as a key regulator of reactive oxygen species production in diabetic rat heart. *J. Mol. Cell. Cardiol.* **2012**, *52*, 1103–1111. [CrossRef] [PubMed]
11. Roe, N.; Thomas, D.; Ren, J. Inhibition of NADPH oxidase alleviates experimental diabetes-induced myocardial contractile dysfunction. *Diabetes Obes. Metab.* **2011**, *13*, 465–473. [CrossRef]
12. Fukuda, M.; Nakamura, T.; Kataoka, K.; Nako, H.; Tokutomi, Y.; Dong, Y.-F.; Yasuda, O.; Ogawa, H.; Kim-Mitsuyama, S. Ezetimibe ameliorates cardiovascular complications and hepatic steatosis in obese and type 2 diabetic db/db mice. *J. Pharmacol. Exp. Ther.* **2010**, *335*, 70–75. [CrossRef]
13. Gharib, M.; Tao, H.; Fungwe, T.V.; Hajri, T. Cluster Differentiating 36 (CD36) deficiency attenuates obesity-associated oxidative stress in the heart. *PLoS ONE* **2016**, *11*, e0155611. [CrossRef]
14. Jaishy, B.; Zhang, Q.; Chung, H.S.; Riehle, C.; Soto, J.; Jenkins, S.; Abel, P.; Cowart, L.A.; Van Eyk, J.E.; Abel, E.D. Lipid-induced NOX2 activation inhibits autophagic flux by impairing lysosomal enzyme activity. *J. Lipid Res.* **2015**, *56*, 546–561. [CrossRef]
15. Aasum, E.; Hafstad, A.D.; Severson, D.L.; Larsen, T.S. Age-dependent changes in metabolism, contractile function, and ischemic sensitivity in hearts from db/db mice. *Diabetes* **2003**, *52*, 434–441. [CrossRef]
16. Belke, D.D.; Larsen, T.S.; Gibbs, E.M.; Severson, D.L. Altered metabolism causes cardiac dysfunction in perfused hearts from diabetic (db/db) mice. *Am. J. Physiol. Endocrinol. Metab.* **2000**, *279*, E1104–E1113. [CrossRef]
17. Peterson, L.R.; Herrero, P.; Schechtman, K.B.; Racette, S.B.; Waggoner, A.D.; Kisrieva-Ware, Z.; Dence, C.; Klein, S.; Marsala, J.; Meyer, T. Effect of obesity and insulin resistance on myocardial substrate metabolism and efficiency in young women. *Circulation* **2004**, *109*, 2191–2196. [CrossRef]
18. Scheuermann-Freestone, M.; Madsen, P.L.; Manners, D.; Blamire, A.M.; Buckingham, R.E.; Styles, P.; Radda, G.K.; Neubauer, S.; Clarke, K. Abnormal cardiac and skeletal muscle energy metabolism in patients with type 2 diabetes. *Circulation* **2003**, *107*, 3040–3046. [CrossRef]
19. How, O.-J.; Aasum, E.; Kunnathu, S.; Severson, D.L.; Myhre, E.S.; Larsen, T.S. Influence of substrate supply on cardiac efficiency, as measured by pressure-volume analysis in ex vivo mouse hearts. *Am. J. Physiol. Heart Circ. Physiol.* **2005**, *288*, H2979–H2985. [CrossRef]

20. Boardman, N.; Hafstad, A.D.; Larsen, T.S.; Severson, D.L.; Aasum, E. Increased O_2 cost of basal metabolism and excitation-contraction coupling in hearts from type 2 diabetic mice. *Am. J. Physiol. Heart Circ. Physiol.* **2009**, *296*, H1373–H1379. [CrossRef]
21. Hafstad, A.D.; Khalid, A.M.; How, O.-J.; Larsen, T.S.; Aasum, E. Glucose and insulin improve cardiac efficiency and postischemic functional recovery in perfused hearts from type 2 diabetic (db/db) mice. *Am. J. Physiol. Endocrinol. Metab.* **2007**, *292*, E1288–E1294. [CrossRef]
22. Boardman, N.T.; Hafstad, A.D.; Lund, J.; Rossvoll, L.; Aasum, E. Exercise of obese mice induces cardioprotection and oxygen sparing in hearts exposed to high-fat load. *Am. J. Physiol. Heart Circ. Physiol.* **2017**, *313*, H1054–H1062. [CrossRef]
23. Hafstad, A.D.; Lund, J.; Hadler-Olsen, E.; Höper, A.C.; Larsen, T.S.; Aasum, E. High-and moderate-intensity training normalizes ventricular function and mechanoenergetics in mice with diet-induced obesity. *Diabetes* **2013**, *62*, 2287–2294. [CrossRef]
24. Boudina, S.; Sena, S.; O'Neill, B.T.; Tathireddy, P.; Young, M.E.; Abel, E.D. Reduced mitochondrial oxidative capacity and increased mitochondrial uncoupling impair myocardial energetics in obesity. *Circulation* **2005**, *112*, 2686–2695. [CrossRef]
25. Joseph, L.C.; Barca, E.; Subramanyam, P.; Komrowski, M.; Pajvani, U.; Colecraft, H.M.; Hirano, M.; Morrow, J.P. Inhibition of NAPDH oxidase 2 (NOX2) prevents oxidative stress and mitochondrial abnormalities caused by saturated fat in cardiomyocytes. *PLoS ONE* **2016**, *11*, e0145750. [CrossRef]
26. Zhang, M.; Prosser, B.L.; Bamboye, M.A.; Gondim, A.N.; Santos, C.X.; Martin, D.; Ghigo, A.; Perino, A.; Brewer, A.C.; Ward, C.W. Contractile Function During Angiotensin-II Activation. *J. Am. Coll. Cardiol.* **2015**, *66*, 261–272. [CrossRef]
27. Roussel, J.; Thireau, J.; Brenner, C.; Saint, N.; Scheuermann, V.; Lacampagne, A.; Le Guennec, J.-Y.; Fauconnier, J. Palmitoyl-carnitine increases RyR2 oxidation and sarcoplasmic reticulum Ca^{2+} leak in cardiomyocytes: Role of adenine nucleotide translocase. *Biochim. Biophys. Acta Mol. Basis Dis.* **2015**, *1852*, 749–758. [CrossRef]
28. Valdés, Á.; Treuer, A.; Barrios, G.; Ponce, N.; Fuentealba, R.; Dulce, R.; González, D. Nox inhibition improves β-adrenergic stimulated contractility and intracellular calcium handling in the aged rat heart. *Int. J. Mol. Sci.* **2018**, *19*, 2404. [CrossRef]
29. Joseph, L.C.; Kokkinaki, D.; Valenti, M.-C.; Kim, G.J.; Barca, E.; Tomar, D.; Hoffman, N.E.; Subramanyam, P.; Colecraft, H.M.; Hirano, M. Inhibition of NADPH oxidase 2 (NOX2) prevents sepsis-induced cardiomyopathy by improving calcium handling and mitochondrial function. *JCI Insight* **2017**, *2*, e94248. [CrossRef]
30. Meng, R.; Zhu, D.-L.; Bi, Y.; Yang, D.-H.; Wang, Y.-P. Apocynin improves insulin resistance through suppressing inflammation in high-fat diet-induced obese mice. *Med. Inflamm.* **2010**, *2010*, 9. [CrossRef]
31. Matthews, D.; Hosker, J.; Rudenski, A.; Naylor, B.; Treacher, D.; Turner, R. Homeostasis model assessment: Insulin resistance and β-cell function from fasting plasma glucose and insulin concentrations in man. *Diabetologia* **1985**, *28*, 412–419. [CrossRef]
32. Laurindo, F.R.; Fernandes, D.C.; Santos, C.X. Chapter thirteen-assessment of superoxide production and nadph oxidase activity by hplc analysis of dihydroethidium oxidation products. *Methods Enzymol.* **2008**, *441*, 237–260.
33. Palmer, J.W.; Tandler, B.; Hoppel, C.L. Biochemical properties of subsarcolemmal and interfibrillar mitochondria isolated from rat cardiac muscle. *J. Biol. Chem.* **1977**, *252*, 8731–8739.
34. Lund, J.; Hafstad, A.D.; Boardman, N.T.; Rossvoll, L.; Rolim, N.P.; Ahmed, M.S.; Florholmen, G.; Attramadal, H.; Wisløff, U.; Larsen, T.S. Exercise training promotes cardioprotection through oxygen-sparing action in high fat-fed mice. *Am. J. Physiol. Heart Circ. Physiol.* **2015**, *308*, H823–H829. [CrossRef]
35. How, O.-J.; Aasum, E.; Severson, D.L.; Chan, W.A.; Essop, M.F.; Larsen, T.S. Increased myocardial oxygen consumption reduces cardiac efficiency in diabetic mice. *Diabetes* **2006**, *55*, 466–473. [CrossRef]
36. Pepping, J.K.; Freeman, L.R.; Gupta, S.; Keller, J.N.; Bruce-Keller, A.J. NOX2 deficiency attenuates markers of adiposopathy and brain injury induced by high-fat diet. *Am. J. Physiol. Endocrinol. Metab.* **2012**, *304*, E392–E404. [CrossRef]
37. Du, J.; Fan, L.M.; Mai, A.; Li, J.M. Crucial roles of N ox2-derived oxidative stress in deteriorating the function of insulin receptors and endothelium in dietary obesity of middle-aged mice. *Br. J. Pharmacol.* **2013**, *170*, 1064–1077. [CrossRef]
38. Meng, R.; Zhu, D.-L.; Bi, Y.; Yang, D.-H.; Wang, Y.-P. Anti-oxidative effect of apocynin on insulin resistance in high-fat diet mice. *Ann. Clin. Lab. Sci.* **2011**, *41*, 236–243.

39. De Figueiredo, A.S.P.; Salmon, A.B.; Bruno, F.; Jimenez, F.; Martinez, H.G.; Halade, G.V.; Ahuja, S.S.; Clark, R.A.; DeFronzo, R.A.; Abboud, H.E. Nox2 mediates skeletal muscle insulin resistance induced by a high fat diet. *J. Biol. Chem.* **2015**, *290*, 13427–13439. [CrossRef]
40. García-Ruiz, I.; Solís-Muñoz, P.; Fernández-Moreira, D.; Grau, M.; Muñoz-Yagüe, T.; Solís-Herruzo, J.A. NADPH oxidase is implicated in the pathogenesis of oxidative phosphorylation dysfunction in mice fed a high-fat diet. *Sci. Rep.* **2016**, *6*, 23664. [CrossRef]
41. Costford, S.R.; Castro-Alves, J.; Chan, K.L.; Bailey, L.J.; Woo, M.; Belsham, D.D.; Brumell, J.H.; Klip, A. Mice lacking NOX2 are hyperphagic and store fat preferentially in the liver. *Am. J. Physiol. Endocrinol. Metab.* **2014**, *306*, E1341–E1353. [CrossRef]
42. Huynh, K.; Kiriazis, H.; Du, X.-J.; Love, J.E.; Gray, S.P.; Jandeleit-Dahm, K.A.; McMullen, J.R.; Ritchie, R.H. Targeting the upregulation of reactive oxygen species subsequent to hyperglycemia prevents type 1 diabetic cardiomyopathy in mice. *Free Radic. Biol. Med.* **2013**, *60*, 307–317. [CrossRef]
43. Guo, Z.; Qi, W.; Yu, Y.; Du, S.; Wu, J.; Liu, J. Effect of exenatide on the cardiac expression of adiponectin receptor 1 and NADPH oxidase subunits and heart function in streptozotocin-induced diabetic rats. *Diabetol. Metab. Syndr.* **2014**, *6*, 29. [CrossRef]
44. Joseph, L.C.; Avula, U.M.R.; Wan, E.Y.; Reyes, M.V.; Lakkadi, K.R.; Subramanyam, P.; Nakanishi, K.; Homma, S.; Muchir, A.; Pajvani, U.B. Dietary saturated fat promotes arrhythmia by activating NOX2 (nadph oxidase 2). *Circ. Arrhythm. Electrophysiol.* **2019**, *12*, e007573. [CrossRef]
45. Grieve, D.J.; Byrne, J.A.; Siva, A.; Layland, J.; Johar, S.; Cave, A.C.; Shah, A.M. Involvement of the nicotinamide adenosine dinucleotide phosphate oxidase isoform Nox2 in cardiac contractile dysfunction occurring in response to pressure overload. *J. Am. Coll. Cardiol.* **2006**, *47*, 817–826. [CrossRef]
46. Boardman, N.T.; Rossvoll, L.; Lund, J.; Hafstad, A.D.; Aasum, E. 3-Weeks of Exercise Training Increases Ischemic-Tolerance in Hearts from High-Fat Diet Fed Mice. *Front. Physiol.* **2019**, *10*, 1274. [CrossRef]
47. Kuster, G.M.; Lancel, S.; Zhang, J.; Communal, C.; Trucillo, M.P.; Lim, C.C.; Pfister, O.; Weinberg, E.O.; Cohen, R.A.; Liao, R. Redox-mediated reciprocal regulation of SERCA and Na+–Ca^{2+} exchanger contributes to sarcoplasmic reticulum Ca 2+ depletion in cardiac myocytes. *Free Radic. Biol. Med.* **2010**, *48*, 1182–1187. [CrossRef]
48. Belke, D.D.; Dillmann, W.H. Altered cardiac calcium handling in diabetes. *Curr. Hypertens. Rep.* **2004**, *6*, 424–429. [CrossRef]
49. Stølen, T.O.; Høydal, M.A.; Kemi, O.J.; Catalucci, D.; Ceci, M.; Aasum, E.; Larsen, T.; Rolim, N.; Condorelli, G.; Smith, G.L. Interval training normalizes cardiomyocyte function, diastolic Ca2+ control, and SR Ca2+ release synchronicity in a mouse model of diabetic cardiomyopathy. *Circ. Res.* **2009**, *105*, 527–536. [CrossRef]
50. Opie, L.H. *Heart Physiology: From Cell to Circulation*; Lippincott Williams & Wilkins: Philadelphia, PA, USA, 2004.
51. Boardman, N.T.; Larsen, T.S.; Severson, D.L.; Essop, M.F.; Aasum, E. Chronic and acute exposure of mouse hearts to fatty acids increases oxygen cost of excitation-contraction coupling. *Am. J. Physiol. Heart Circ. Physiol.* **2011**, *300*, H1631–H1636. [CrossRef]
52. Hutter, J.; Piper, H.; Spieckerman, P. Effect of fatty acid oxidation on efficiency of energy production in rat heart. *Am. J. Physiol. Heart Circ. Physiol.* **1985**, *249*, H723–H728. [CrossRef]
53. Heumüller, S.; Wind, S.; Barbosa-Sicard, E.; Schmidt, H.H.; Busse, R.; Schröder, K.; Brandes, R.P. Apocynin is not an inhibitor of vascular NADPH oxidases but an antioxidant. *Hypertension* **2008**, *51*, 211–217. [CrossRef]
54. Kim, J.-C.; Wang, J.; Son, M.-J.; Woo, S.-H. Shear stress enhances Ca^{2+} sparks through Nox2-dependent mitochondrial reactive oxygen species generation in rat ventricular myocytes. *Biochim. Biophys. Acta Mol. Cell Res.* **2017**, *1864*, 1121–1131. [CrossRef]
55. Echtay, K.S.; Roussel, D.; St-Pierre, J.; Jekabsons, M.B.; Cadenas, S.; Stuart, J.A.; Harper, J.A.; Roebuck, S.J.; Morrison, A.; Pickering, S. Superoxide activates mitochondrial uncoupling proteins. *Nature* **2002**, *415*, 96–99. [CrossRef]

Paper II:

Overexpression of NOX2 Exacerbates AngII-Mediated Cardiac Dysfunction and Metabolic Remodelling

antioxidants

MDPI

Article

Overexpression of NOX2 Exacerbates AngII-Mediated Cardiac Dysfunction and Metabolic Remodelling

Synne S. Hansen [1,*,†], Tina M. Pedersen [1,†], Julie Marin [1], Neoma T. Boardman [1], Ajay M. Shah [2], Ellen Aasum [1] and Anne D. Hafstad [1]

[1] Cardiovascular Research Group, Department of Medical Biology, Faculty of Health Science, UiT—The Arctic University of Norway, 9019 Tromsø, Norway; tipe@biomed.au.dk (T.M.P.); Julie.MARIN@student.umons.ac.be (J.M.); neoma.boardman@uit.no (N.T.B.); ellen.aasum@uit.no (E.A.); anne.hafstad@uit.no (A.D.H.)

[2] School of Cardiovascular Medicine & Sciences, King's College London, British Heart Foundation Centre of Excellence, London SE5 9NU, UK; ajay.shah@kcl.ac.uk

* Correspondence: synne.s.hansen@uit.no

† These authors contributed equally to this work.

Abstract: The present study aimed to examine the effects of low doses of angiotensin II (AngII) on cardiac function, myocardial substrate utilization, energetics, and mitochondrial function in C57Bl/6J mice and in a transgenic mouse model with cardiomyocyte specific upregulation of NOX2 (csNOX2 TG). Mice were treated with saline (sham), 50 or 400 ng/kg/min of AngII ($AngII_{50}$ and $AngII_{400}$) for two weeks. In vivo blood pressure and cardiac function were measured using plethysmography and echocardiography, respectively. Ex vivo cardiac function, mechanical efficiency, and myocardial substrate utilization were assessed in isolated perfused working hearts, and mitochondrial function was measured in left ventricular homogenates. $AngII_{50}$ caused reduced mechanical efficiency despite having no effect on cardiac hypertrophy, function, or substrate utilization. $AngII_{400}$ slightly increased systemic blood pressure and induced cardiac hypertrophy with no effect on cardiac function, efficiency, or substrate utilization. In csNOX2 TG mice, $AngII_{400}$ induced cardiac hypertrophy and in vivo cardiac dysfunction. This was associated with a switch towards increased myocardial glucose oxidation and impaired mitochondrial oxygen consumption rates. Low doses of AngII may transiently impair cardiac efficiency, preceding the development of hypertrophy induced at higher doses. NOX2 overexpression exacerbates the AngII -induced pathology, with cardiac dysfunction and myocardial metabolic remodelling.

Keywords: angiotensin II; NOX2; cardiac disease; hypertension; cardiac efficiency; cardiac hypertrophy

Citation: Hansen, S.S.; Pedersen, T.M.; Marin, J.; Boardman, N.T.; Shah, A.M.; Aasum, E.; Hafstad, A.D. Overexpression of NOX2 Exacerbates AngII-Mediated Cardiac Dysfunction and Metabolic Remodelling. *Antioxidants* **2022**, *11*, 143. https://doi.org/10.3390/antiox11010143

Academic Editors: Nicola King and M.-Saadeh Suleiman

Received: 2 December 2021
Accepted: 5 January 2022
Published: 10 January 2022

1. Introduction

Activation of the renin–angiotensin–aldosterone system (RAAS) is known to play an important role in a range of conditions known to increase the risk of developing cardiovascular diseases. Angiotensin (AngII) induces systemic effects, including arterial vasoconstriction as well as sodium and water retention, which may result in hypertension, increased cardiac workload, and development of heart failure. However, AngII has also been shown to have a direct effect on cardiomyocytes, affecting intracellular processes such as increased production of reactive oxygen species (ROS), fibrosis, hypertrophy, apoptosis, endoplasmic reticulum stress (ER stress), and inhibition of autophagy [1–3]. Therefore, AngII likely has a key role in cardiac remodelling and the development of cardiac dysfunction, also in the absence of hypertension.

In experimental studies of AngII-mediated heart failure, the AngII dose and treatment protocols are highly variable. High doses, >1000 ng/kg/min, typically cause an overt hypertension and hypertrophy [4–6], creating severe models of heart disease and possibly

cachexia. Low doses, particularly those of ≤500 ng/kg/min, will cause an initial prehypertensive period characterized by auto potentiation to AngII, and subsequent development of hypertension, depending on the duration of treatment [7,8]. Although the phenotypic changes are easily studied in models using pressor doses, lower doses (no or slow pressor doses) are required to study the initial effect of AngII, without introducing confounding disease factors that may mask the direct effects of AngII. Additionally, although the suppression of the RAAS is an important medical therapy in heart failure patients, this alone does not prevent the progression, even in optimally treated patients. Thus, investigating the development of early AngII-induced disease can be an important step to discover relevant treatment options and novel therapies.

Altered substrate metabolism and loss of metabolic flexibility are hallmarks in heart failure [9–14]. In addition, decreased cardiac efficiency is an early indicator of the failing heart, often preceding development of cardiac dysfunction [12,14]. Although it is well known that AngII induces structural remodelling in the heart [15,16], its effect on cardiac metabolic remodelling is less clear. There is evidence showing that the prevention of metabolic alterations in the failing heart is beneficial [17]; thus, studying the metabolic adaptations and possible maladaptation in early AngII-induced disease could provide important insight into the therapeutic potential. A common mediator of AngII-induced processes is increased production of ROS, which is detectible even with very low doses of AngII and in early stages of heart failure [3,7,18,19]. Although there are several sources of ROS in cardiomyocytes, studies have confirmed that NADPH oxidase 2 (NOX2) is a crucial contributor to AngII-induced ROS production in the pathogenesis of heart failure [20–22]. We have previously found elevated myocardial ROS levels to be associated with increased myocardial oxygen consumption [14], and abrogation of NOX2 was shown to reduce cardiac ROS levels and improve cardiac efficiency in obesity-induced heart-failure [23]. Furthermore, non-pressor doses of AngII (50 ng/kg/min) have been shown to induce mitochondrial uncoupling in skeletal muscles [19], which could suggest an impact on mitochondrial efficiency.

The aim of the present study was therefore to examine the effects of a non-pressor dose of AngII (50 ng/kg/min) as well as a slow pressor dose of AngII (400 ng/kg/min) on cardiac function, substrate utilization, efficiency, and mitochondrial respiration. We also included mice with cardiomyocyte specific NOX2 overexpression to investigate whether NOX2 exacerbates AngII-induced cardiac metabolic remodelling.

2. Materials and Methods

2.1. Animal Models

Male 11-week-old C57BL/6J mice (Charles River Laboratories, Sulzfeld, Germany) were used in the study. In addition, age-matched male wild-type (WT) and transgenic mice with a cardiomyocyte-specific overexpression of NOX2 (csNOX2 TG), obtained from Professor Ajay M. Shah's lab (King's College, London, UK) were also included. The csNOX2 were created on a C57BL/6J background by cloning a 1.8 kb human NOX2 cDNA downstream of the myosin light chain-2 promoter, prior to injection into fertilized oocytes [22]. The expression of the NOX2 protein is approximately five times higher in csNOX2 TG mice than in WT mice, but the basal NOX2 activity and cardiac phenotype are unaltered. However, in response to pathological stressors, such as AngII stimulation, cardiomyocytes from csNOX2 TG mice exhibit increased NOX2-mediated ROS production [22].

All mice were acclimatized to the animal facilities for one week and kept on a 12:12 hour reversed light–dark cycle, in a room with a constant temperature of 21 °C and 55% humidity. The animals were given ad libitum access to a normal chow diet and water and were otherwise treated in accordance with the guidelines on accommodation and care of animals given by the European Convention for the Protection of Vertebrate Animals for Experimental and Other Scientific Purposes.

C57BL/6J WT and csNOX2 TG mice were given either saline (sham), non-pressor dose, 50 ng/kg/min AngII ($AngII_{50}$) or slow pressor dose, 400 ng/kg/min AngII ($AngII_{400}$).

Micro-osmotic pumps (Model 1002, Alzet, Cupertino, CA, USA) were inserted subcutaneously, and the treatment lasted for two weeks. Animals were given a standard volume of 100 µL of saline or AngII (A9525, Sigma Aldrich, Saint-Louis, MO, USA). Prior to pump implantation, animals were given buprenorphine (0.05 mg/kg SC) as an analgesic. Experiments were done in our laboratory at the UiT—The Arctic University of Norway and were approved by the Animal Welfare Committee at the university and the Norwegian Food Safety Authority (FOTS id: 7435).

2.2. Echocardiography and Blood Pressure Measurements

Echocardiographic measurements were performed at baseline and repeated after two weeks. Animals were lightly anaesthetized with isoflurane (1.5–2% isoflurane) while lying in a supine position on a heated platform [24]. Measurements were obtained and analysed from parasternal short-axis M-mode and, for a more comprehensive examination, apical four-chamber Doppler images, as previously described [24]. A blinded operator imaged all mice and performed the subsequent analyses.

Blood pressures were obtained using tail-cuff plethysmography (Coda High Throughput Non-Invasive Blood Pressure System, Kent Scientific, Torrington, CT, USA) on awake animals.

2.3. Isolated Heart Perfusions

Isolated heart perfusion was performed the day after the last echocardiography. Animals were anesthetized with pentobarbital (100 mg/kg i.p.) and heparin (100 U, i.p.), and hearts were excised and placed in ice-cold buffer before being fixed in a perfusion system, in working heart mode. A modified Krebs–Henseleit buffer containing 5 mM of glucose and 0.4 mM of palmitate bound to 3% fat free bovine serum albumin (EQBAH66 Europa Bioproducts, Cambridge, UK) was used with ^{4}C-U-labelled glucose (NEC04B005MC, Perken Elmer, Boston, MA, USA) and ^{3}H-9,10-labelled palmitate (NET043005MC, Perken Elmer, Boston, MA, USA) in order to measure fatty acid and glucose oxidation rates [13]. Preload and afterload pressures were kept at a constant standardized level throughout the protocol (10 mmHg and 55 mmHg, respectively). A pressure catheter (Codman Microsensor, DePuy Synthes Co, MA, USA) was placed in the aortic line close to the heart, measuring peak systolic pressure (PSP). Left ventricular (LV) stroke work was calculated as the product of stroke volume * (PSP-filling pressure). Data were obtained and analysed using LabChart 7Pro software (AD Instruments, Bella Vista, Australia).

Fibre-optic O_2 sensors (FOXY-AL 300; Ocean Optics, Duiven, The Netherlands) were placed in the buffer flow above the aorta (i.e., in the buffer entering the coronary vessels) and in the pulmonary trunk (in the buffer leaving the heart), to obtain the arterial–venous difference in PO_2, in order to measure myocardial oxygen consumption (MVO_2) as previously described [25]. Total mechanical efficiency was calculated as the ratio between LV stroke work and MVO_2 [14]. Finally, MVO_2 was also measured in unloaded retrograde perfused hearts ($MVO_{2Unloaded}$) and in electrically arrested hearts to measure MVO_2 for basal metabolism (MVO_{2BM}). MVO_2 for processes associated with excitation–contraction coupling (MVO_{2ECC}) was calculated as $MVO_{2unloaded}$-MVO_{2BM} [26]. After ex vivo perfusion protocol, heart tissue samples were harvested for mRNA analysis and respirometry measurements.

2.4. Real-Time Quantitative PCR

LV tissue from perfused hearts was immersed in RNAlater (Qiagen, Hilden, Germany), and total RNA was extracted according to the RNeasy Fibrous Tissue kit Protocol (Qiagen Nordic, Oslo, Norway). Real-time qPCR analysis was performed on tissue samples using an ABI PRISM 7900 HT Fast real-time thermal cycler as previously described [27]. Details about primer/probe sequences are given in supplemented data.

2.5. Respirometry in Frozen Samples

Oxygen consumption rates (OCR) were measured in homogenates from frozen (−70 °C) LV biopsies according to the method previously described by Acin-Perez et al., 2020 [28]. This method has been shown to allow assessment of OCR in the respiratory chain complexes comparable to uncoupled mitochondria from fresh tissue [28]. We added homogenate to the closed chambers of the oxygraph (O2K, Oroboros Instrument, Innsbruck, Austria). Data were recorded using DatLab 5 software (Oroboros Instrument, Innsbruck, Austria). Measurements were done at 37 °C. Two respiration protocols were performed in two separate chambers after recording a stable basal respiration. Protocol A: 1 mM NADH (Sigma Aldrich, Saint-Louis, MO, USA) was added to the chamber to stimulate complex I (CI) respiration. Then, 0.5 µM rotenone (Sigma Aldrich, Saint-Louis, MO, USA) was added to inhibit CI respiration. Protocol B: 0.5 µM rotenone was added to the oxygraph chamber, followed by 10 mM succinate to assess complex II (CII) respiration. Finally, 5 mM malonic acid (Sigma Aldrich, Saint-Louis, MO, USA) and 2.5 mM antimycin A (Sigma Aldrich, Saint-Louis, MO, USA) were added sequentially to inhibit CII and complex III (CIII), respectively, and to assess non-mitochondrial residual OCR (ROX). The recorded O_2 flux in each state was normalized to protein concentration quantified by Bradford protein Assay (Bio-Rad Laboratories, Hercules, CA, USA).

2.6. Blood Glucose Levels

Blood was drawn after two weeks of treatment at the point of euthanasia. We used a standard blood glucose measuring device (Freestyle, Blood glucose measuring system, Abbott Park, IL, USA).

2.7. Statistics

The results are presented as mean ± standard error of means in tables, line charts, and column bar graphs. When comparing differences between groups or individuals, unpaired and paired Student's t-tests were performed, respectively.

3. Results

Two weeks of AngII treatment (50 or 400 ng/kg/min) did not alter body weight, blood glucose, or liver weight in C57BL/6J mice. Following $AngII_{50}$ treatment there were no signs of cardiac hypertrophy; however, using the slow pressor dose ($AngII_{400}$), hypertrophy was evident as increased heart weight and increased cardiac mRNA expression of the gene encoding for the hypertrophic markers natriuretic peptide A(*nppa*) and natriuretic peptide B (*nppb*) (Table 1). We did not find $AngII_{400}$ to alter the mean arterial pressure (MAP), but there was a modest elevation of the arterial systolic blood pressure (SBP) at two weeks of treatment when compared to baseline (106 ± 3 vs. 94 ± 4 mmHg, respectively, $p < 0.05$).

Cardiomyocyte specific upregulation of NOX2 did not aggravate the effects of Ang_{400} treatment in terms of body weight, cardiac hypertrophy, or expression of hypertrophic markers in csNOX2 TG mice (Table 1). Both the SBP and the MAP were slightly elevated compared to baseline in $AngII_{400}$ treated csNOX2 TG mice (SBP 110 ± 4 vs. 90 ± 2 mmHg, and MAP 90 ± 4 vs. 72 ± 2 mmHg, $p < 0.05$) (Table 1).

Baseline measurements of in vivo cardiac parameters were not different between treatment groups or genetic phenotype (Tables 2 and 3). Echocardiographic measurements of cardiac dimensions support the findings of $AngII_{400}$-induced hypertrophy with increased LV posterior wall thickness in diastole (LVPW;d) and increased LV mass (Table 2). The $AngII_{400}$ induced hypertrophy was not associated with deterioration of cardiac function in C57BL/6J mice.

Table 1. Animal characteristics of C57BL/6J, wild-type (WT), and csNOX2 transgenic (TG) mice treated for two weeks with micro-osmotic pumps containing either saline (sham), 50 or 400 ng/kg/min angiotensin II ($AngII_{50}$ and $AngII_{400}$). The data are presented as mean ± SEM.

	Sham	$AngII_{50}$	Sham	$AngII_{400}$	WT $AngII_{400}$	TG $AngII_{400}$
n	**9**	**11**	**10**	**10**	**6**	**6**
MAP (mmHg)	n.m.	n.m.	99 ± 6	105 ± 6	86 ± 3	90 ± 4 #
SBP	n.m.	n.m.	136 ± 12	131 ± 7	107 ± 3 #	110 ± 4 #
Body weight (g)	26 ± 0.3	27 ± 0.2	25 ± 0.3	25 ± 0.4	27.2 ± 0.8	27.0 ± 0.2
Liver weight (g)	1.33 ± 0.7	1.48 ± 0.05	0.99 ± 0.03	1.00 ± 0.04	0.95 ± 0.07	0.96 ± 0.04
Blood glucose (mM)	5.2 ± 0.3	4.6 ± 0.3	5.8 ± 0.5	5.5 ± 0.3	6.2 ± 0.6	6.2 ± 0.5
HW/BW (mg)	5.1 ± 0.2	4.9 ± 0.1	5.1 ± 0.1	5.5 ± 0.1 *	6.0 ± 0.2	5.7 ± 0.3
$nppa_{heart}$	1.0 ± 0.1	1.2 ± 0.2	1.0 ± 0.2	2.5 ± 0.3 *	1.0 ± 0.2	0.7 ± 0.2
$nppb_{heart}$	1.0 ± 0.1	1.3 ± 0.2	1.0 ± 0.1	1.4 ± 0.1 *	1.0 ± 0.1	0.9 ± 0.1

Blood samples were obtained from fed animals. The cardiac tissue mRNA expression of genes encoding for Natriuretic Peptide A ($nppa_{heart}$) and Natriuretic Peptide B ($nppb_{heart}$) were normalized to the corresponding expression in respective sham C57Bl-6J or WT $AngII_{400}$; heart weight/body weight, HW/BW; MAP, mean arterial pressure. * $p < 0.05$ vs. sham, # $p < 0.05$ vs. baseline.

Table 2. In vivo left ventricular function assessed by transthoracic echocardiography in C57BL/6J mice treated with slow pressure dose of angiotensin II ($AngII_{400}$) or saline (sham) for two weeks. Measurements were obtained and analysed from parasternal short-axis M-mode. Data are presented as mean ± SEM.

	Sham		$AngII_{400}$	
	Baseline	**Week 2**	**Baseline**	**Week 2**
n	**7**	**7**	**7**	**7**
Heart rate (BPM)	460 ± 21	451 ± 13	470 ± 9	458 ± 19
LVPW;d (mm)	0.71 ± 0.04	0.74 ± 0.02	0.77 ± 0.02	0.81 ± 0.02 *
LVID;d (mm)	3.7 ± 0.1	3.9 ± 0.1	3.7 ± 0.1	4.0 ± 0.1 #
LV mass (mg)	74 ± 7	88 ± 3 *	82 ± 2	102 ± 3 #,*
LV Mass/BW (mg/g)	3.1 ± 0.2	3.9 ± 0.1	3.6 ± 0.1	4.4 ± 0.2
LVEDV (µL)	57 ± 3	65 ± 4	59 ± 3	69 ± 2 #
LVESV (µL)	19 ± 1	22 ± 3	20 ± 2	24 ± 2
SV (µL)	38 ± 2	43 ± 2 #	39 ± 2	45 ± 2 #
FS (%)	37 ± 1	36 ± 1	36 ± 1	36 ± 2
EF (%)	67 ± 1	67 ± 2	66 ± 2	66 ± 3
LV Volume/LV Mass (µL/mg)	0.78 ± 0.05	0.74 ± 0.04	0.69 ± 0.04	0.68 ± 0.01

LVPW;d, left ventricular (LV) posterior wall thickness; LVID;d, LV internal diameter in diastole; BW, body weight; EDV and ESV, end-diastolic and end-systolic volumes; SV, stroke volume; FS, fractional shortening; EF, ejection fraction. # $p < 0.05$ vs. baseline, * $p < 0.05$ vs. sham.

Again, overexpression of csNOX2 did not aggravate the hypertrophic effects of $AngII_{400}$, as $AngII_{400}$ LV mass and posterior wall thickness were not altered in the csNOX2 TG mice as compared to WT mice. However, the ratio between end-diastolic volume and LV mass was elevated in csNOX2 TG $AngII_{400}$ mice, signifying an eccentric hypertrophy with dilation and increased intraventricular volume. Upregulation of csNOX2 deteriorated LV systolic function, as it increased the systolic LV internal diameter in csNOX2 TG $AngII_{400}$, but not WT $AngII_{400}$ mice. This led to a decrease in fractional shortening (FS) in csNOX2 TG $AngII_{400}$ mice (Table 3). Similarly, csNOX2 TG $AngII_{400}$ mice also showed an increase in end-systolic volume (ESV), resulting in a decreased ejection fraction (EF) (Table 3). In addition, $AngII_{400}$ was found to significantly increase the E/E' ratio only in csNOX2 TG. As elevation of the E/E' ratio indicates increased LV filling pressure and decreased compliance, these data suggest progression of LV diastolic dysfunction. Thus, although hypertrophy was not exacerbated per se, the pathological phenotype was aggravated, signifying progression of cardiac disease in the csNOX2 TG mice. Interestingly, ex vivo function measured in

isolated working hearts did not reveal differences in ventricular function between treatment groups or genotypes (Table S5).

Table 3. In vivo left ventricular function assessed by transthoracic echocardiography in wild-type (WT) and csNOX2 transgenic (TG) mice treated with angiotensin II ($AngII_{400}$) for two weeks. Measurements were obtained and analysed from parasternal short-axis M-mode and apical four-chamber view. Data are presented as mean ± SEM.

	WT $AngII_{400}$		**TG $AngII_{400}$**	
	Baseline	**Week 2**	**Baseline**	**Week 2**
n	**4**	**6**	**6**	**5**
Heart rate (BPM)	491 ± 12	526 ± 14	484 ± 7	515 ± 13 #
LVPW;d (mm)	0.82 ± 0.05	0.92 ± 0.05 #	0.77 ± 0.02	0.89 ± 0.02 #
LVID;d (mm)	4.1 ± 0.1	4.0 ± 0.1	4.2 ± 0.1	4.3 ± 0.2
LV mass (mg)	101 ± 5	118 ± 4 #	95 ± 4	113 ± 6 #
LV Mass/BW (mg/g)	3.6 ± 0.1	4.3 ± 0.1 #	3.5 ± 0.1	4.2 ± 0.1 #
LVEDV (µL)	73 ± 3	71 ± 6	77 ± 2	84 ± 8
LVESV (µL)	27 ± 1	30 ± 4	32 ± 2	43 ± 5 #,*
SV (µL)	45 ± 2	40 ± 2	45 ± 2	41 ± 3
FS (%)	33 ± 1	30 ± 2	31 ± 1	25 ± 1 #,*
EF (%)	62 ± 2	58 ± 2	59 ± 2	50 ± 2 #,*
LV Volume/LV Mass (µL/mg)	0.72 ± 0.04	0.60 ± 0.05	0.83 ± 0.02 *	0.74 ± 0.04 #,*
E/A	1.3 ± 0.1	1.5 ± 0.2	1.4 ± 0.0	1.4 ± 0.2
E/E′	28 ± 2	30 ± 2	29 ± 1	34 ± 2 #
Deceleration time (ms)	24 ± 1	20 ± 2	23 ± 2	19 ± 2

LVPW;d, left ventricular (LV) posterior wall thickness; LVID;d, left ventricular (LV) internal diameter in diastole; EDV and ESV, end-diastolic and end-systolic volumes; SV, stroke volume; FS, fractional shortening; EF, ejection fraction; E/A, ratio of velocity of early to late ventricular filling; E/E′; ratio of velocity of early ventricular filling to early diastolic mitral annular velocity. # $p < 0.05$ vs. baseline, * $p < 0.05$ vs. WT.

In this study, we also investigated the effects of AngII-treatment on myocardial energetics. We found a significant reduction in cardiac mechanical efficiency in $AngII_{50}$ mice compared to sham mainly due to increased myocardial oxygen consumption in unloaded hearts ($MVO_{2unloaded}$, $p = 0.085$) (Figure 1A,D). Further, increasing the dose of AngII did not impair myocardial energetics as there were no differences in mechanical efficiency, $MVO_{2unloaded}$, or MVO_2 for processes associated with excitation–contraction coupling (MVO_{2ECC}) or basal metabolism (MVO_{2BM}). Furthermore, upregulation of NOX2 did not alter the response to $AngII_{400}$ with regards to mechanical efficiency or MVO_2.

Altered myocardial substrate utilization has previously been linked to myocardial energetics [11,29], and we therefore assessed myocardial glucose and fatty acid oxidation rates in response to AngII treatment. Neither $AngII_{50}$ nor $AngII_{400}$ was found to alter substrate oxidation rates (Figure 2). This was supported by unchanged gene expression of markers of metabolic reprogramming, such as peroxisome proliferator-activated receptor α (*pparα*), *cd36*, protein pyruvate dehydrogenase kinase 4 (*pdk4*), and hexokinase (*hk*) (Table S2). Cardiac overexpression of NOX2, however, induced a metabolic shift in response to AngII treatment, as we found increased glucose oxidation rates in csNOX2 TG $AngII_{400}$ (Figure 2F). This metabolic reprogramming was associated with a significant increase in *pdk4* mRNA levels in csNOX2 TG. There were no differences in other markers of metabolic reprogramming (*pparα*, *cd36*, *ldh* and *hk*) between $AngII_{400}$ treated csNOX2 TG and WT (Table S3).

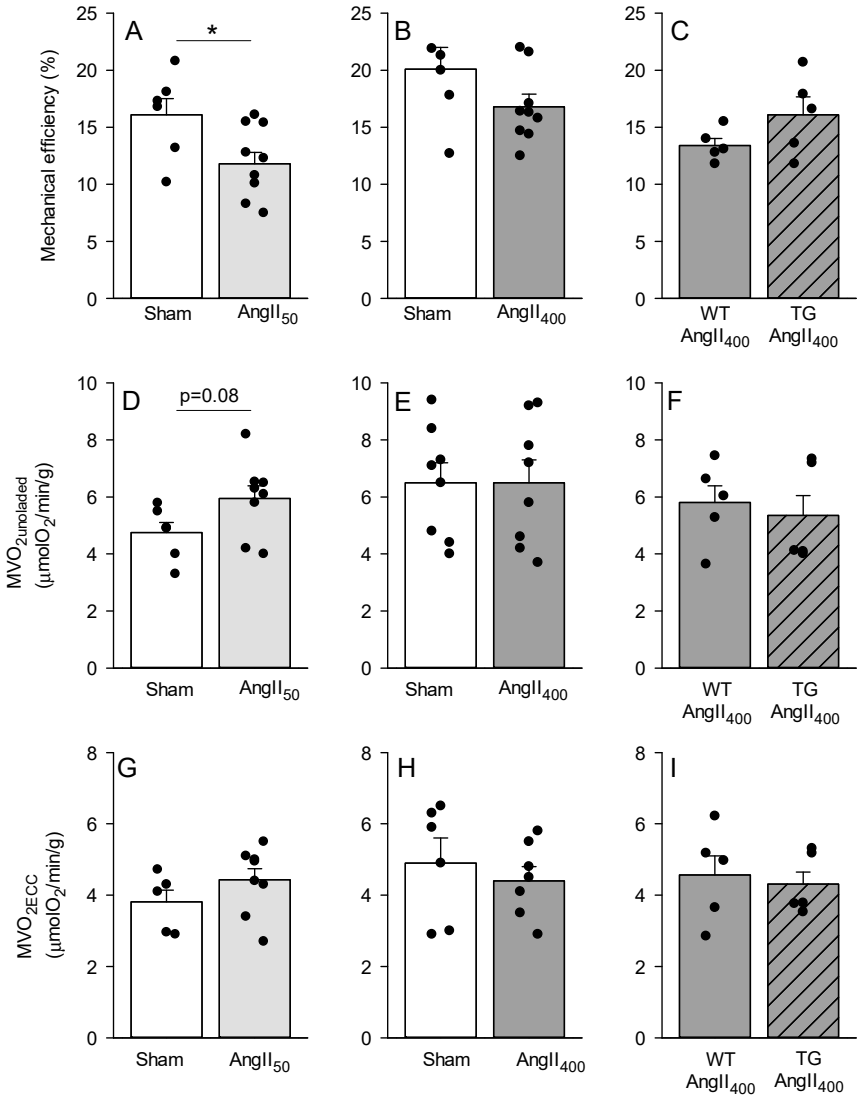

Figure 1. Mechanical efficiency (**A**–**C**), myocardial oxygen consumption in mechanically unloaded hearts ($MVO_{2unloaded}$, **D**–**F**) and MVO_2 for processes associated with excitation-contraction coupling (MVO_{2ECC}, **G**–**I**), measured in isolated perfused hearts from C57BL/6J, wild-type (WT), and csNOX2 transgenic (TG) mice treated for two weeks with micro-osmotic pumps containing either saline (sham), 50 or 400 ng/kg/min angiotensin II ($AngII_{50}$ and $AngII_{400}$). The data are presented as mean ± SEM. * $p < 0.05$ vs. sham.

The oxygen consumption rate (OCR) through the complexes in the electron transport system in the mitochondria was measured in homogenates from LV heart tissue that had been previously frozen. There was no difference in OCR in homogenates from sham and AngII-treated LV heart tissue (Figure 3A,B). In the csNOX2 TG, $AngII_{400}$ resulted in a significant reduction in basal and residual oxygen consumption rates (ROX) compared to WT (Figure 3C). In addition, there was a non-significant tendency towards lower OCR in complex I (CI) in homogenate from csNOX2 TG $AngII_{400}$, which might indicate altered mitochondrial respiration.

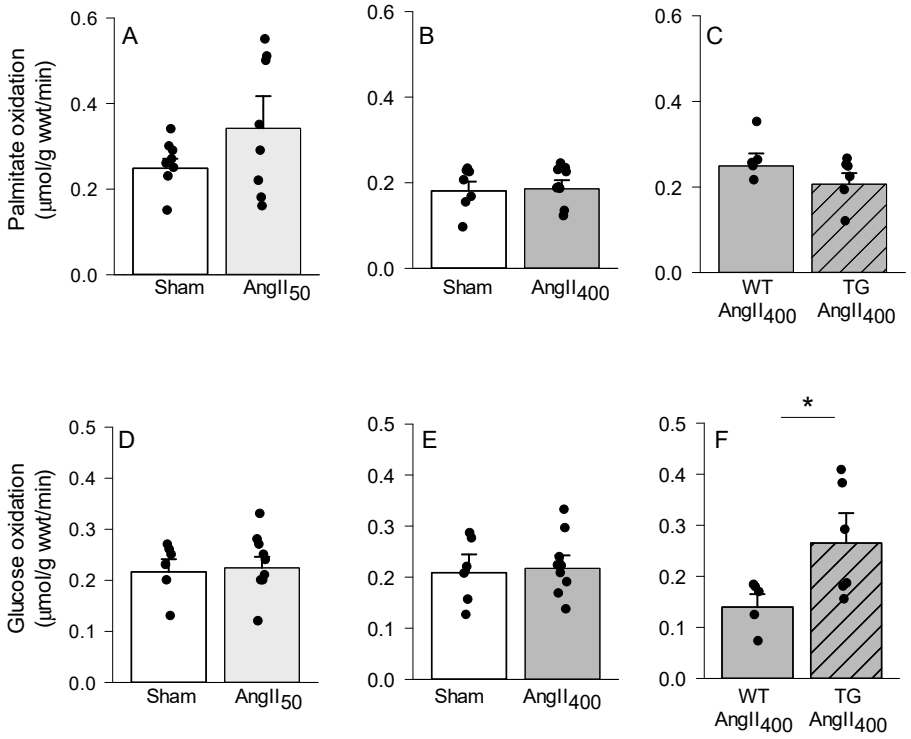

Figure 2. Palmitate (**A**–**C**) and glucose (**D**–**F**) oxidation rates assessed in isolated working hearts from C57BL/6J, wild-type (WT), and csNOX2 transgenic (TG) mice treated for two weeks with micro-osmotic pumps containing either saline (sham), 50 or 400 ng/kg/min angiotensin II ($AngII_{50}$ and $AngII_{400}$). The data are presented as mean ± SEM. * $p < 0.05$ vs. WT.

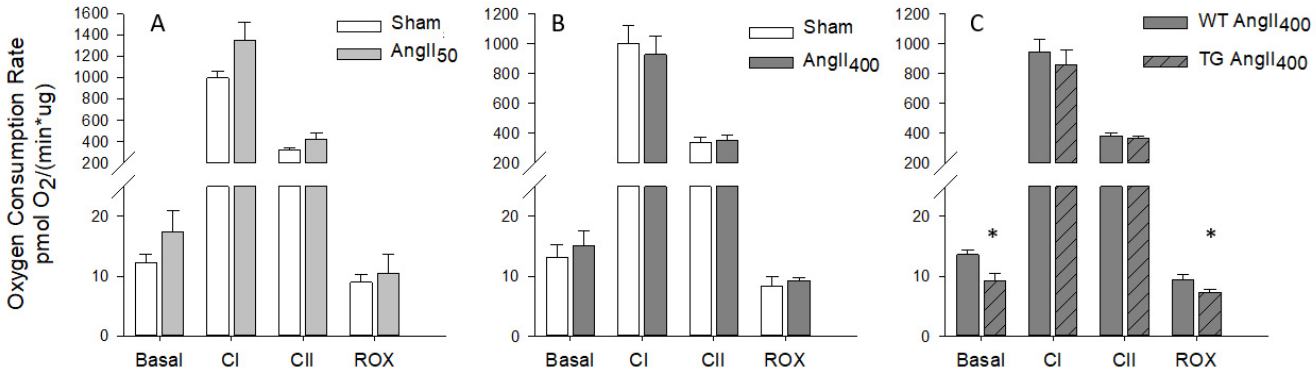

Figure 3. Oxygen consumption rate measured in homogenate from frozen left ventricular heart tissue from C57BL/6J, wild-type (WT), and cardiomyocyte specific NOX2 transgenic (TG) mice treated for two weeks with micro-osmotic pumps containing either saline (sham), 50 or 400 ng/kg/min angiotensin II ($AngII_{50}$ and $AngII_{400}$). (**A**) Sham and $AngII_{50}$. (**B**) Sham and $AngII_{400}$. (**C**) WT $AngII_{400}$ and TG $AngII_{400}$. Basal, homogenate with cytochrome C; Complex I (CI), homogenate and NADH; Complex II (CII) is homogenate with rotenone (CI-blocker) and succinate; Residual Oxygen consumption (ROX), homogenate with malonate (CII-blocker) and antimycin A (CIII-blocker). Data are means ± SEM. * $p < 0.05$ vs. WT.

4. Discussion

While it is well documented that high doses of AngII lead to a rapid and overt pressor response accompanied by development of cardiac dysfunction [4–6], the functional effect of low doses and their impact on cardiac metabolism has been less described. In the present study we have examined metabolic and functional changes in the heart associated with two-week treatment of mice using non-pressor dose (50 ng/kg/min) or slow pressor

dose (400 ng/kg/min) of AngII. These doses were used to mimic early phase of heart failure, prior to the introduction of confounding effects that follow the complexity of overt hypertension. Knowing that NOX2 is an important target for AngII in the heart, we also included a transgenic model with cardiomyocyte specific NOX2 overexpression (csNOX2 TG) to evaluate the potential role of NOX2.

We did not detect changes in body weight development following $AngII_{50}$ or $AngII_{400}$ treatment, similar to other reports [19]. These data support that there were no cachexic effects of the doses used as compared to the effect of higher doses [30]. Previously, studies using slow pressor doses (400 and 500 ng/kg/min) have reported elevations in systolic blood pressure (SBP) and mean arterial pressure (MAP) [7,31,32]. We did not detect changes in MAP but did observe a slight increase in SBP, which was subtle compared to previous reports [7,31,32]. It should be noted, however, that there are limitations in sensitivity when using tail-cuff plethysmography compared to more invasive measurements, and this could explain the inconsistencies in reports regarding the effect of slow pressor dose of AngII on blood pressure.

In a study by Byrne and colleagues, 2003 [21], AngII-mediated elevation of blood pressure was linked to the expression of NOX2, as mice with a global knockdown of NOX2 ($gp91^{phox-/-}$ mice) did not exhibit the same increased SBP in response to AngII-pressor doses. A previous study on csNOX2 TG mice treated with 300 ng/kg/min of AngII did not report any blood pressure differences between csNOX2 TG and WT mice [22]. In the present study, both MAP and SBP were slightly increased in the csNOX2 TG mice, which could be linked to increased cardiac output during the awake blood pressure measurements.

$AngII_{50}$ did not induce any hypertrophic changes in the myocardium, in line with previous reports [19]. Mice treated with $AngII_{400}$, however, display a hypertrophic phenotype, confirmed by increased wall thickness and increased gene expression of *nppa* and *nppb*. Our data therefore show that AngII can mediate direct hypertrophic effects also in the absence of overt changes in MAP. This also supports other studies on using low doses of AngII (50–300 ng/kg/min) for two to four weeks where mice developed cardiac hypertrophy and signs of fibrosis, despite an absence of increased blood pressure [6,20,22,33].

Slow pressure doses of AngII have been shown to increase both ROS production and NOX2 activity during the development of cardiac hypertrophy [31]. In addition, Byrne et al., 2003 [21] demonstrated that NOX2 is essential for the development of AngII-induced hypertrophy, as NOX2 KO mice failed to develop hypertrophy even in the presence of pressor doses of AngII (>1000 ng/kg/min). Additionally, Zhang et al., 2015 [22], using slightly lower doses of AngII (300 ng/kg/min for two weeks), reported aggravated hypertrophic response in csNOX2 TG mice. In contrast to this, we could not detect any differences in hypertrophy in csNOX2 TG or WT mice in the present study.

Non-pressor doses (50 ng/kg/min) of AngII did not cause changes in LV functional parameters, in coherence with the findings of Inoue and colleagues [19]. However, reduced diastolic function, both with and without systolic dysfunction, has previously been reported following treatment with both 150 ng/kg/min [6] and 500 ng/kg/min [32] of AngII. This contrasts with the current study, where we could not detect any in vivo or ex vivo ventricular dysfunction in $AngII_{400}$ treated mice. We did however observe that an overexpression of NOX2 lead to AngII-mediated cardiac dysfunction as indicated by increased end-systolic volume (ESV) accompanied by reduced ejection fraction (EF) in csNOX2 TG mice. In addition to the systolic dysfunction, these hearts also showed increased LV filling pressure and reduced compliance, indicative of diastolic dysfunction. There are several plausible mechanisms behind the development of LV dysfunction, as NOX2-induced ROS production has been shown to impair calcium handling [22,34,35] and induce a range of pathological cardiac changes such as fibrosis, apoptosis, and hypertrophy [36,37]. Our findings are consistent with those of Zhang et al. [22], who showed that prolonged activation of NOX2 in csNOX2 TG mice resulted in deterioration of cardiac function similar to the current results. Taking these studies together, our data support the notion that the

functional consequence of increased NOX2 activation in the heart may depend on type and proportion of stress applied to the heart [38].

Pathological hypertrophy and heart failure are known to be associated with changes in myocardial substrate utilization [39]. We did not find any changes in oxygen consumption rates (OCR) in ventricular homogenates or a shift in myocardial substrate oxidation rates in non-transgenic mice treated with $AngII_{50}$ or $AngII_{400}$. Although changes in myocardial substrate utilization have been reported following chronic exposure to AngII, there are discrepancies in terms of substrate preference [16,17,40,41]. A study utilizing slightly higher doses of AngII (<800 ng/kg/min for 2–4 weeks) reported reduced in myocardial fatty acid oxidation rates with increased utilization of glucose [17]. Moreover, studies using pressor doses (>1000 ng/kg/min for two weeks) generally report systemic insulin resistance, with a subsequent increased cardiac preference for fatty acids and diminished glucose and lactate oxidation [16,40]. Although the metabolic phenotype in these studies varies, the AngII-treated mice all displayed ventricular dysfunction [16,17,40,41], suggesting that a metabolic shift becomes evident at the onset of cardiac failure. The present study shows that C57Bl/6J mice treated with the $AngII_{400,}$ showed neither cardiac dysfunction nor changes in myocardial substrate utilization, further supporting the notion that the metabolic alterations occur only when the AngII-induced pathological condition has progressed far enough to manifest as cardiac dysfunction.

In the csNOX2 TG, $AngII_{400}$ treatment led to a significant reduction in basal OCR in ventricular homogenates. Previous reports have shown that AngII-induced oxidative stress results in mitochondrial damage and dysfunction [3]. In addition, we found an increase in myocardial glucose oxidation, accompanied by a tendency towards reduced palmitate oxidation in ex vivo csNOX2 TG hearts. There was also a significant increase in *pdk4*, a marker of metabolic switch. To our knowledge, no one has previously investigated the metabolic changes in response to slow pressor dose of AngII in csNOX2 TG mice, but our finding corroborates the metabolic shift previously reported in animal models with AngII-induced heart failure [17,41]. Oxidative stress has previously been associated with induction of translocation of GLUT4 to the plasma membrane, deacetylation of the pyruvate dehydrogenase complex, and enhanced glucose utilization [40,42–44]. Interestingly, Pellieux and collaborators reported that AngII-treatment led to downregulation of several key regulatory proteins of fatty acid oxidation and that these effects were impeded by inhibition of ROS production [45]. Accordingly, the overexpression and subsequent increase in ROS production following AngII treatment in the csNOX2 TG animals in this study could mediate downregulation of regulatory proteins and cause the observed substrate shift through the same signalling pathways that were described by Pellieux and Aikawa with colleagues [42,45].

In a previous study performed by our group, we demonstrated that ablation and pharmacological inhibition of NOX2 in obese mice improved the mechanical efficiency and reduced myocardial oxygen consumption (MVO_2) for non-mechanical cardiac work [23]. We have also previously demonstrated an association between increased ROS and increased MVO_2 [14], which together suggest a link between myocardial oxygen wasting and NOX2 activation. Increased NOX2 activity has in several studies been linked to altered calcium handling [22,34,35] such as increased calcium leak through the Ryanodine Receptor (RyR) in the sarcoplasmic reticulum [34,35]. This could potentially lead to oxygen wasting processes in the myocardium. Thus, we were surprised to find that the slow pressor dose, $AngII_{400}$, did not cause altered mechanical efficiency or altered MVO_2 in neither non-transgenic nor in the csNOX2 TG mice. In contrast, we observed a decline in mechanical efficiency in the $AngII_{50}$ mice. In addition, these hearts showed a somewhat higher unloaded MVO_2. As they did not show altered oxygen cost of excitation contraction coupling (ECC), it suggests that the decline in mechanical efficiency most likely is caused by a higher basal metabolism and/or a higher work-dependent oxygen cost. The same treatment has previously showed increased oxygen wasting processes in skeletal muscle in mice, including increased residual oxygen consumption (ROX) as well as increased expression of uncoupling proteins in

mitochondria [19]. Although there was a tendency for increased OCR and ROX in the $AngII_{50}$ group, ROX was unaltered in $AngII_{400}$ and reduced in csNOX2 TG $AngII_{400}$, suggesting that there might indeed be transient effects of AngII-mediated signalling in the myocardium.

The current study only includes male mice, and therefore we acknowledge the gender bias. It is well known that there are differences between males and females in symptoms and frequency of heart failure [46]. In addition, sex steroids have been shown to influence the progression of AngII-mediated cardiovascular diseases [31,47]. In specific, AngII only led to increased NOX2 activity in cardiac tissue from male and ovariectomized female mice as compared to control female mice [31], suggesting oestrogens to protect against NOX2 upregulation. Therefore, more studies on gender differences in cardiometabolic adaptations to cardiac stressors are warranted in the future.

5. Conclusions

This study shows that cardiac efficiency may be reduced by non-pressure doses of AngII (50 ng/kg/min), preceding apparent cardiac hypertrophy, ventricular dysfunction, or changes in myocardial substrate utilization. Interestingly, a slow pressor dose of AngII (400 ng/kg/min), which did induce cardiac hypertrophy, was not associated with impaired cardiac efficiency. This dose did not impact ventricular function or myocardial substrate utilization in WT mice. However, the same slow pressure dose, in mice with cardiomyocyte-specific overexpression of NOX2, led to cardiac dysfunction and metabolic reprogramming without any apparent effect on cardiac energetics. Our data therefore suggest that impaired cardiac energetics may precede AngII-induced ventricular structural and metabolic remodelling. Hence, increased NOX2 activity may aggravate metabolic as well as structural cardiac remodelling of AngII-mediated signalling.

Supplementary Materials: The following supporting information can be downloaded at https://www.mdpi.com/article/10.3390/antiox11010143/s1, Table S1: mRNA expression of genes in cardiac tissue from C57BL/6J mice treated with 50ng/kg/min AngII ($AngII_{50}$) or saline (sham) for two weeks; Table S2: mRNA expression of genes in cardiac tissue from C57BL/6J mice treated with 400 ng/kg/min AngII ($AngII_{400}$) or saline (sham) for two weeks; Table S3: mRNA expression of genes in cardiac tissue from male (WT) and cs NOX2 transgenic (TG) mice treated with 400 ng/kg/min AngII ($AngII_{400}$) for two weeks. Table S4. Primers for real-time quantitative PCR; Table S5. Ex vivo steady-state measurements of cardiac function from C57Bl/6J, WT and csNOX2 transgenic (TG) mice treated for two weeks with micro-osmotic pumps containing either Saline (sham), 50 or 400 ng/kg/min Angiotensin II ($AngII_{50}$ and $AngII_{400}$).

Author Contributions: Conceptualization, A.D.H. and E.A.; formal analysis, A.D.H., T.M.P., S.S.H. and J.M.; investigation, A.D.H., T.M.P., J.M. and S.S.H.; resources, A.D.H., A.M.S. and E.A.; data curation, A.D.H., T.M.P., S.S.H. and E.A.; writing—original draft preparation, S.S.H., T.M.P. and A.D.H.; writing—review and editing, A.D.H., S.S.H., N.T.B., T.M.P., A.M.S., J.M. and E.A.; visualization, S.S.H. and A.D.H.; supervision, A.D.H., N.T.B. and E.A.; project administration, A.D.H., T.M.P.; funding acquisition, A.D.H., E.A. and A.M.S. All authors have read and agreed to the published version of the manuscript.

Funding: This research was funded by The Norwegian Health Association grant number 2013.ST.080 (fellowship to T.M.P) and the UiT-The Arctic University of Norway (fellowship to S.S.H. and publication charges of the article). A.M.S. is supported by the British Heart foundation, grant number CH/1999001/11735, RE/18/2/34213.

Institutional Review Board Statement: The study was conducted according to the guidelines of the Declaration of Helsinki and approved by the Animal Welfare Committee at the University and the Norwegian Food and Safety Authority (FOTS id: 7435).

Informed Consent Statement: Not applicable.

Data Availability Statement: The data is contained within the article or supplementary materials.

Acknowledgments: Trine Lund's expert technical assistance is gratefully acknowledged. The authors would also like to thank Ajay M. Shah's group at the BHF Centre of Research Excellence, Cardiovascular Division at King's College London, UK, especially Min Zhang and Norman Catibog for their guidance regarding animal experimental protocols and echocardiography.

Conflicts of Interest: The authors declare no conflict of interest. The funders had no role in the design of the study; in the collection, analyses, or interpretation of data; in the writing of the manuscript, or in the decision to publish the results.

References

1. Domenighetti, A.A.; Wang, Q.; Egger, M.; Richards, S.M.; Pedrazzini, T.; Delbridge, L.M. Angiotensin II–mediated phenotypic cardiomyocyte remodeling leads to age-dependent cardiac dysfunction and failure. *Hypertension* **2005**, *46*, 426–432. [CrossRef] [PubMed]
2. Mazzolai, L.; Nussberger, J.r.; Aubert, J.-F.; Brunner, D.B.; Gabbiani, G.; Brunner, H.R.; Pedrazzini, T. Blood pressure–independent cardiac hypertrophy induced by locally activated renin-angiotensin system. *Hypertension* **1998**, *31*, 1324–1330. [CrossRef]
3. Zablocki, D.; Sadoshima, J. Angiotensin II and oxidative stress in the failing heart. *Antioxid. Redox Signal.* **2013**, *19*, 1095–1109. [CrossRef] [PubMed]
4. Hauck, L.; Grothe, D.; Billia, F. p21CIP1/WAF1-dependent inhibition of cardiac hypertrophy in response to Angiotensin II involves Akt/Myc and pRb signaling. *Peptides* **2016**, *83*, 38–48. [CrossRef]
5. Zhang, Y.; Yan, H.; Guang, G.-c.; Deng, Z.-r. Overexpressed connective tissue growth factor in cardiomyocytes attenuates left ventricular remodeling induced by angiotensin II perfusion. *Clin. Exp. Hypertens.* **2017**, *39*, 168–174. [CrossRef] [PubMed]
6. Zhong, J.; Basu, R.; Guo, D.; Chow, F.L.; Byrns, S.; Schuster, M.; Loibner, H.; Wang, X.-h.; Penninger, J.M.; Kassiri, Z. Angiotensin-converting enzyme 2 suppresses pathological hypertrophy, myocardial fibrosis, and cardiac dysfunction. *Circulation* **2010**, *122*, 717–728. [CrossRef] [PubMed]
7. Kawada, N.; Imai, E.; Karber, A.; Welch, W.J.; Wilcox, C.S. A mouse model of angiotensin II slow pressor response: Role of oxidative stress. *J. Am. Soc. Nephrol.* **2002**, *13*, 2860–2868. [CrossRef]
8. Simon, G.; Abraham, G.; Cserep, G. Pressor and subpressor angiotensin II administration two experimental models of hypertension. *Am. J. Hypertens.* **1995**, *8*, 645–650. [CrossRef]
9. Stanley, W.C.; Recchia, F.A.; Lopaschuk, G.D. Myocardial substrate metabolism in the normal and failing heart. *Physiol. Rev.* **2005**, *85*, 1093–1129. [CrossRef]
10. How, O.-J.; Aasum, E.; Severson, D.L.; Chan, W.A.; Essop, M.F.; Larsen, T.S. Increased myocardial oxygen consumption reduces cardiac efficiency in diabetic mice. *Diabetes* **2006**, *55*, 466–473. [CrossRef]
11. Buchanan, J.; Mazumder, P.K.; Hu, P.; Chakrabarti, G.; Roberts, M.W.; Yun, U.J.; Cooksey, R.C.; Litwin, S.E.; Abel, E.D. Reduced cardiac efficiency and altered substrate metabolism precedes the onset of hyperglycemia and contractile dysfunction in two mouse models of insulin resistance and obesity. *Endocrinology* **2005**, *146*, 5341–5349. [CrossRef]
12. Peterson, L.R.; Waggoner, A.D.; Schechtman, K.B.; Meyer, T.; Gropler, R.J.; Barzilai, B.; Dávila-Román, V.G. Alterations in left ventricular structure and function in young healthy obese women: Assessment by echocardiography and tissue Doppler imaging. *J. Am. Coll. Cardiol.* **2004**, *43*, 1399–1404. [CrossRef]
13. Aasum, E.; Hafstad, A.D.; Larsen, T.S. Changes in substrate metabolism in isolated mouse hearts following ischemia-reperfusion. In *Biochemistry of Diabetes and Atherosclerosis*; Springer: Berlin/Heidelberg, Germany, 2003; pp. 97–103.
14. Hafstad, A.D.; Lund, J.; Hadler-Olsen, E.; Höper, A.C.; Larsen, T.S.; Aasum, E. High-and moderate-intensity training normalizes ventricular function and mechanoenergetics in mice with diet-induced obesity. *Diabetes* **2013**, *62*, 2287–2294. [CrossRef]
15. Wu, C.-H.; Mohammadmoradi, S.; Chen, J.Z.; Sawada, H.; Daugherty, A.; Lu, H.S. Renin-angiotensin system and cardiovascular functions. *Arterioscler. Thromb. Vasc. Biol.* **2018**, *38*, 108–116. [CrossRef]
16. Mori, J.; Basu, R.; McLean, B.A.; Das, S.K.; Zhang, L.; Patel, V.B.; Wagg, C.S.; Kassiri, Z.; Lopaschuk, G.D.; Oudit, G.Y. Agonist-induced hypertrophy and diastolic dysfunction are associated with selective reduction in glucose oxidation: A metabolic contribution to heart failure with normal ejection fraction. *Circ. Heart Fail.* **2012**, *5*, 493–503. [CrossRef] [PubMed]
17. Choi, Y.S.; de Mattos, A.B.M.; Shao, D.; Li, T.; Nabben, M.; Kim, M.; Wang, W.; Tian, R.; Kolwicz Jr, S.C. Preservation of myocardial fatty acid oxidation prevents diastolic dysfunction in mice subjected to angiotensin II infusion. *J. Mol. Cell. Cardiol.* **2016**, *100*, 64–71. [CrossRef]
18. Brand, S.; Amann, K.; Schupp, N. Angiotensin II-induced hypertension dose-dependently leads to oxidative stress and DNA damage in mouse kidneys and hearts. *J. Hypertens.* **2013**, *31*, 333–344. [CrossRef] [PubMed]
19. Inoue, N.; Kinugawa, S.; Suga, T.; Yokota, T.; Hirabayashi, K.; Kuroda, S.; Okita, K.; Tsutsui, H. Angiotensin II-induced reduction in exercise capacity is associated with increased oxidative stress in skeletal muscle. *Am. J. Physiol.-Heart Circ. Physiol.* **2012**, *302*, 1202–1210. [CrossRef] [PubMed]
20. Bendall, J.K.; Cave, A.C.; Heymes, C.; Gall, N.; Shah, A.M. Pivotal role of a gp91phox-containing NADPH oxidase in angiotensin II-induced cardiac hypertrophy in mice. *Circulation* **2002**, *105*, 293–296. [CrossRef]

21. Byrne Jonathan, A.; Grieve, D.J.; Bendall, J.K.; Li, J.-M.; Gove, C.; Lambeth, J.D.; Cave, A.C.; Shah, A.M. Contrasting roles of NADPH oxidase isoforms in pressure-overload versus angiotensin II–induced cardiac hypertrophy. *Circ. Res.* **2003**, *93*, 802–805. [CrossRef]
22. Zhang, M.; Prosser, B.L.; Bamboye, M.A.; Gondim, A.N.; Santos, C.X.; Martin, D.; Ghigo, A.; Perino, A.; Brewer, A.C.; Ward, C.W. Contractile function during angiotensin-II activation: Increased Nox2 activity modulates cardiac calcium handling via phospholamban phosphorylation. *J. Am. Coll. Cardiol.* **2015**, *66*, 261–272. [CrossRef] [PubMed]
23. Hafstad, A.D.; Hansen, S.S.; Lund, J.; Santos, C.X.; Boardman, N.T.; Shah, A.M.; Aasum, E. NADPH Oxidase 2 Mediates Myocardial Oxygen Wasting in Obesity. *Antioxidants* **2020**, *9*, 171. [CrossRef]
24. Pedersen, T.M.; Boardman, N.T.; Hafstad, A.D.; Aasum, E. Isolated perfused working hearts provide valuable additional information during phenotypic assessment of the diabetic mouse heart. *PLoS ONE* **2018**, *13*, e0204843. [CrossRef] [PubMed]
25. How, O.-J.; Aasum, E.; Kunnathu, S.; Severson, D.L.; Myhre, E.S.; Larsen, T.S. Influence of substrate supply on cardiac efficiency, as measured by pressure-volume analysis in ex vivo mouse hearts. *Am. J. Physiol.-Heart Circ. Physiol.* **2005**, *288*, 2979–2985. [CrossRef]
26. Boardman, N.; Hafstad, A.D.; Larsen, T.S.; Severson, D.L.; Aasum, E. Increased O_2 cost of basal metabolism and excitation-contraction coupling in hearts from type 2 diabetic mice. *Am. J. Physiol.-Heart Circ. Physiol.* **2009**, *296*, 1373–1379. [CrossRef] [PubMed]
27. Hafstad, A.D.; Boardman, N.T.; Lund, J.; Hagve, M.; Khalid, A.M.; Wisløff, U.; Larsen, T.S.; Aasum, E. High intensity interval training alters substrate utilization and reduces oxygen consumption in the heart. *J. Appl. Physiol.* **2011**, *111*, 1235–1241. [CrossRef]
28. Acin-Perez, R.; Benador, I.Y.; Petcherski, A.; Veliova, M.; Benavides, G.A.; Lagarrigue, S.; Caudal, A.; Vergnes, L.; Murphy, A.N.; Karamanlidis, G. A novel approach to measure mitochondrial respiration in frozen biological samples. *EMBO J.* **2020**, *39*, e104073. [CrossRef]
29. Hafstad, A.D.; Khalid, A.M.; How, O.-J.; Larsen, T.S.; Aasum, E. Glucose and insulin improve cardiac efficiency and postischemic functional recovery in perfused hearts from type 2 diabetic (db/db) mice. *Am. J. Physiol.-Endocrinol. Metab.* **2007**, *292*, 1288–1294. [CrossRef]
30. Sugiyama, M.; Yamaki, A.; Furuya, M.; Inomata, N.; Minamitake, Y.; Ohsuye, K.; Kangawa, K. Ghrelin improves body weight loss and skeletal muscle catabolism associated with angiotensin II-induced cachexia in mice. *Regul. Pept.* **2012**, *178*, 21–28. [CrossRef] [PubMed]
31. Ebrahimian, T.; He, Y.; Schiffrin, E.L.; Touyz, R.M. Differential regulation of thioredoxin and NAD (P) H oxidase by angiotensin II in male and female mice. *J. Hypertens.* **2007**, *25*, 1263–1271. [CrossRef]
32. Glenn, D.J.; Cardema, M.C.; Ni, W.; Zhang, Y.; Yeghiazarians, Y.; Grapov, D.; Fiehn, O.; Gardner, D.G. Cardiac steatosis potentiates angiotensin II effects in the heart. *Am. J. Physiol.-Heart Circ. Physiol.* **2015**, *308*, 339–350. [CrossRef]
33. Regan, J.A.; Mauro, A.G.; Carbone, S.; Marchetti, C.; Gill, R.; Mezzaroma, E.; Valle Raleigh, J.; Salloum, F.N.; Van Tassell, B.W.; Abbate, A. A mouse model of heart failure with preserved ejection fraction due to chronic infusion of a low subpressor dose of angiotensin II. *Am. J. Physiol.-Heart Circ. Physiol.* **2015**, *309*, H771–H778. [CrossRef]
34. Joseph, L.C.; Avula, U.M.R.; Wan, E.Y.; Reyes, M.V.; Lakkadi, K.R.; Subramanyam, P.; Nakanishi, K.; Homma, S.; Muchir, A.; Pajvani, U.B. Dietary saturated fat promotes arrhythmia by activating NOX2 (NADPH Oxidase 2). *Circ. Arrhythmia Electrophysiol.* **2019**, *12*, e007573. [CrossRef] [PubMed]
35. Donoso, P.; Finkelstein, J.P.; Montecinos, L.; Said, M.; Sánchez, G.; Vittone, L.; Bull, R. Stimulation of NOX2 in isolated hearts reversibly sensitizes RyR2 channels to activation by cytoplasmic calcium. *J. Mol. Cell. Cardiol.* **2014**, *68*, 38–46. [CrossRef]
36. Zhang, Y.; Fan, S.; Hu, N.; Gu, M.; Chu, C.; Li, Y.; Lu, X.; Huang, C. Rhein reduces fat weight in db/db mouse and prevents diet-induced obesity in C57Bl/6 mouse through the inhibition of PPARγ signaling. *PPAR Res.* **2012**, *2012*, 374936. [CrossRef]
37. Burgoyne, J.R.; Mongue-Din, H.; Eaton, P.; Shah, A.M. Redox signaling in cardiac physiology and pathology. *Circ. Res.* **2012**, *111*, 1091–1106. [CrossRef]
38. Prosser, B.L.; Ward, C.W.; Lederer, W. X-ROS signaling: Rapid mechano-chemo transduction in heart. *Science* **2011**, *333*, 1440–1445. [CrossRef] [PubMed]
39. Karwi, Q.G.; Uddin, G.M.; Ho, K.L.; Lopaschuk, G.D. Loss of metabolic flexibility in the failing heart. *Front. Cardiovasc. Med.* **2018**, *5*, 68. [CrossRef]
40. Mori, J.; Alrob, O.A.; Wagg, C.S.; Harris, R.A.; Lopaschuk, G.D.; Oudit, G.Y. ANG II causes insulin resistance and induces cardiac metabolic switch and inefficiency: A critical role of PDK4. *Am. J. Physiol.-Heart Circ. Physiol.* **2013**, *304*, 1103–1113. [CrossRef] [PubMed]
41. Pellieux, C.; Aasum, E.; Larsen, T.S.; Montessuit, C.; Papageorgiou, I.; Pedrazzini, T.; Lerch, R. Overexpression of angiotensinogen in the myocardium induces downregulation of the fatty acid oxidation pathway. *J. Mol. Cell. Cardiol.* **2006**, *41*, 459–466. [CrossRef]
42. Aikawa, R.; Nawano, M.; Gu, Y.; Katagiri, H.; Asano, T.; Zhu, W.; Nagai, R.; Komuro, I. Insulin prevents cardiomyocytes from oxidative stress–induced apoptosis through activation of PI3 kinase/Akt. *Circulation* **2000**, *102*, 2873–2879. [CrossRef] [PubMed]
43. Chen, Y.; Chen, C.; Dong, B.; Xing, F.; Huang, H.; Yao, F.; Ma, Y.; He, J.; Dong, Y. AMPK attenuates ventricular remodeling and dysfunction following aortic banding in mice via the Sirt3/Oxidative stress pathway. *Eur. J. Pharmacol.* **2017**, *814*, 335–342. [CrossRef] [PubMed]

44. Wang, M.; Sun, G.-b.; Sun, X.; Wang, H.-w.; Meng, X.-b.; Qin, M.; Sun, J.; Luo, Y.; Sun, X.-b. Cardioprotective effect of salvianolic acid B against arsenic trioxide-induced injury in cardiac H9c2 cells via the PI3K/Akt signal pathway. *Toxicol. Lett.* **2013**, *216*, 100–107. [CrossRef] [PubMed]
45. Pellieux, C.; Montessuit, C.; Papageorgiou, I.; Lerch, R. Angiotensin II downregulates the fatty acid oxidation pathway in adult rat cardiomyocytes via release of tumour necrosis factor-α. *Cardiovasc. Res.* **2009**, *82*, 341–350. [CrossRef]
46. Levinsson, A.; Dubé, M.P.; Tardif, J.C.; de Denus, S. Sex, drugs, and heart failure: A sex-sensitive review of the evidence base behind current heart failure clinical guidelines. *ESC Heart Fail.* **2018**, *5*, 745–754. [CrossRef] [PubMed]
47. Xue, B.; Pamidimukkala, J.; Hay, M. Sex differences in the development of angiotensin II-induced hypertension in conscious mice. *Am. J. Physiol.-Heart Circ. Physiol.* **2005**, *288*, 2177–2184. [CrossRef]

Paper III:

Hydrolyzed Wax Ester from Calanus Oil Protects H9c2 Cardiomyoblasts from Palmitate-Induced Lipotoxicity

Hydrolyzed wax ester from Calanus oil protects H9c2 cardiomyoblasts from palmitate-induced lipotoxicity

Synne S. Hansen[1]*, Kirsten M. Jansen[1]*, Kenneth B. Larsen[2], Anne D. Hafstad[1], Ragnar L. Olsen[3], Terje S. Larsen[1] and Ellen Aasum[1].

[1]Cardiovascular Research Group, Department of Medical Biology, Faculty of Health Sciences, University of Tromsø- The Arctic University of Norway. synne.s.hansen@uit.no

[2]Advanced Microscopy Core Facility, Department of Medical Biology, Faculty of Health Sciences, University of Tromsø-The Arctic University of Norway.

[3]The Norwegian College of Fishery Science, Faculty of Biosciences, Fisheries and Economics, University of Tromsø-The Arctic University of Norway.

* These authors contributed equally.

Short title: Hydrolyzed wax ester prevents lipotoxic stress

Key words: palmitic acid, lipotoxicity, ER stress, wax ester, autophagy, PUFA

Abstract

Lipotoxicity induced by an excessive load of saturated fatty acids, plays an important role in the development of obesity-induced heart failure. Accordingly, palmitate-induced lipotoxicity has been linked to increased oxidative stress, endoplasmic reticulum (ER) stress, impaired autophagic flux and apoptotic cell death. Previous reports have shown that Calanus oil and purified wax ester (WE) from this oil have beneficial systemic and cardiac effects in diet-induced obese mice. Here we evaluated the effect of hydrolysed WE (WE_H) from Calanus oil during palmitate-induced nutritional stress in H9c2 cells. Incubation of the cells with 100μM palmitate for 20-hours resulted in approximately 80% cell death. Co-incubation with WE_H resulted in a dose-dependent increase in cell survival, where 10 μM of WE_H almost completely abolished the palmitate-induced cell death. Although palmitate caused increased production of reactive oxygen species, this was not affected by co-incubation with WE_H. Palmitate-induced ER stress, as reflected by a significant increase of C/EBP homologous protein expression and nuclear translocation, was markedly reduced by co-incubation with WE_H. Palmitate-treated cells also displayed numerous enlarged LC3B-positive vesicles and p62-positive aggregates, suggesting impaired autophagic flux, which was markedly diminished by co-incubation with WE_H. To conclude, WE_H from Calanus had a direct protective effect on cardiomyoblasts during nutritional stress by inhibiting or preventing ER stress and impairment of autophagic flux. However, this was not mediated through reduced oxidative stress.

Introduction

Obesity and diabetes can result in an excessive accumulation of lipids in the myocardium [1,2] which, together with their intermediate products, may cause lipotoxicity and consequently disturbances of the cellular metabolism [3-5]. Cardiac lipotoxicity can be induced by both chronic high fat feeding of mice and by acute palmitate-treatment in H9c2 cells [6-8]. There are several proposed mechanisms for the detrimental effects observed in cardiac lipotoxicity. Both chronic and acute high lipid load are reported to cause increased myocardial oxidative stress, which is proposed as a major cause of lipotoxicity-induced cell death [3,9-11]. In addition, palmitate load has been shown to cause altered myocardial metabolism [12] increased myocardial endoplasmic reticulum (ER) stress [7,9] and altered autophagic flux [9,13] both of which can result in activation of apoptotic pathways.

Omega-3 poly-unsaturated fatty acids has been suggested as a potential strategy to counteract obesity-induced lipotoxicity, acting as reactive oxygen species (ROS) scavengers in vascular endothelial cells [14] as well as attenuating ER stress in primary rat hepatocytes [15]. We have previously reported that dietary supplementation with a small amount of Calanus oil from the marine crustacean Calanus *finmarchicus,* reduces intra-abdominal fat deposition, as well as adipose tissue inflammation in diet induced obese (DIO) mice [16,17]. More recently, we found that Calanus oil supplementation improved cardiac metabolism in DIO mice by alleviating the obesity-induced over-reliance on fatty acid oxidation [18]. Of particular interest was the finding that hearts from DIO mice who were supplemented with Calanus oil showed significantly better recovery of ventricular function following an ischemic insult. The mechanism behind this cardioprotective effect of Calanus oil is however not clear. The purpose of this study was therefore to explore potential beneficial effects of fatty acid and fatty alcohols derived from Calanus oil, during palmitate-induced nutritional stress in H9c2 cells.

Material and methods

Isolation and hydrolysis of wax ester from Calanus oil

Neutral lipids from Calanus oil were isolated by solid phase extraction, using five Mega Bond Elut aminopropyl SPE disposable columns (Varian Inc., Middelburg, Netherlands) mounted on a Visiprep vacuum manifold (Supelco, Pennsylvania, USA), as described by Vang et al. [19]. Following conditioning with heptane, each column was loaded with 80-100 mg Calanus oil (in 2 mL chloroform). The neutral lipids were eluted with chloroform: isopropanol (2:1), dried under a stream of nitrogen and re-dissolved in 1 mL heptane. The lipid extracts were loaded on new columns, and the wax esters (WE) subsequently eluted with heptane, dried and re-dissolved in chloroform. The WE were subsequently hydrolyzed in ethanolic potassium hydroxide, thereby separating the free fatty acids from the WE, creating WE hydrolysate (WE_H), according to the procedure described by Han and Christie [20].

Cell culture

H9c2 cells (rat embryonic cardiomyoblasts, ECACC Cell Lines, Sigma-Aldrich, England) were cultured at 37°C with 5% CO_2 using Dulbecco's modified eagles' medium with high glucose (DMEM D5796, Sigma-Aldrich, Missouri, USA), 10% fetal bovine serum (FBS, Sigma-Aldrich, Missouri, USA) and 100 U/mL penicillin and 100 µg/mL streptomycin (p0781, Sigma-Aldrich, Darmstadt, Germany). Cells from passage 10 to 15 were used in this study. To induce a lipotoxic stress, the cells were incubated with 100 µM palmitate (palmitic acid, P0500, Sigma-Aldrich, Darmstadt, Germany) dissolved in ethanol. Cells incubated in the presence of ethanol (vehicle) served as controls. In addition, palmitate-treated cells were co-incubated with WE_H, 0.2-10 µM from Calanus oil. To inhibit ER stress, the cells were incubated with 60 µM salubrinal (Sigma-Aldrich, Darmstadt, Germany). To induced ER stress cells were incubated with either 2.5 µg/mL tunicamycin (Sigma-Aldrich, Darmstadt,

Germany) or 1μM thapsigargin (Sigma-Aldrich, Darmstadt, Germany). To inhibit autophagy, the cells were incubated with either 20 μM LY294002 (Sigma-Aldrich, Darmstadt, Germany) or 0.2 μM bafilomycin A_1 (B1793, Sigma-Aldrich, Darmstadt, Germany). To induce autophagy cells were either treated with 1 μM rapamycin (R0395, Sigma-Aldrich, Darmstadt, Germany) or by acute amino acid starvation for 2 hours (Hank's treatment).

Determination of cell viability

The effect of WE_H on palmitate-induced cell death was assessed by Live Cell Imaging (Zeiss Celldiscoverer, Carl Zeiss Microscopy, GmbH 07745 Jena, Germany). The number of live and dead cells were manually counted in images obtained at different time points throughout a 20-hour incubation. In addition, cell viability was analyzed by xCELLigence biosensor technology (xCELLigence® Biosensor Technology RTCA, ACEA, Etterbeek, Belgium) which measures the strength of adhesion (in terms of electrical impedance) of cells to high-density gold electrode arrays printed on custom-designed E-plates, plates with gold microelectrodes fused to the bottom surface. Baseline impedance, termed cell index (CI) was measured after 24-hour pre-incubation of the cells (time zero), and measurements of impedance at 10- and 20-hours were normalized to the zero-time value.

Palmitate uptake in H9c2 cells

To determine if WE_H affected the uptake of fatty acids, we measured palmitate uptake in H9c2 cells over an 8-hour period, using 0.2 μCi/mL ^{3}H-labelled palmitate as a tracer. Cells were collected at timed intervals and washed several times with cold PBS. Lipids were extracted by the method of Folch [21] and the radioactivity determined by liquid scintillation (1900 TR Liquid Scintillation Analyser, Packard, Laborel, Oslo, Norway) .

ROS measurements

H9c2 cells were incubated with either 100μM palmitate, a combination of 100 μM palmitate and 10μM WE_H or 10μM WE_H exclusively for 6 hours. During the last 30 minutes of incubation 10 μM of the ROS binding probe, 2',7' –dichlorofluorescin diacetate (DCFDA / H2DCFDA – Cellular ROS Assay cit. Abcam, Cambridge, UK), was added directly to the wells. ROS measurements were performed by flow cytometry (LSRFortessa™, BD, New Jersey, U.S.) and registered as fluorescens emitted in the FITC channel.

Immunofluorescence

H9c2 cells grown in Lab-Tek chambered cover glass (Thermo Fisher Scientific, Massachusetts, USA) were fixed for 20 minutes with 4% formaldehyde in PHEM buffer, permeabilized with 0.3% Triton X-100 in PBS for 5 minutes and incubated with 3% goat serum in PBS for 60 minutes to block unspecific binding. The cells were then incubated overnight at 4° C with primary antibodies against C/EBP homologous protein (CHOP, Cell Signaling #2895, diluted 1:400), LC3B (Sigma-Aldrich, Darmstadt, Germany, #L7543, diluted 1:1300,), and p62/SQSTM1 (Progen, Heidelberg, Germany, #GP62-C, diluted 1:2000). After primary antibody incubation, cells were washed 6 x 5 minutes with PBS and then incubated with AlexaFluor-conjugated secondary antibodies (Sigma-Aldrich, Darmstadt, Germany, diluted 1:500) for 30 minutes at room temperature. Both primary and secondary antibodies were diluted in 1% goat serum in PBS. Finally, cells were washed 4 x 5 minutes with PBS, cell nuclei were stained with 1 μg/mL DAPI (Sigma-Aldrich, Darmstadt, Germany) in PBS for 10 minutes, followed by two additional washes with PBS. The cells were imaged using an LSM880 confocal microscope or a CD7 widefield microscope (Carl Zeiss Microscopy, Jena, Germany). Images were collected in ZEN software (Carl Zeiss Microscopy, Jena, Germany) using a 40x NA1.2 W C-Apochromat objective for confocal microscopy, or a 50x NA1.2 W Plan-Apochromat objective for widefield microscopy. Images were recorded with a pixel size of

0.42 μm for confocal acquisition and 0.13 μm for widefield acquisition. In both cases, optimal excitation and emission settings for each fluorophore were determined using the Smart Setup function in ZEN software. All fluorescence channels were recorded at non-saturating levels and acquisition settings were kept identical between all samples used for comparisons or quantifications. For scoring CHOP nuclear translocation and quantifying the per-cell number of p62/SQSTM1 bodies, between 15 and 20 confocal stacks (z step size = 1.00 μm, z range = 5.00 μm) were collected at random positions in each well and used for subsequent image analysis.

Real-time quantitative PCR

Cells were collected and immersed in RNAlater (Qiagen, Hilden, Germany), and total RNA was extracted according to the RNeasy plus mini kit Protocol (Qiagen Nordic, Norway). Quantification and purity of RNA was measured spectrophotometrically. RNA was reverse transcribed into cDNA using High-Capacity cDNA Reverse Transcription Kit (Thermo Fisher, Massachusetts, USA) and real-time PCR was performed in a LightCycler®96 System (Roche, Basel, Switzerland) with the cDNA and FastStart Essential DNA Green Master (Roche, Basel, Switzerland). Target gene expression levels were normalized to a stable expressed housekeeping gene (HMBS, GAPDH, SDHA, Cyclo). The stability of the housekeeping gene was determined by geNorm [22].

Statistics

Cells derived from one passage were regarded as n=1. The difference between treatment groups and within individual passages were analysed with paired one-way ANOVA together with Tukey's post hoc test. The overall significance level was set to $p < 0.05$. Results are presented as mean ± standard error of the mean (SEM) in tables and with individual data points in column bar graphs.

Results

WE_H protects H9c2 cells from palmitate-induced cell death

Incubation of H9c2 cells in the presence of 100 μM palmitate resulted in a time-dependent increase in cell death, as assessed by visual examination and scoring of live cell microscopy images (Fig. 1A). Cell death occurred after about 6-8-hours of incubation, while almost all cells were dead after 20 hours. The percentage of live palmitate-treated cells after 10- and 20-hours were approximately 65% and 25%, respectively, while the corresponding numbers for cells incubated in the presence of vehicle, were 99% and 97% (Fig. 1 B and D). Co-incubation of palmitate-exposed cells with WE_H resulted in a clear dose-dependent increase in cell viability. Thus, after 20 hours, cell viability was significantly improved in WE_H treated cells, even at very low concentrations (1 and 2 μM), while the highest dose (10 μM) almost completely rescued the cells from palmitate-induced death (Fig. 1 B and D).

In addition to the live cell imaging, we used xCELLigence real-time cell analysis. Baseline cell index (CI) was measured following 24-hour preincubation (time zero) and thereafter every 10 min over the next 20-hour period. In vehicle-treated cells, CI increased continuously throughout the full 20-hour period, while it started to decay after about 10-hour in palmitate-exposed cells. In the same manner as with live cell imaging, we found that co-incubation with WE_H dose-dependently antagonized the palmitate-induced decline in CI, and the CI curve obtained with 10 μM WE_H was not significantly different from that of vehicle-treated cells (Fig. 1 C and E).

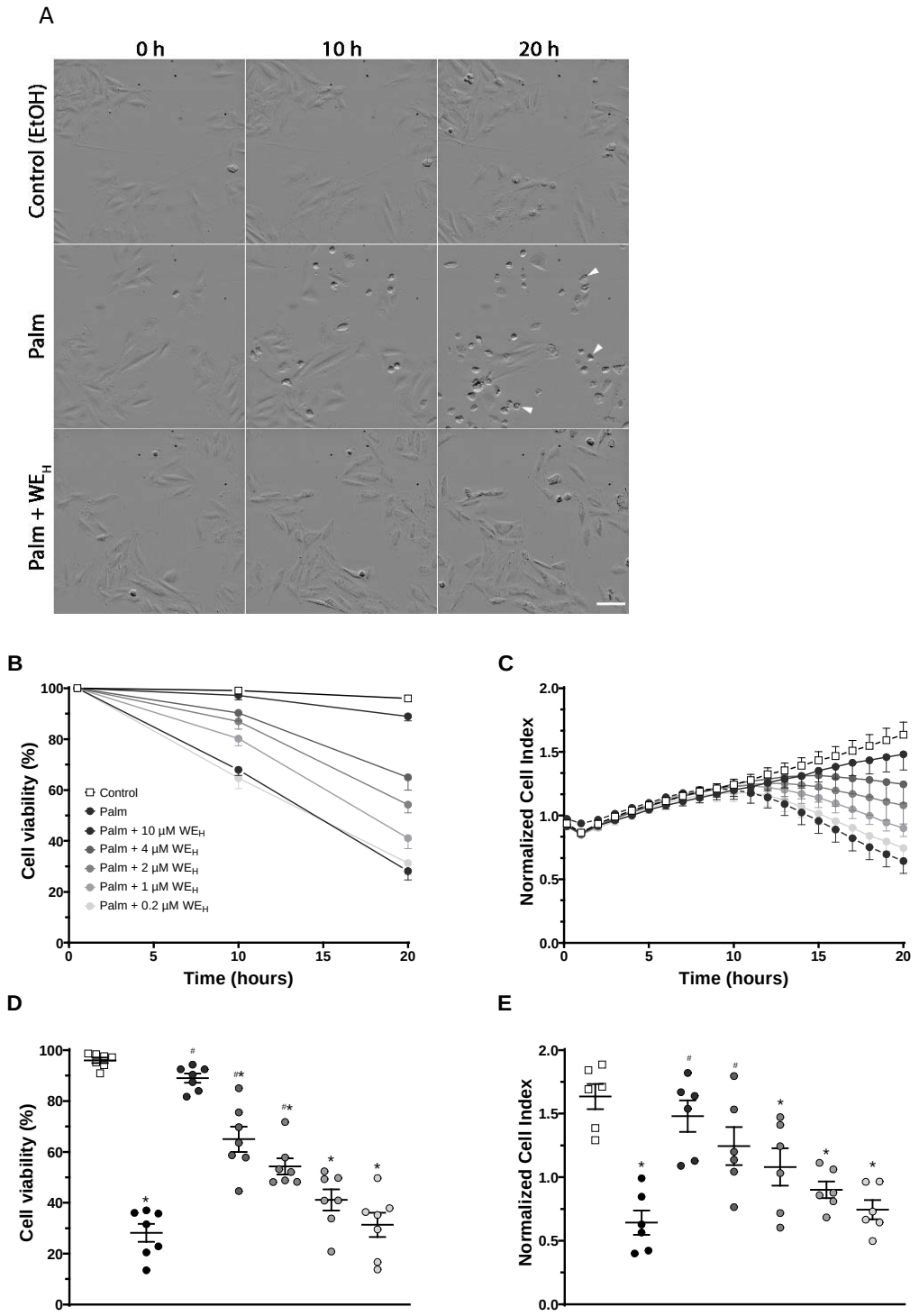

Figure 1. Effect of palmitate (Palm) and hydrolyzed wax ester (WE_H) from Calanus oil on viability of palmitate exposed H9c2 cells. The cells were incubated with 100 µM Palm and 0-10 µM WE_H for 20 hours. Ethanol (vehicle)-treated cells were included as controls**. A:** Representative live cell images showing palmitate-induced cell death at 0, 10 and 20 hours, arrowheads indicate examples of dead cells. Scale bar 100 µm. **B and C**: Time courses of cell viability of palmitate exposed H9c2 cells in the absence and presence of increasing concentrations of WE_H. Cell viability assessed as % live cells from the live cell images or Normalized Cell Index, using Live Cell Imaging and xCELLigence RTCA Biosensor Technology, respectively. **D and E**: Cell viability in individual experiments at the end of the 20-hour incubation period. Data are mean ± SEM (Live Cell Imaging and xCELLigence, respectively). * $p<0.05$ vs. control; # $p<0.05$ vs palmitate.

Co-incubation with WEH does not alter palmitate uptake or ROS production

WEH did not affect the palmitate uptake in the H9c2 cells (Figure 2A). Of note, measurements of palmitate uptake over time showed a drop in uptake after about 6-8 hours in cells treated with palmitate exclusively, as expected considering the cell viability data shown in Fig. 1. Although palmitate-treatment increased cellular ROS in the H9c2 cells (Figure 2 B) as previously described [7,11], co-treatment with WEH did not inhibit ROS production. Finally, WEH incubation alone did not significantly alter ROS production in H9c2 cells.

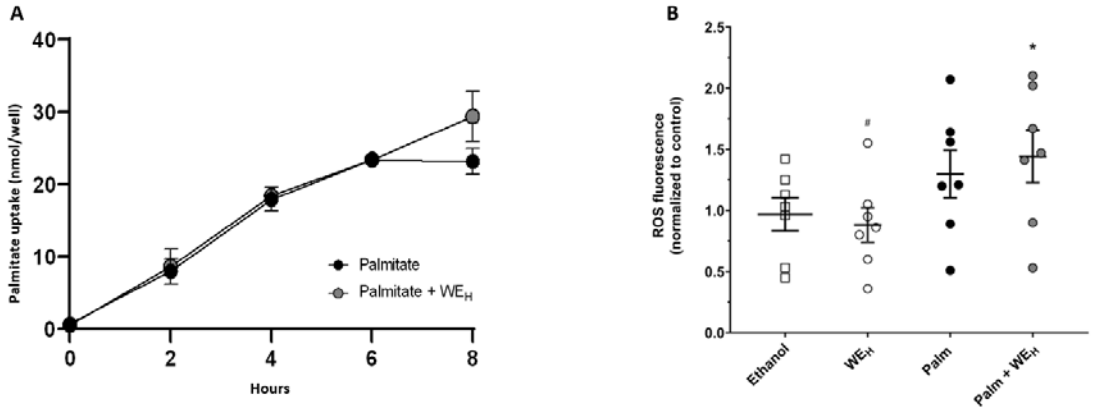

Figure 2. Effect of palmitate (Palm)- and hydrolysed wax ester (WEH)-treatment on palmitate uptake and ROS production. The cells were incubated with 100 μM Palm and 10 μM WEH. Ethanol (vehicle)-treated cells were included as controls. **A:** The cells were incubated with Palm or WEH for 8 hours. Palm uptake was measured using ^{3}H-labeled palmitate as a tracer, n=2. **B:** ROS production in H9c2 cells were measured by flow cytometry using redox sensitive probe DCFDA following a 6-hour incubation Palm or WEH. Data are presented as mean ± SEM. * $p<0.05$ vs. control, # $p<0.05$ vs palmitate.

WEH reduces palmitate-induced ER stress

Palmitate has previously been shown to induce ER stress in H9c2 cells [6]. Thus, we investigated whether the observed protective effect of WEH could be accompanied by reduced ER stress. Salubrinal is a selective inhibitor of eukaryotic initiation factor-2α (eIF2α) dephosphorylation, consequently protecting cells from ER stress [23]. Interestingly, we found that salubrinal significantly reduced the palmitate-induced

cell death (Fig. 3A), suggesting that survival of H9c2 cells after palmitate exposure is strongly affected by eIF2α phosphorylation. To examine if WE_H could have a direct effect on chemically induced ER stress, we induced ER stress in control cells using tunicamycin, a protein glycosylation inhibitor [23]. As expected, tunicamycin significantly reduced cell viability, however, co-incubation with WE_H did not alter tunicamycin-induced cell death.

We also measured gene expression of the transcription factor CHOP, a marker of ER stress, and found a 7-fold increase following 6-hour palmitate incubation (Fig. 3B). These data were supported by immunofluorescence microscopy of CHOP after 15 hours, showing a clear increase in CHOP nuclear translocation after palmitate exposure (Fig. 3C). Taken together these results confirm that palmitate causes severe ER stress in H9c2 cells, which is in line with previous findings [6]. Importantly, although WE_H could not abrogate tunicamycin-induced ER stress, co-incubation with 10 μM WE_H caused a marked reduction in both palmitate-induced CHOP expression (Fig. 3B) and nuclear translocation (Fig. 3C). These data clearly show that WE_H can counteract palmitate-induced up-regulation of CHOP in H9c2 cells. Incubation with WE_H alone had no effect on CHOP expression (Fig. 3B) or nuclear translocation (data not shown).

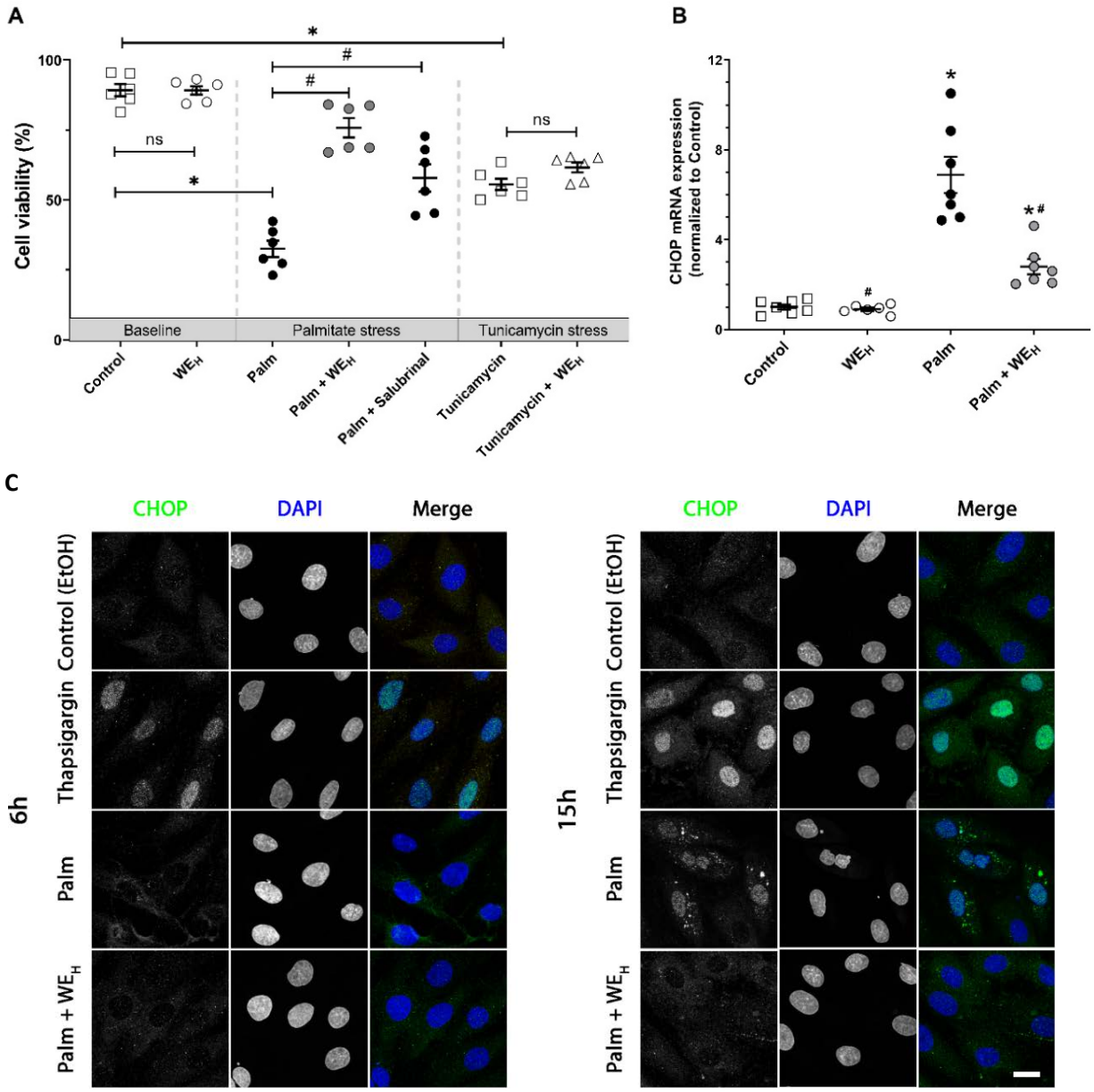

Figure 3. Effect of hydrolyzed wax ester (WE_H) from Calanus oil and ER stress inhibition and induction in H9c2 cells. The cells were incubated with 100 μM palmitate (Palm) and 10 μM WE_H. Ethanol (vehicle)-treated cells were included as controls. **A**: Cell viability (% live cells assessed from Live Cell Images) following 20-hour incubation with Palm and WE_H. Cells were also incubated in the presence of 60 μM salubrinal (ER stress inhibitor) or 2.5 μg/mL tunicamycin (ER stress inducer) as indicated. **B**: The mRNA expression of the CHOP gene in cells incubated with Palm and WE_H for 6 hours. **C:** Representative pictures showing the nuclear translocation of CHOP in cells incubated with Palm and WE_H for 6 and 15 hours. Cells were also incubated in the presence of 1 μM thapsigargin (ER stress inducer) as positive control. The cells were imaged by confocal microscopy. Data are presented as mean± SEM, * $p<0.05$ vs. control; # $p<0.05$ vs palmitate. Scale bar 20μM.

WE_H counteracts the palmitate-induced impairment of autophagy flux

ER stress is dynamically interrelated with autophagy, and several reports have suggested that palmitate can impair autophagic flux. Thus, we also examined whether the observed protective effect of WE_H was accompanied by restored autophagic flux. For this, we used live cell imaging experiments for assessment of cell viability (Fig. 4A), immunofluorescence studies with the autophagosome marker LC3B and the selective autophagy cargo receptor p62 (Fig. 4B). We first confirmed that H9c2 cells elicit a normal autophagy response with typical LC3B-positive autophagosomes appearing after acute amino acid starvation (Hank's treatment) as well as an accumulation of both LC3B and p62 in cytosolic puncta after lysosomal inhibition with bafilomycin A_1 (Fig. S2). In coherence with this, we found that palmitate exposure (6 hours) induced numerous enlarged LC3B-positive vesicles (Fig. 4B, middle panel) and a dramatic increase in p62-positive aggregates/inclusions. It should be noted that these structures appeared already within two hours of palmitate-treatment and were present at all later timepoints (data not shown). Importantly, in cells co-treated with WE_H the presence of LC3B vesicles and p62 aggregates was greatly diminished (Fig. 4B, lower panel), which suggests that WE_H can counteract this palmitate-induced impairment of the autophagic flux. Therefore, we tested if activation of autophagy could increase viability in palmitate-treated cells. However, inducing autophagy with rapamycin did not counteract the palmitate-induced cell death. In addition, we examined whether WE_H could ameliorate the cell death induced by inhibiting endogenous autophagy using LY294002, but as shown in Fig. 4A, WE_H did not protect against cell death following a chemical inhibition of autophagy. Taken together, these results suggest that autophagy is impaired by palmitate-induced stress in H9c2 cells, but chemical activation of autophagy does not alleviate this.

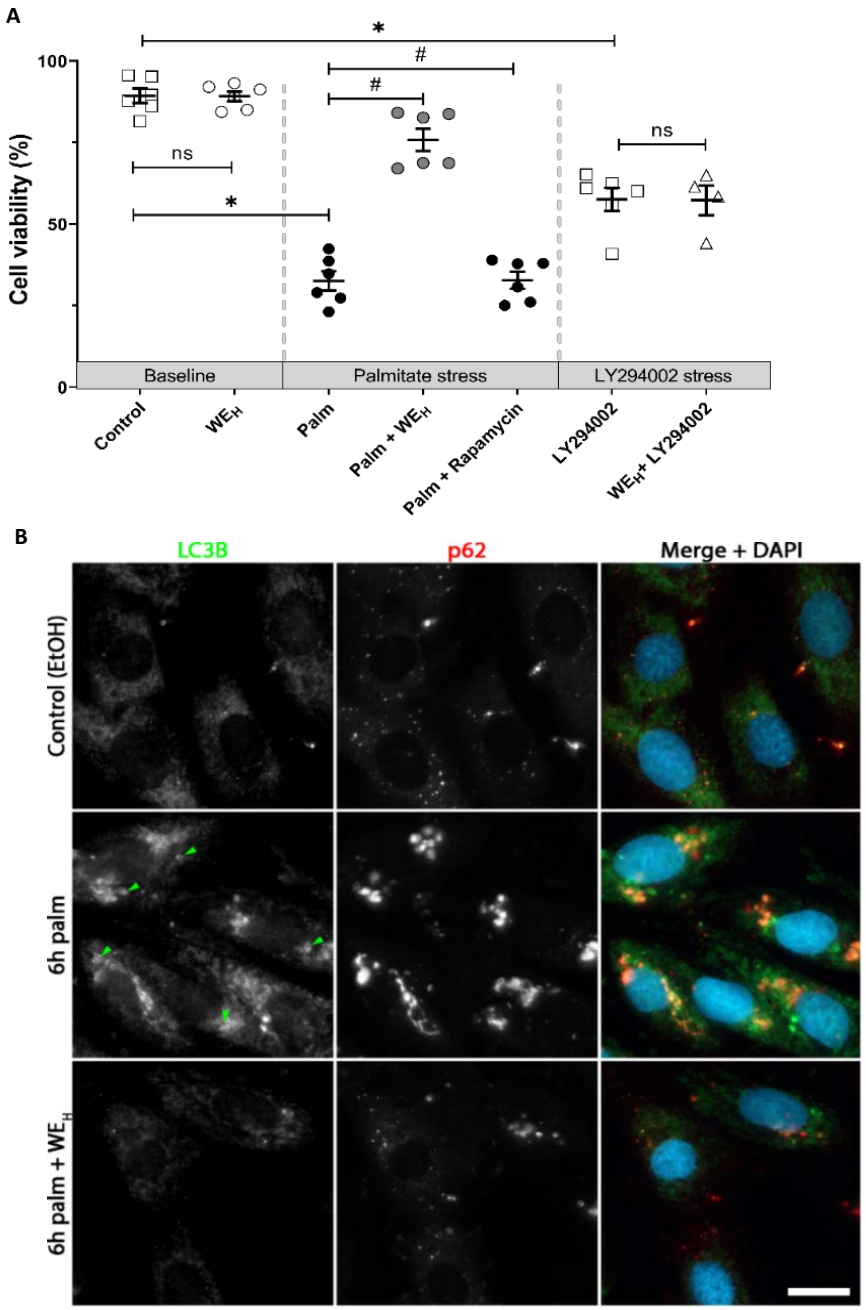

Figure 4. Effect of palmitate (Palm) and hydrolyzed wax ester (WE_H) from Calanus oil on cell viability and autophagy in H9c2 cells. The cells were incubated with 100 µM Palm and 10 µM WE_H. Ethanol (vehicle)-treated cells were included as controls. **A**: Cell viability (% live cells assessed from Live Cell Imaging) following 20-hour incubation with Palm and WE_H. Cells were also incubated in the presence of 1µM rapamycin or 20 µM LY294002 as indicated. **B:** Representative pictures showing the abundance and localization of LC3B and p62 (autophagy markers) in cells incubated with Palm and WE_H for 6 hours. The cells were imaged by confocal microscopy. Green arrowheads point to enlarged LC3B vesicles. Data are presented as mean ± SEM. $p<0.05$ vs. control; # $p<0.05$ vs palmitate. Scale bar 20µm.

Discussion

Animal experiments have reported cardioprotective effects of dietary fish oil supplements by improved functional recovery or decreased infarct size following ischemia [24,25]. In a previous study, the dietary supplementation with Calanus oil was found to be cardioprotective, in the sense that it attenuates ischemic damage in perfused hearts from diet-induced obese mice [18]. This oil has a chemical composition where 80-85% of the lipids are in the form of wax esters (WE). In the present study, we show that hydrolyzed WE (WE_H) from Calanus oil effectively and dose-dependently protects H9c2 cells from palmitate-induced cell death.

A protective effect of marine polyunsaturated fatty acids (PUFA), such as EPA and/or DHA, was also previously reported in palmitate exposed H9c2 cells. However, in these experiments, the concentrations of PUFA were considerably higher than those used in the current study. Cetrullo et al. [26] reported that 80 μM EPA significantly increased survival of H9c2 cells incubated with 500 μM palmitate. The same group also found that the combination of EPA and DHA (60 μM each) protected the cells from the palmitate-induced stress [27]. In the present study we demonstrate that 10 μM of WE_H nearly completely abolished the palmitate-induced cell death. It is not obvious why the WE_H afforded protection at concentrations below 10 μM, but the combination of several PUFAs, including a relatively high concentration of stearidonic acid (SDA) as well as monounsaturated fatty acids, could probably explain its efficacy. In addition, fatty acids and fatty alcohols were present at the same molar concentrations in the WE_H, and although the beneficial effects of marine oils are normally attributed to their content of PUFA, the presence of fatty alcohols could also contribute to the potency of the hydrolysate [28].

PUFA play a pivotal role in regulating the biophysical properties of cellular membranes [29], and human studies suggest that replacement of saturated fat in the diet by PUFA may contribute to lower uptake of lipids in skeletal muscle [30]. We

therefore examined whether the protective effect of WE_H could be explained in terms of reduced lipotoxicity due to reduced palmitate uptake. However, the results showed that palmitate uptake was not affected by the presence of WE_H.

Palmitate-treatment in H9c2 cells has been shown to increase ROS production, generating oxidative stress [5,7,11,31], which was confirmed in the preset study. Despite the fact that omega-3 fatty acids have been shown to exhibit antioxidant properties, acting as a ROS scavengers [14], co-incubation with WE_H did not alter palmitate-induced ROS production. It should however be noted that WE_H treatment alone, although non-significant, tended to have lower ROS production then the control.

Sustained ER stress plays a critical role in the development of cardiac dysfunction by contributing to apoptotic cell death [6,32]. In addition, cellular stress will also activate autophagy to remove damaged organelles and misfolded proteins [33,34], and palmitate has been reported to facilitate autophagosome accumulation in H9c2 cells [6,35]. In coherence with previous reports [6,32], we observed that palmitate exposure resulted in a significant increase in the expression and nuclear translocation of CHOP (ER stress marker), and that inhibition of ER stress with salubrinal significantly improved viability in palmitate-treated cells. Importantly, co-incubation with WE_H markedly ameliorated both the palmitate-induced increase in CHOP expression and translocation to the nuclei. These data might suggest that prevention or reduction of ER stress, at least in part, accounts for the cardioprotective effect of WE_H. On the other hand, WE_H did not inhibit the chemically induced ER stress caused by tunicamycin, which indicates that the cardioprotective effect of WE_H might be upstream of the palmitate-induced ER stress.

The present study supports previous reports, which show that palmitate induces LC3B-positive vesicles in H9c2 cells [6,35]. This increase was accompanied by p62-positive aggregates, as also shown by Jaishy et al. [35]. These structures were

apparent within two hours of treatment and did not diminish over time, suggesting an impairment of autophagic flux already at an early stage of the process. Of particular interest, however, was the observation that the presence of LC3B vesicles and p62 aggregates/inclusions were absent in palmitate-exposed cells co-treated with WE_H. In our hands, however, chemical activation of autophagy (by co-treatment with rapamycin) failed to affect viability of palmitate treated H9c2, indicating that chemical activation of autophagy alone is not sufficient to alleviate cellular toxicity caused by palmitate. Taken together, these data suggest that palmitate impairs autophagic flux, and that WE_H prevents the formation of palmitate-induced aggregates/inclusions. Our results points to the notion of autophagy being a very complex cellular process. Although, several findings suggest that increased autophagy has a protective effect against cell death during cellular stress, sustained activation may have detrimental effects [6,36].

In conclusion, this study demonstrates for the first time that the wax ester from Calanus oil, has a direct protective effect on cardiac cells during nutritional stress. This cardio-protective effect was not mediated through reduced oxidative stress but seems to be associated with amelioration of palmitate-induced ER stress and impaired autophagic flux. Further studies are however needed to fully reveal the mechanisms involved.

Acknowledgements
Trine Lund's and Thomas V. Andreasen's expert technical assistance is gratefully acknowledged.

Author Contributions: Conceptualization, S.S.H., K.M.J., T.L., A.D.H., E.A. and K.L.B.; formal analysis, S.S.H., K.M.J., E.A. and K.B.L.; investigation, S.S.H., K.M.J. and K.B.L.; data curation, S.S.H., K.M.J., E.A. and K.B.L. and E.A.; writing—original draft preparation, S.S.H., K.M.J., T.L. and K.B.L.; writing—review and editing, S.S.H., K.M.J., T.L., A.D.H., E.A., R.B.O and K.B.L. visualization, S.S.H., K.M.J. and K.B.L. supervision T.L., A.D.H. and E.A.; project administration, T.L. and E.A.; funding acquisition, T.L.

Funding: This research was funded by The Norwegian Heart Foundation (fellowship K.M.J) and the UIT-The Arctic University of Norway (fellowship to S.S.H.) as well as Calanus AS; and the Northern Norway Regional Health Authority [HNF– 1341-17].

Conflicts of Interest: The authors declare no conflict of interest. The funders had no role in the design of the study; in the collection, analyses, or interpretation of data; in the writing of the manuscript, or in the future decision to publish the results.

References

1. Kenchaiah, S.; Evans, J.C.; Levy, D.; Wilson, P.W.; Benjamin, E.J.; Larson, M.G.; Kannel, W.B.; Vasan, R.S. Obesity and the risk of heart failure. *N Engl J Med* **2002**, *347*, 305-313, doi:10.1056/NEJMoa020245.
2. Van Gaal, L.F.; Mertens, I.L.; De Block, C.E. Mechanisms linking obesity with cardiovascular disease. *Nature* **2006**, *444*, 875-880, doi:10.1038/nature05487.
3. Joseph, L.C.; Barca, E.; Subramanyam, P.; Komrowski, M.; Pajvani, U.; Colecraft, H.M.; Hirano, M.; Morrow, J.P. Inhibition of NAPDH oxidase 2 (NOX2) prevents oxidative stress and mitochondrial abnormalities caused by saturated fat in cardiomyocytes. *PloS one* **2016**, *11*, e0145750.
4. Haffar, T.; Berube-Simard, F.; Bousette, N. Impaired fatty acid oxidation as a cause for lipotoxicity in cardiomyocytes. *Biochemical and Biophysical Research Communications* **2015**, *468*, 73-78, doi:10.1016/j.bbrc.2015.10.162.
5. Haffar, T.; Akoumi, A.; Bousette, N. Lipotoxic palmitate impairs the rate of β-oxidation and citric acid cycle flux in rat neonatal cardiomyocytes. *Cellular Physiology and Biochemistry* **2016**, *40*, 969-981.

6. Park, M.; Sabetski, A.; Kwan Chan, Y.; Turdi, S.; Sweeney, G. Palmitate induces ER stress and autophagy in H9c2 cells: implications for apoptosis and adiponectin resistance. *J Cell Physiol* **2015**, *230*, 630-639, doi:10.1002/jcp.24781.
7. Yang, L.; Guan, G.; Lei, L.; Liu, J.; Cao, L.; Wang, X. Oxidative and endoplasmic reticulum stresses are involved in palmitic acid-induced H9c2 cell apoptosis. *Bioscience Reports* **2019**, *39*.
8. Hsu, H.C.; Chen, C.Y.; Lee, B.C.; Chen, M.F. High-fat diet induces cardiomyocyte apoptosis via the inhibition of autophagy. *Eur J Nutr* **2016**, *55*, 2245-2254, doi:10.1007/s00394-015-1034-7.
9. Jaishy, B.; Zhang, Q.; Chung, H.S.; Riehle, C.; Soto, J.; Jenkins, S.; Abel, P.; Cowart, L.A.; Van Eyk, J.E.; Abel, E.D. Lipid-induced NOX2 activation inhibits autophagic flux by impairing lysosomal enzyme activity. *Journal of Lipid Research* **2015**, *56*, 546-561.
10. Yang, M.; Wei, D.; Mo, C.; Zhang, J.; Wang, X.; Han, X.; Wang, Z.; Xiao, H. Saturated fatty acid palmitate-induced insulin resistance is accompanied with myotube loss and the impaired expression of health benefit myokine genes in C2C12 myotubes. *Lipids in health and disease* **2013**, *12*, 104.
11. Wei, C.D.; Li, Y.; Zheng, H.Y.; Tong, Y.Q.; Dai, W. Palmitate induces H9c2 cell apoptosis by increasing reactive oxygen species generation and activation of the ERK1/2 signaling pathway. *Molecular Medicine Reports* **2013**, *7*, 855-861.
12. How, O.-J.; Aasum, E.; Severson, D.L.; Chan, W.A.; Essop, M.F.; Larsen, T.S. Increased myocardial oxygen consumption reduces cardiac efficiency in diabetic mice. *Diabetes* **2006**, *55*, 466-473.
13. Park, M.; Sabetski, A.; Kwan Chan, Y.; Turdi, S.; Sweeney, G. Palmitate induces ER stress and autophagy in H9c2 cells: implications for apoptosis and adiponectin resistance. *Journal of Cellular Physiology* **2015**, *230*, 630-639.
14. Richard, D.; Kefi, K.; Barbe, U.; Bausero, P.; Visioli, F. Polyunsaturated fatty acids as antioxidants. *Pharmacological Research* **2008**, *57*, 451-455.
15. Zhang, Y.; Dong, L.; Yang, X.; Shi, H.; Zhang, L. α-Linolenic acid prevents endoplasmic reticulum stress-mediated apoptosis of stearic acid lipotoxicity on primary rat hepatocytes. *Lipids Health Dis* **2011**, *10*, 81, doi:10.1186/1476-511x-10-81.
16. Höper, A.C.; Salma, W.; Khalid, A.M.; Hafstad, A.D.; Sollie, S.J.; Raa, J.; Larsen, T.S.; Aasum, E. Oil from the marine zooplankton Calanus finmarchicus improves the cardiometabolic phenotype of diet-induced obese mice. *British Journal of Nutrition* **2013**, *110*, 2186-2193, doi:10.1017/s0007114513001839.
17. Höper, A.C.; Salma, W.; Sollie, S.J.; Hafstad, A.D.; Lund, J.; Khalid, A.M.; Raa, J.; Aasum, E.; Larsen, T.S. Wax esters from the marine copepod Calanus finmarchicus reduce diet-induced obesity and obesity-related metabolic disorders in mice. *The Journal of nutrition* **2014**, *144*, 164-169, doi:10.3945/jn.113.182501.
18. Jansen, K.M.; Moreno, S.; Garcia-Roves, P.M.P.; Larsen, T.S. Dietary Calanus oil recovers metabolic flexibility and rescues post-ischemic cardiac function in obese female mice. *Am J Physiol Heart Circ Physiol* **2019**, doi:10.1152/ajpheart.00191.2019.
19. Vang, B.; Pedersen, A.M.; Olsen, R.L. Oil extraction From the Copepod Calanus finmarchicus Using Proteolytic Enzymes. *Journal of aquatic food product technology* **2013**, *22*, 619-628.
20. Han, X.; Christie, W. Lipid Analysis: Isolation, Separation, Identification and Lipidomic Analysis. **2010**.
21. Folch, J.; Lees, M.; Sloane Stanley, G.H. A simple method for the isolation and purification of total lipides from animal tissues. *J Biol Chem* **1957**, *226*, 497-509.
22. Vandesompele, J.; De Preter, K.; Pattyn, F.; Poppe, B.; Van Roy, N.; De Paepe, A.; Speleman, F. Accurate normalization of real-time quantitative RT-PCR data by geometric averaging of multiple internal control genes. *Genome biology* **2002**, *3*, Research0034, doi:10.1186/gb-2002-3-7-research0034.
23. Boyce, M.; Bryant, K.F.; Jousse, C.; Long, K.; Harding, H.P.; Scheuner, D.; Kaufman, R.J.; Ma, D.; Coen, D.M.; Ron, D.; et al. A selective inhibitor of eIF2alpha dephosphorylation protects cells from ER stress. *Science* **2005**, *307*, 935-939, doi:10.1126/science.1101902.

24. Zhu, B.Q.; Sievers, R.E.; Sun, Y.P.; Morse-Fisher, N.; Parmley, W.W.; Wolfe, C.L. Is the reduction of myocardial infarct size by dietary fish oil the result of altered platelet function? *American Heart Journal* **1994**, *127*, 744-755, doi:10.1016/0002-8703(94)90540-1.
25. Yang, B.C.; Saldeen, T.G.; Bryant, J.L.; Nichols, W.W.; Mehta, J.L. Long-term dietary fish oil supplementation protects against ischemia-reperfusion-induced myocardial dysfunction in isolated rat hearts. *American Heart Journal* **1993**, *126*, 1287-1292, doi:10.1016/0002-8703(93)90524-d.
26. Cetrullo, S.; Tantini, B.; Flamigni, F.; Pazzini, C.; Facchini, A.; Stefanelli, C.; Caldarera, C.M.; Pignatti, C. Antiapoptotic and antiautophagic effects of eicosapentaenoic acid in cardiac myoblasts exposed to palmitic acid. *Nutrients* **2012**, *4*, 78-90, doi:10.3390/nu4020078.
27. Cetrullo, S.; D'Adamo, S.; Panichi, V.; Borzì, R.M.; Pignatti, C.; Flamigni, F. Modulation of Fatty Acid-Related Genes in the Response of H9c2 Cardiac Cells to Palmitate and n-3 Polyunsaturated Fatty Acids. *Cells* **2020**, *9*, doi:10.3390/cells9030537.
28. Schots, P.C.; Pedersen, A.M.; Eilertsen, K.E.; Olsen, R.L.; Larsen, T.S. Possible Health Effects of a Wax Ester Rich Marine Oil. *Front Pharmacol* **2020**, *11*, 961, doi:10.3389/fphar.2020.00961.
29. Harayama, T.; Shimizu, T. Roles of polyunsaturated fatty acids, from mediators to membranes. *J Lipid Res* **2020**, *61*, 1150-1160, doi:10.1194/jlr.R120000800.
30. Jans, A.; Konings, E.; Goossens, G.H.; Bouwman, F.G.; Moors, C.C.; Boekschoten, M.V.; Afman, L.A.; Müller, M.; Mariman, E.C.; Blaak, E.E. PUFAs acutely affect triacylglycerol-derived skeletal muscle fatty acid uptake and increase postprandial insulin sensitivity. *The American Journal of Clinical Nutrition* **2012**, *95*, 825-836, doi:10.3945/ajcn.111.028787.
31. Wu, K.-M.; Hsu, Y.-M.; Ying, M.-C.; Tsai, F.-J.; Tsai, C.-H.; Chung, J.-G.; Yang, J.-S.; Tang, C.-H.; Cheng, L.-Y.; Su, P.-H. High-density lipoprotein ameliorates palmitic acid-induced lipotoxicity and oxidative dysfunction in H9c2 cardiomyoblast cells via ROS suppression. *Nutrition & metabolism* **2019**, *16*, 1-13.
32. Zou, L.; Li, X.; Wu, N.; Jia, P.; Liu, C.; Jia, D. Palmitate induces myocardial lipotoxic injury via the endoplasmic reticulum stress-mediated apoptosis pathway. *Molecular Medicine Reports* **2017**, *16*, 6934-6939.
33. Bernales, S.; McDonald, K.L.; Walter, P. Autophagy counterbalances endoplasmic reticulum expansion during the unfolded protein response. *PLoS Biol* **2006**, *4*, e423, doi:10.1371/journal.pbio.0040423.
34. Ding, W.X.; Ni, H.M.; Gao, W.; Hou, Y.F.; Melan, M.A.; Chen, X.; Stolz, D.B.; Shao, Z.M.; Yin, X.M. Differential effects of endoplasmic reticulum stress-induced autophagy on cell survival. *J Biol Chem* **2007**, *282*, 4702-4710, doi:10.1074/jbc.M609267200.
35. Jaishy, B.; Zhang, Q.; Chung, H.S.; Riehle, C.; Soto, J.; Jenkins, S.; Abel, P.; Cowart, L.A.; Van Eyk, J.E.; Abel, E.D. Lipid-induced NOX2 activation inhibits autophagic flux by impairing lysosomal enzyme activity. *J Lipid Res* **2015**, *56*, 546-561, doi:10.1194/jlr.M055152.
36. Shintani, T.; Klionsky, D.J. Autophagy in health and disease: a double-edged sword. *Science* **2004**, *306*, 990-995, doi:10.1126/science.1099993.

Supplemented data

Thin layer chromatography

Thin layer chromatography (TLC) was performed as previously described [19] and confirmed total hydrolysis of the wax esters (Fig. S1, appendix). In brief, lipids extracts and standards (18-5 from Nu-check prep inc. MN, USA) were applied to high performance thin layer chromatography (HPTLC) plates (silica gel 60 matrix, Merck, Darmstadt, Germany), which were developed using a mobile phase consisting of heptane: diethyl ether: acetic acid (80:20:2). The TLC plates were dried and sprayed with 10% copper sulphate in 8% phosphoric acid. The major lipid species were visualized by heating for 10 minutes at 180 °C. A standard was used to determine the concentration of fatty acid in the hydrolysate. We assumed equimolar concentration of fatty acid and fatty alcohol.

A separate TLC run, including several concentrations of a known fatty acid, was performed to determine the fatty acid concentration in the wax ester hydrolysate. The plate was scanned using Image Studio Lite v5.2.5 (LI-COR Biosciences - GmbH), and the data were subsequently used to establish a fatty acid standard curve, which in turn was used for determination of the fatty acid concentration in the wax ester hydrolysate. Since the hydrolysis of the wax ester was complete, and the wax ester is composed of one fatty alcohol and one fatty acid, we assumed equimolar concentrations of fatty acids and fatty alcohols in the hydrolysate.

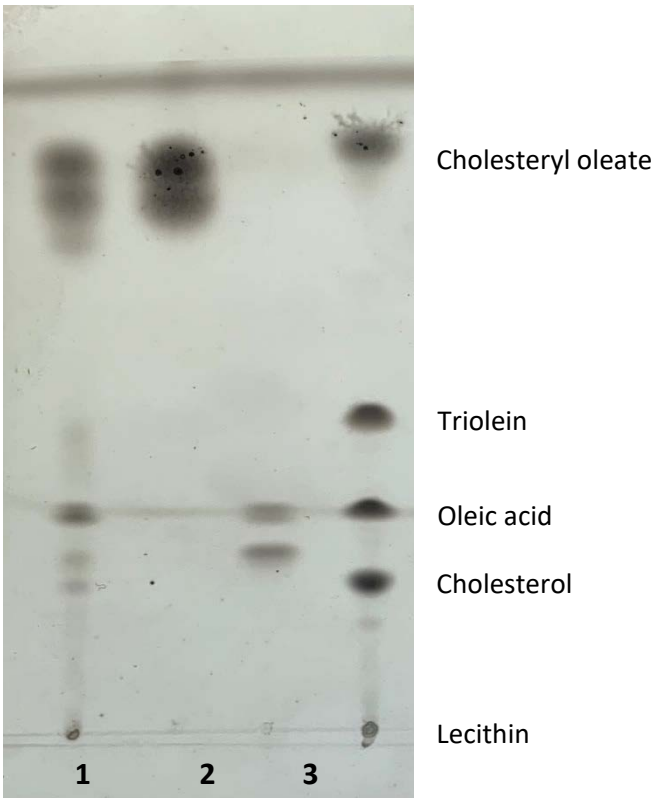

Figure S1. Thin layer chromatography showing the various lipid classes in crude Calanus oil in line 1; purified wax ester in lane 2; hydrolyzed wax ester (i.e. fatty acids and fatty alcohols) in lane 3; lipid standard (18:5 from Nu-check prep inc.) in lane 4.

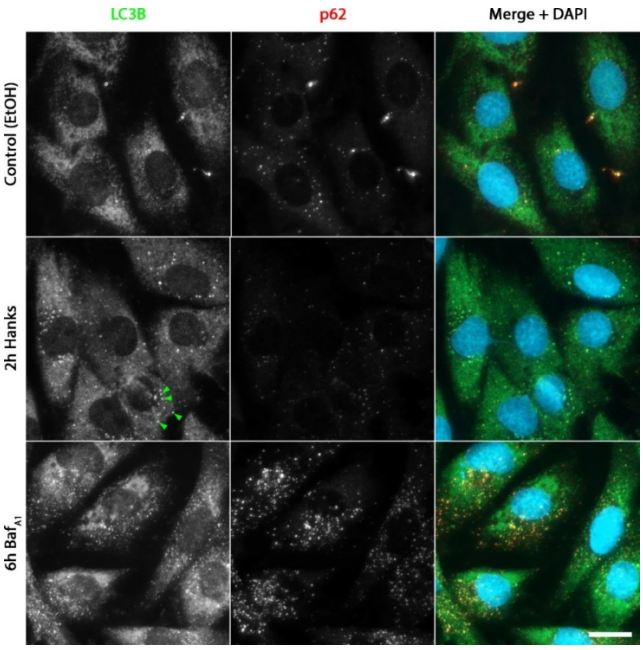

Figure S2. Effect of autophagy activation and autophagic flux inhibition on localization and abundance of LC3B and p62. Immunofluorescence microscopy of H9c2 cells acute amino acid starvation (2 hours with Hank's buffer) or lysosomal inhibition (6 hours with bafilomycin A_1). Ethanol-treated (vehicle) cells were included as a control. Scale bar 20 μm.